

# **Studies with a Beta Particle Emitting Radionuclide in the Context of Radioimmunotherapy**

*By*

**CHANDAN KUMAR**

**Enrolment No. LIFE01200804009**

**Bhabha Atomic Research Centre**

*A thesis submitted to the  
Board of Studies in Life Sciences*

*In partial fulfillment of requirements  
For the Degree of*

**DOCTOR OF PHILOSOPHY**

*of*

**HOMI BHABHA NATIONAL INSTITUTE**



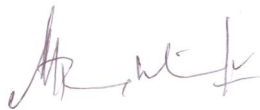
**October, 2013**

# Homi Bhabha National Institute

## Recommendations of the Viva Voce Board

As members of the Viva Voce Board, we certify that we have read the dissertation prepared by Chandan Kumar entitled “**Studies with a beta particle emitting radionuclide in the context of radioimmunotherapy**” and recommend that it may be accepted as fulfilling the dissertation requirement for the Degree of Doctor of Philosophy.

Chairman- Dr. M. G. R. Rajan



Date: 9/12/14

External Examiner- Dr. B. S. Dwarakanath



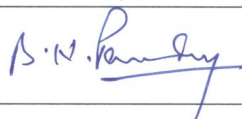
Date:

Guide- Dr. Meera Venkatesh



Date: 09<sup>th</sup> Dec 2014

Co-Guide & Member 1 - Dr. B. N. Pandey



Date: 9.12.14

Member 2- Dr. B. S. Shankar



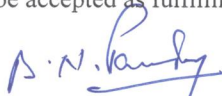
Date: 9/12/14

---

Final approval and acceptance of this dissertation is contingent upon the candidate's submission of the final copies of the dissertation to HBNI.

I hereby certify that I have read this dissertation prepared under my direction and recommend that it may be accepted as fulfilling the dissertation requirement.

Date:



Place: Mumbai

Co-Guide - Dr. B. N. Pandey

Guide - Dr. Meera Venkatesh

## **STATEMENT BY AUTHOR**

This dissertation has been submitted in partial fulfillment of requirements for an advanced degree at Homi Bhabha National Institute (HBNI) and is deposited in the Library to be made available to borrowers under rules of the HBNI.

Brief quotations from this dissertation are allowable without special permission, provided that accurate acknowledgement of source is made. Requests for permission for extended quotation from or reproduction of this manuscript in whole or in part may be granted by the Competent Authority of HBNI when in his or her judgment the proposed use of the material is in the interests of scholarship. In all other instances, however, permission must be obtained from the author.



**(Chandan Kumar)**

## DECLARATION

I, hereby declare that the investigation presented in the thesis has been carried out by me. The work is original and has not been submitted earlier as a whole or in part for a degree / diploma at this or any other Institution / University.



**(Chandan Kumar)**

*Dedicated to My Beloved  
Lordship Radhagopinathjee*

## ACKNOWLEDGEMENTS

I wish to express gratitude to my research guide, Prof. Meera Venkatesh, former Head, Radiopharmaceuticals Division (RPhD), Bhabha Atomic Research Centre (BARC) for her encouragement, technical suggestions and good wishes, blessed me to prepare this thesis.

I wish to express sincere and heartfelt gratitude to my research co-guide and member, Dr. B. N. Pandey, Head, Radiation Signaling and Cancer Biology Section, Radiation Biology & Health Sciences Division, Bhabha Atomic Research Centre (BARC) for his constant and valuable scientific suggestions, and motivation lead to complete the Ph.D. thesis work.

I wish to express my deep sense of gratitude to Dr. Grace Samuel for her keen observations of work, moral support and strong faith in me to complete my work.

It is my great honor to thank the Chairman Prof. Dr. M. G. R. Rajan, Head, RMC, BARC, Ex- members of the doctoral committee Dr. R. C. Chaubey, Dr. S. M. Zingde and Dr. T. B. Poduval for their critical reviews and suggestions throughout the Ph.D. work and the progress review presentations. I wish to thank the present member of doctoral committee Dr. Bhavani Shankar for her suggestions for the improvement of thesis.

I am grateful to my colleagues Dr. Aruna Korde, Dr. Mythili Kameswaran, Shri Suresh Subramanian and Shri A.D. Kadam of IP&AD, and Shri Jayakumar of RBHSD, BARC for their help during my experimental work to finalize the present thesis.

It is my pleasure to acknowledge Mr. P. V. Joshi Ex-Head former Radiochemicals Section and his group for regular supply of  $\text{Na}^{131}\text{I}$  to carry out the

research work and other colleagues of IP &AD and RPhCS for their help render during the work. I would be like to acknowledge the help rendered by the technical staffs Shri Umesh Kumar, Shri U. K. Sukhale, Shri E. G. Mohite and Mrs. Savita Gawarne, of IP&AD and Shri Sanjay Shinde of RBHSD, BARC for various technical assistance and irradiation during Ph.D. thesis work.

I would like to express soulwise gratitude from the core of heart to my beloved Lordship Radhagopinath Jee and Lord Jaganath- Baldev- Subhadra Maharani for showering the choicest blessing upon me. I will be eternally grateful and indebted for the sources of inspiration given by HH Radhanath Swami Maharaj and His Divine Grace Srila Prabhupad by their mercy I received the crest jewels which I do not deserve at least in this life time.

My special thanks to HG Radhavallabh Das, HG BankimRaya Das, HG Sudhanidhi Das, HG Sridamasakha Das, HG Avtar Leela Das, HG Surver Krishna Das, HG Prem Hari Das, HG Prem Kunj Devi Dasi, Pranaw Kumar and many more whose associations inspired me.

Last but not the least, without blessing, good wishes, constant moral support, love and encouragement of my best friend and wife Priyadarshni, daughter Shubhangi, father Shri Mahatma Prasad, mother Smt. Usha Devi, father-in-law Shri Ganga Dass and other relatives, this work would not be completed. It will be incomplete if I do not mention the good wishes and blessings of my late grandfather Shri Chandrika Prasad and late grandmother Smt. Sangami Devi.

Trombay, Mumbai

  
(Chandan Kumar)

15 December, 2014

# Index

CONTENTS	Page No.
Synopsis .....	ix-xxiii
Abbreviations.....	xxiv-xxvii
List of Figures.....	xxviii-xxxiii
List of Tables.....	xxxiv
CHAPTER 1 Introduction.....	1-29
1.1.Preamble.....	2
1.2. History of radionuclides.....	2-4
1.3. Production of radioisotopes.....	4-5
1.4. Application of radionuclides in healthcare.....	5-10
1.5. Cancer and therapeutic modalities.....	11-24
1.6. Iodine -131 based radiopharmaceuticals.....	25-26
1.7. Biological effects of radiation.....	26-27
1.8. Rationale of the thesis .....	27-28
1.9. Scope and objectives of the thesis.....	28-29
CHAPTER 2 Comparison of effects of beta radiation emitted from <sup>131</sup> I with an equivalent dose of γ-rays in human cancer cells .....	30-53
2.1. Introduction.....	30-31
2.2. Scope and objectives of the chapter.....	32-33
2.3. Materials and methods .....	34-39
2.4. Results .....	40-48



2.5. Discussion .....	49-53
<b>CHAPTER 3</b> Study on cellular internalization and mechanism of toxicity of <sup>131</sup> I-rituximab in Raji cells.....	54-88
3.1. Introduction .....	55-58
3.2. Scope and objectives of the chapter.....	58-59
3.3. Materials and methods .....	60-69
3.4. Results .....	70-85
3.5. Discussion.....	86-88
<b>CHAPTER 4</b> Study on effect of <sup>131</sup> I-rituximab in combination with doxorubicin on Raji cells.....	89-109
4.1.Introduction.....	90-91
4.2.Scope and objectives of the chapter.....	91-92
4.3.Materials and methods.....	93-96
4.4.Results.....	97-105
4.5.Discussion.....	106-109
<b>CHAPTER 5</b> Summary, conclusions and future directions.....	110-116
5.1.Summary of the thesis.....	111-114
5.2.Major conclusions of the thesis.....	115
5.3.Future directions.....	116
<b>REFERENCES</b> .....	117-138
<b>LIST OF PUBLICATIONS</b> .....	139-140

## SYNOPSIS

### Preamble

Use of radiation is very well established and is one of the primary modalities of treatment of various cancers. While external beam therapy using gamma radiation from  $^{60}\text{Co}$  or from linear accelerators is widely practised. In-vivo radionuclides therapy using radiopharmaceuticals are very effective in selected cancers, such as thyroid cancer. Radionuclides therapy is most often accomplished using radioisotopes capable of emitting alpha and or beta, as it is important to deliver the radiation dose to the target tissue, while sparing the neighboring healthy tissues. In this context,  $^{131}\text{I}$  has been used for therapy since more than six decades and is still among the most promising therapeutic radionuclide, despite the associated gamma emissions as well the emergence of other radionuclides for therapy such as Lutetium-177. While thyroid cancer has been treated since several decades using radiopharmaceuticals, attempt to treat many other cancers over the past 10-15 years have opened the avenue for effective treatment of several malignancies that were not very responsive to other modes of treatment. One of the causes for these new radiopharmaceuticals is the availability, of highly specific targeting molecules such as antibodies and peptides, resulting from the great advances in the area of cancer research. One such malignancy is non-Hodgkin's lymphoma (NHL), where radiolabeled monoclonal antibodies against the CD20 antigen are being explored for use in therapy. Application of radiolabeled antibodies provides a tool for targeted therapy for lymphoma, highlighting the concept of "magic bullets" coined by Ehrlich (Ehrlich, 1960) that was meant to eradicate disease by targeting the diseased tissues/organs. NHL is a clinically heterogeneous group of malignancies arising from B, T or NK-lymphoid

cells and the 11<sup>th</sup> most common cause of cancer incidence. Most of the B-cell lymphoma tumor cells express higher number of CD20 receptors and therefore it becomes one of the possible targets for therapy (Anderson *et al.*1984). There are several anti CD20 antibodies used in clinics but rituximab is currently available. Rituximab is a genetically engineered, chimeric monoclonal antibody against CD20 receptor and has been approved by FDA in 1997 for use in immunotherapy (Boye *et al.* 2003). The therapeutic efficacy of rituximab could be increased by labeling the antibody with a radioisotope having high energy beta particle thus enabling the targeted delivery of radionuclide to the tumor tissue. Earlier, Tositumomab and Ibritumomab, both anti CD20 mouse antibodies were radiolabeled with <sup>131</sup>I and <sup>90</sup>Y respectively and have been approved by FDA for clinical use. But, with the availability of rituximab, many are working to develop radiolabeled rituximab to achieve better treatment devoid of human anti mouse antibody (HAMA) responses.

Among the various therapeutic radionuclides, radioiodine (<sup>131</sup>I) is predominantly used, as it has several advantages such as good radiation properties, amenable chemistry and easy availability at reasonable costs. The high energy beta particles emitted by <sup>131</sup>I have a maximum tissue penetration range of ~2.3 mm, which can lead to irradiation of large mass of tumor. <sup>131</sup>I has a half life of 8 days and is available indigenously at reasonable costs with regular supplies. Biomolecules can be labeled with <sup>131</sup>I without significant changes in biological properties using simple methods. Iodine is easily incorporated into antibodies as well as other molecules with tyrosine/tryptophan/histidine moiety to form stable radiolabeled molecules without steric hindrance and major changes in 3d confirmations.

The aim of this thesis is to study the effect of beta radiations on the human cancer cell lines using <sup>131</sup>I, and compare with an equivalent dose of  $\gamma$ -rays. Further,

studies were carried out to assess whether the use of  $^{131}\text{I}$ -rituximab resulted in enhanced cell toxicity in Raji cells and understand the underlying mechanism for the same. Additionally, the advantage of using  $^{131}\text{I}$ -rituximab in combination with conventionally used chemotherapy agents such as doxorubicin was also explored. Doxorubicin has serious side effects (cardiotoxicity being one of them) and also results in drug resistance. In this study, Raji cells were treated with  $^{131}\text{I}$ -rituximab in combination with doxorubicin, and cell toxicity and mechanism of toxicity were elucidated.

### **RATIONALE OF THE THESIS**

$^{131}\text{I}$  was chosen as the radionuclide for these studies due to its excellent potential for therapy applications and the lack of in-depth studies on the mechanisms of its therapeutic action. As mentioned above, the physical as well as the chemical properties of  $^{131}\text{I}$  render it a very useful therapeutic radioisotope. To reiterate, an ideal therapeutic beta emitting radioisotope should have following characteristics: (a) relatively moderate to long half life to enable adequate irradiation to the target tissues, (b) high energy of beta for effective killing of cancer cells and (c) emission of suitable gamma radiation which can be imaged for monitoring.  $^{131}\text{I}$  fulfills these criteria. NHL is fatal if untreated and survival rates for NHL vary widely, depending on the lymphoma type, stage, age of the patient, and other variables. According to the American Cancer Society, the overall 5-year relative survival rate for patients with NHL is 63 % and the 10-year relative survival rate is 51 %. The treatment modalities are generally based on immunotherapy and chemotherapy. Although rituximab is immunotherapeutic on its own since it induces cell death in B-cell lymphoma, large amounts of antibodies have to be administered for therapy. Use of the antibody for selectively targeting the tumor and combining the antibody with another lethal entity

such as radionuclide is a well proven strategy for increasing the effectiveness in cancer therapy, while using much lower amounts of the precious antibody. Further, it has been found that most of the NHL become non responsive or resistance to either rituximab or chemotherapy. Even radiation therapy alone is not very helpful in the cure of NHL. It is thus, relevant to study the effectiveness of radiolabeled rituximab alone as well as in combination with a chemotherapy agent, with respect to the cell toxicity. Hence,  $^{131}\text{I}$ -rituximab was used in these studies, assuming that the combined modality would have synergistic benefit. Raji cells, which are CD20 positive human lymphoma cell line, were used in these studies too.

### **OBJECTIVES OF THE THESIS**

This research was carried out with the following specific aims:

1. To study the in vitro effect of beta radiation emitted from  $^{131}\text{I}$  in comparison with the  $\gamma$ -radiation in different human tumor cell lines
2. To study the cellular internalization of  $^{131}\text{I}$ -rituximab and mechanism of toxicity in Raji cells
3. To study the effect of doxorubicin on  $^{131}\text{I}$ -rituximab treated Raji cells

The thesis entitled “Studies with a beta particle emitting radionuclide in context of radioimmunotherapy” has been summarized in the following chapters:

#### **CHAPTER 1** Introduction

**CHAPTER 2** Comparison of effect of beta radiation emitted from  $^{131}\text{I}$  with an equivalent dose of  $\gamma$ -radiation in human cancer cell lines

**CHAPTER 3** Study on cellular internalization and mechanism of toxicity of  $^{131}\text{I}$ -rituximab in Raji cells

**CHAPTER 4** Study on effect of  $^{131}\text{I}$ -rituximab in combination with doxorubicin on Raji cells

**CHAPTER 5** Summary, conclusions and future directions

Chapter 2-4 contains separate introduction pertaining to respective chapter, detailed materials and methods, results and discussion.

### **CHAPTER 1 Introduction**

This chapter deals with a brief history of radioisotopes from the discovery of atom to the radioactivity, production of radionuclides and its applications in human health care. The application of radionuclides in healthcare began almost 70 years ago with the use of  $^{131}\text{I}$  as sodium iodide in treatment of thyroid cancers and  $^{32}\text{P}$  for treatment of polycythemia vera. The specialty of ‘Nuclear Medicine’, where radioactive formulations known as radiopharmaceuticals are used for either diagnosis or therapy, evolved over time as a branch of medicine. A steep increase in diagnostic applications was seen after the advent of Technetium-99m ( $^{99\text{m}}\text{Tc}$ ) in the 1960’s and the invention of the gamma camera by Anger designed to detect the 140 keV gammas from  $^{99\text{m}}\text{Tc}$  efficiently.

Around the same period, the pioneering work of Rosalyn Yalow and Solomon Aaron Berson in the USA (Yalow et. al., 1960), and Ekins in the UK described techniques known as radioimmunoassay or competitive radioligand assay, which led to the use of radioisotopes, essentially,  $^{131}\text{I}$ ,  $^{125}\text{I}$  and tritium for estimating very minute quantities of hormones, tumor markers, drugs and other metabolites in blood and other body fluids.

The production of clinically useful radioisotopes by radiochemists and the parallel understanding of the pathophysiology of cancers, viz., cancer biochemistry,

molecular biology, etc. had a great influence on the growth of nuclear medicine. Many diseases could be diagnosed easily without a biopsy sample. In oncology, malignant tumors especially of the prostate, breast, lung etc., could be detected with tumor localizing radiopharmaceuticals, with  $^{18}\text{F}$ FDG being the most prominent. In advanced cases, the malignancy metastasizes to the other organs including the bone. Bone-metastasis cause unbearable pain, which is usually treated with analgesics drugs and radiolabeled bisphosphonates. When these drugs no longer relieve the pain, bone seeking simple radioisotopes ( $^{89}\text{SrCl}$  and  $^{32}\text{P}$ ) or radiolabeled phosphonates ( $^{153}\text{Sm}$ -EDTMP,  $^{177}\text{Lu}$ -EDTMP and  $^{166}\text{Ho}$ -DOTMP) is used for bone pain palliation (Finlay et al. 2005).

Among the radionuclides used in therapy, radioiodine ( $^{131}\text{I}$ ) is the earliest known radionuclide used in thyroid disorder (Hertz et al. 1940). Its beta energy is used for therapy and gamma rays for imaging. The latter contributes very little in therapy but can be employed for dosimetric calculation and imaging during therapy. Targeted delivery of radionuclides is possible by several means viz., antibodies, peptides, antisense RNA, aptamer of DNA and RNA, target specific small molecules and affibody (Jamous *et al.* 2013, Hicke *et al.* 2006, Boswell *et al.* 2007, Hoppman et al. 2011). Amongst them, antibodies have taken a lead role in radiopharmaceuticals for cancer therapy as several FDA approved antibodies are commercially available, which could be tagged with radionuclides for use in therapy.

## **CHAPTER 2 Comparison of effect of beta radiation emitted from $^{131}\text{I}$ with an equivalent dose of $\alpha$ -radiation in human cancer cells**

Cancer treatment using external beam of gamma rays is very well established and the effects of gamma rays on cancer cells have been studied and reported extensively (Steel et al. 1987, Bracey et al. 1995). Despite the fact that many beta emitting

radionuclides are in clinical use, the studies about the mechanism of cell death induced by beta radiation are very limited in the literature.  $^{131}\text{I}$  ( $\text{Na}^{131}\text{I}$ ) which emits beta particles is an established effective therapeutic radionuclide. However, the cytotoxic effect of  $^{131}\text{I}$  in comparison of  $\gamma$ -ray is not well understood. Hence, in this chapter the effect of the beta radiation from  $^{131}\text{I}$  was studied on tumor cells of different tissue origin, which was compared with an equivalent dose of  $\gamma$  radiation. The cell toxicity study was further extended to investigate regulation of genes involved in DNA damage and apoptosis.

Four different human cancer cell lines viz. Raji (Burkitt Lymphoma), U937 (Histiocytic Lymphoma), MCF-7 (Breast carcinoma) and A431 (skin carcinoma) were treated with 1.85 MBq of  $^{131}\text{I}$  for 2 h (dose 0.4 Gy and dose rate 0.003 Gy/min) and non radioactive sodium iodide (NaI) at the same chemical concentration was used as vehicle control. The cells were washed thoroughly and further incubated for 24 h. Likewise, similar number of cells were irradiated with 0.4 Gy of gamma rays (dose rate: 0.4 Gy/min) and incubated under same conditions. After incubation, the cells were harvested and the cell death was assessed using trypan blue dye. The results showed that  $^{131}\text{I}$  induced 16 % cell death in Raji cells which is significantly higher ( $p < 0.05$ ) compared to (10 %) by the 0.4 Gy given by  $^{60}\text{Co}$ -gamma radiation. Amongst all the cell lines, maximum cell death was observed in Raji cells and the least in A431 cells. Due to the lower radiation dose component from the gamma rays in comparison with the beta particles, it is assumed that contribution of gamma radiation from  $^{131}\text{I}$  is negligible towards radiation induced cytotoxicity in cancer cells.

In order to investigate the underlying mechanism of cell death in Raji, U937, MCF-7 and A431 cells after  $^{131}\text{I}$  and equivalent dose of gamma rays treatment, apoptotic DNA fragmentation study was carried out. The results showed that,  $^{131}\text{I}$



induced DNA fragmentation measured in terms of enrichment factor (1.8 to 2.4) was significantly higher ( $p < 0.05$ ) than fragmentation induced by the equivalent dose of  $\gamma$ -rays (1.2). It was also observed that maximum fragmentation was observed in the Raji cell line. Significant PARP cleavage ( $p < 0.05$ ) was observed in  $^{131}\text{I}$  treated cell lines when compared to the equivalent dose of  $\gamma$ -rays.

Since Raji cell line exhibited maximum cell toxicity and apoptosis compared to the other cell lines, it was of interest to further study the expression of genes involved in DNA damage response after irradiation at 30 and 240 min. Expressions of *BAX*, *P21* and *RAD51* genes were analyzed by real time PCR. It was found that *BAX* gene is upregulated in  $^{131}\text{I}$  and 0.4 Gy treated Raji cells when the time of incubation was increased from 30 min to 4 h ( $p < 0.05$ ). However, no significant change in *BAX* expression was observed between  $^{131}\text{I}$  and gamma treated Raji cells. At 30 min of incubation, it was observed that the *P21* expression was much higher for 0.4 Gy from gamma but decreased subsequently with time. This might be due to the high dose rate of  $\gamma$ -rays, causing more DNA damage and hence *P21* expression was higher compared to the equivalent dose of  $^{131}\text{I}$ . However, in case of  $^{131}\text{I}$ , *P21* expression increased from 30 min to 4 h ( $p < 0.05$ ) because the DNA damage accumulated with time and hence the expression was more at 4 h time period than at 30 min. *RAD51* gene, involved in DSB repair by homologous recombination, was found to remain constant with time for  $^{131}\text{I}$  irradiated cells. In case of gamma irradiated cells, the *RAD51* expression was relatively higher within 30 min, but decreased by 4 h ( $p < 0.05$ ). The initial higher expression could be due to the higher dose rate of  $\gamma$ -rays causing more DNA damage, but subsequently decreasing due to repair taking place via homologous repair (Khanna et al. 2001). In case of  $^{131}\text{I}$ , it is possible that the natures of damages are different and probably involve other repair mechanism(s).

These studies show that cell toxicity and apoptotic death induced by beta radiation from  $^{131}\text{I}$  is higher than that produced by an equivalent dose of  $\gamma$ -rays. Raji cells were found to be sensitive to both beta and gamma radiation than other cancer cell lines studied.

### **Chapter 3 Study on cellular internalization and mechanism of toxicity of $^{131}\text{I}$ -rituximab of in Raji cells**

In Chapter 2,  $^{131}\text{I}$  was found to induce higher cytotoxicity than equivalent dose of gamma radiation, which was again highest in Raji cells. Hence, in this chapter to further increase the efficacy and selectivity of  $^{131}\text{I}$ , we have labeled a CD20 specific antibody i.e. rituximab with  $^{131}\text{I}$  ( $^{131}\text{I}$ -rituxmab). The efficacies of the  $^{131}\text{I}$ -rituximab radiopharmaceutical in binding to the CD20 receptors of Raji cells were studied. Initial studies were performed, for labeling characterization, localization and subsequent fate of  $^{131}\text{I}$ -rituxmab in this cell line. Once  $^{131}\text{I}$ -rituxmab internalized, it would exert its radio-toxicity depending on cellular target and dose received. This Chapter is aimed to study cellular localization/stability of  $^{131}\text{I}$ -rituximab bound to CD20 receptor and the mechanism underlying the cytotoxicity in Raji cells.

The magnitude of expression of CD20 receptors on Raji cells (CD20 positive) was evaluated using anti-CD20-FITC by flow cytometry with negative control of human lymphoma U937 cells (CD20 negative). Results showed that  $69.4 \pm 1.2$  % populations are CD20 FITC positive in Raji cells, while it was very low ( $3.5 \pm 0.376$  %) in U937 cells. Hence, the choice of Raji cells were made in these experiments.

Rituximab was labeled with  $^{131}\text{I}$  by Iodogen method (Fraker et al. 1978) and radioiodination yield was  $>90$  %. The radiochemical purity of  $^{131}\text{I}$ -rituximab was  $>99$  % after PD10 Sephadex column purification as determined by HPLC. The specific

activity of  $^{131}\text{I}$ -rituximab is 0.30-0.35 MBq/ $\mu\text{g}$ . Cell binding and inhibition studies were carried out in Raji cell line and it was found that immunoreactivity of rituximab was retained even after radiolabeling with  $^{131}\text{I}$ , while the non specific binding in U937 cell line was <0.5 %. Cell binding was carried out with increasing concentrations (0.037-3.7 MBq) of  $^{131}\text{I}$ -rituximab and incubated for 30 min to 6 h. It was found that 1.85 MBq of  $^{131}\text{I}$ -rituximab and 2 h time period of incubation were optimum for carrying out further experiments. The dose delivered by  $^{131}\text{I}$ -rituximab was calculated with an assumption that beta particles deposited 100 % of its energy in the cells/media while  $\gamma$ -rays has negligible contribution, and it was found to be 0.38 Gy for 2 h incubation period. The cumulative dose received by cells during incubation period of 2, 6 12 and 24 h were 0.39, 0.40, 0.42 and 0.46 Gy, respectively.

Cellular internalization study of  $^{131}\text{I}$ -rituximab was carried out at different time periods of incubation by membrane stripping, which results in removal of membrane bound activity. It was observed that cellular internalization (radioactivity after stripping) increased with the time of incubation. It was also found that the radioactivity in the cell bound fraction (membrane stripped fraction) decreased during course of incubation. Hence, the fraction of de-iodination was assessed in protein precipitation using trichloroacetic acid (TCA) and paper electrophoresis of medium/supernatant obtained from  $^{131}\text{I}$ -rituximab treated Raji cells, collected at different time points. It was found that only ~10 % free iodide was observed in the supernatant at 24 h time point.

For cell toxicity studies, Raji cells were incubated with 1.85 MBq of  $^{131}\text{I}$ -rituximab for 2 h then washed and further incubated for 2, 6, 12 and 24 h. Cell toxicity was measured by LDH release. It was observed that cells treated with  $^{131}\text{I}$ -rituximab showed increase in LDH release depending on increase in incubation period

compared to the unlabeled rituximab. Likewise, it was found that  $^{131}\text{I}$ -rituximab induced apoptosis with the increase in time of incubation, which was much higher compared to the rituximab. Western blotting of p53 and PARP proteins showed that  $^{131}\text{I}$ -rituximab induced increased PARP cleavage and p53 expression when compared to the rituximab alone, after 6 h of incubation. The increase in PARP cleavage or apoptosis was observed after 6 h which can be related to the fact that internalization of  $^{131}\text{I}$ -rituximab increased from 6 h. On internalization,  $^{131}\text{I}$ -rituximab resides closer to the nucleus than when it was bound to the membrane, causing increased damage to the nucleus and registering increased apoptosis.

From the above studies, it can be concluded that  $^{131}\text{I}$ -rituximab induces higher cell toxicity compared to unlabeled rituximab.

#### **CHAPTER 4 Study on effect of $^{131}\text{I}$ -rituximab in combination with doxorubicin on Raji cells**

Doxorubicin is commonly used in the therapy of a wide range of cancers including leukemia and lymphoma (Tan et al. 1967). The associated side effects and drug-resistance to the therapeutic agent warrants developing combinatorial approach for cancer therapy. It was observed in the previous chapter that  $^{131}\text{I}$ -rituximab enhanced cell death when compared to rituximab. Thus it was envisaged that there could be a further increase in cell toxicity induced by  $^{131}\text{I}$ -rituximab when used in combination with doxorubicin, and hence, the study was carried out to determine the toxicity as well as to understand the underlying mechanism.

Efficacy of rituximab in combination with paclitaxel and other drugs is known (Jazirehi et al. 2003) but the effect of  $^{131}\text{I}$ -rituximab in combination with doxorubicin is not reported. In this experiment, Raji cells were treated with doxorubicin along with

<sup>131</sup>I-rituximab and induced cell death was studied and compared to both rituximab as well as doxorubicin treated cells. Further, the cell toxicity, apoptosis and MAPK signaling pathways were investigated after treatment of <sup>131</sup>I-rituximab in combination with doxorubicin in Raji cells. Raji cells were treated with doxorubicin (0.5, 1, 2 and 10 µg/ml) for 4 h, followed by 2 h incubation of 1.85 MBq of <sup>131</sup>I-rituximab. In all experiments, the cells were washed and incubated for 12 h. Cell viability was estimated by trypan blue dye, apoptotic cell death was assessed by estimation of DNA fragmentation and PARP proteins cleavage by ELISA method. Cell proliferation pathway was studied by measurement of expression of MAPK proteins by Western blotting.

A significant (p 0.05) increase in cell death was observed in Raji cells treated with <sup>131</sup>I-rituximab in combination with doxorubicin (2 µg/ml, ~ 74 %) compared to the corresponding individual control cells i.e. doxorubicin (2 µg/ml, 55 %), and <sup>131</sup>I-rituximab (22 %). Likewise increase in apoptosis was found in the combinatorial treatments. It was observed that expression of p44/42 and p38 were more in cells treated with <sup>131</sup>I-rituximab in combination with doxorubicin. However, strong phosphorylation of p38 was observed in <sup>131</sup>I-rituximab treated cells while phosphorylation of p38 was weak in cells treated with <sup>131</sup>I-rituximab in combination of doxorubicin. Similar pattern was observed in the phospho p44/42 proteins, which was in agreement to previous literature studied for only rituximab treatment (Pedersen et. al., 2002). The anti-apoptotic protein expression (bclxl) was downregulated and cleaved PARP was higher in the cells treated with <sup>131</sup>I-rituximab in combination with doxorubicin compared to the individual treatments.

From these studies, it can be concluded that the efficacy of <sup>131</sup>I-rituximab is enhanced in Raji cells when combined with doxorubicin.

**CHAPTER 5 Summary, conclusions and future directions****Major conclusions of the thesis**

1. Beta radiation emitted from radionuclides is more potent in induction of cell toxicity in tumor cells compared to the equivalent dose and very high dose rate of radiation.
2. *RAD51* and *P21* seem to have major role in discriminating the effect of beta and gamma radiation in tumor cells.
3.  $^{131}\text{I}$ -rituximab enhanced the killing in Raji cells compared to the unlabeled rituximab. This increase in Raji cell death/apoptosis corresponds to the amount of cellular internalization of the  $^{131}\text{I}$ -rituximab.
4. Combinatorial approach of doxorubicin and  $^{131}\text{I}$ -rituximab enhanced toxicity in Raji cell line compared to the individual controls, which involve regulation by *bclxl* and the MAPK signaling pathways.

**Future directions**

1. In future there is a need for detailed studies of the mechanism of DNA damage and repair kinetics of beta radiation and the equivalent dose of gamma radiation. The estimation of SSB and DSB of DNA damage by comet assay and expression of *RAD51* and *KU70/80* will confirm the molecular mechanism involved in the DNA damage repair.
2. To understand the effect of  $^{131}\text{I}$ -rituximab on cytotoxicity and underlying signaling pathways such as apoptosis and MAPK, there is a need to evaluate the efficacy in drug/radiation resistant cell lines.
3. To validate the effect of  $^{131}\text{I}$ -rituximab and its combination with doxorubicin in in-vivo mouse models.

**References**

- Anderson KC, Bates MP, Slau Steelghenhaupt BL, Pinkus GS, Schlossman SF, Nadler LM. Expression of human B cell -associated antigens on leukemia and lymphomas: a model of human B cell differentiation. *Blood* 1984; 63:1424.
- Boswell CA, Brechbiel MW. Development of radioimmunotherapeutic and diagnostic antibodies: an inside-out view. *Nucl Med Biol* 2007; 34:757-778.
- Boye J, Elter T, Engert A. An overview of the current clinical use of the anti CD20 monoclonal antibody Rituximab. *Ann Oncol* 2003; 14: 520-535.
- Bracey TS, Miller JC, Preece A, Paraskeva C. Gamma-radiation-induced apoptosis in human colorectal adenoma and carcinoma cell lines can occur in the absence of wild type p53. *Oncogene* 1995; 15:2391-2396.
- Ehrlich P. The collected papers of Paul Ehrlich, vol 3. London: Pergamon; 1960.
- Ekins RP, Slater JD. A method for the simultaneous estimation of total exchangeable sodium and potassium in man. *Phys Med Biol* 1960; 4:264-70.
- Finlay IG, Mason MD, Shelley M. Radioisotopes for the palliation of metastatic bone cancer: a systematic review. *Lancet Oncol* 2005; 6: 392-400.
- Fraker P, Speck J. Protein and cell membrane iodinations with a sparingly soluble chloroamide 1, 3, 4, 6-tetrachloro-3a, 6a-diphrenylglycoluril. *Biochem Biophys Res Commun* 1978; 80:849-857.
- Hertz S, Roberts A. Radioactive iodine as an indicator in thyroid physiology. *The Am J Physiol* 1940; 128: 565–576.

- Hicke BJ, Stephens AW, Gould T, Chang YF, Lynott CK, Heil J, et al. Tumor Targeting by an Aptamer. *J Nucl Med* 2006; 47: 668–678.
- Hoppmann S, Miao Z , Liu S , Liu H, Ren G, Bao A, Cheng Z. Radiolabeled Affibody-albumin bioconjugates for her2 positive cancer targeting. *Bioconjug Chem* 2011; 22(3): 413-421.
- Jamous M, Mier UHW. Synthesis of peptide radiopharmaceuticals for the therapy and diagnosis of tumor diseases. *Molecules* 2013; 18: 3379-3409.
- Jazirehi AR, Gan XH, De Vos S, Emmanouilides C, Bonavida B. Rituximab (anti-CD20) selectively modifies Bcl-xL and apoptosis protease activating factor-1 (Apaf-1) expression and sensitizes human non-Hodgkin's lymphoma B cell lines to paclitaxel-induced apoptosis. *Mol Cancer Ther* 2003; 2:1183-93.
- Khanna KK., and Jackson SP. DNA double strand breaks: signaling, repair and the cancer connection. *Nat Genet* 2001; 27: 247-254.
- Pedersen IM, Buhl AM, Klausen P, Geisler CH, Jurlander J. The chimeric anti-CD20 antibody Rituximab induces apoptosis in B-cell chronic lymphocytic leukemia cells through a p38 mitogen activated protein-kinase-dependent mechanism. *Blood* 2002; 99:1314-9.
- Steel GG, Deacon JM, Duchesne GM, Horwich A, Kelland LR, Peacock JH. The dose-rate effect in human tumor cells. *Radiother Oncol* 1987; 9: 299-310.
- Tan C, Tasaka H, Yu KP, Murphy ML, Karnofsky DA. Daunomycin, an antitumor antibiotic, in the treatment of neoplastic disease. Clinical evaluation with special reference to childhood leukemia. *Cancer* 1967, 20(3): 333–53.
- Yalow, RS, Berson, SA. Immunoassay of endogenous plasma insulin in man. *J Clin Invest* 1960; 39: 1157–75.



## **ABBREVIATIONS**

ADCC-Antibody Dependent Cell mediated Cytotoxicity

BGO-Bismuth Germanium Oxide

CD3- Cluster of Differentiation 3

CD20- Cluster of Differentiation 20

CDC-Complement Dependent Cytotoxicity

c-DNA-Complementary DeoxyriboNucleic Acid

CP30s-Counts Per 30 Seconds

CPM-Counts Per Minute

DMEM-Dulbecco's Modified Eagle's Media

DMF- Dimethyl Formamide

DNA- DeoxyriboNucleic Acid

DNase- DeoxyriboNuclease

dNTP-deoxy Nucleotide Tri Phosphate

DOTA-TOC- DOTA-octreotide

DOTA-TATE- DOTA-octreotate

EDTA-Ethylene Diamine Tetraacetic Acid

EF-Enrichment Factor

EGTA-Ethylene Glycol Tetraacetic Acid

ELISA-Enzyme Linked Immuno Sorbent Assay

Fab- Fragment of antibody binding

FCS-Fetal Calf Serum

FDA- Food & Drug Administration

FDG-Fluro deoxy Glucose

FITC- Fluorescein IsoThioCyanate

Gy- Gray

HAMA- Human Anti Mouse Antibody

HPLC-High Performance Liquid Chromatography

HRP-HorseRadish Peroxidase

IRMA- Immuno RadioMetric Assay

kDa- kilo Dalton

LDH-Lactate Dehydrogenase

LET-Linear Energy Transfer

MAbs-Monoclonal Antibodies

MBq-Mega Becquerel

MCF-7-Michigan Cancer Research Foundation -7

MeV-Million electron Volt

NaI(Tl)-Sodium Iodide (Thallium)

NHL-Non Hodgkin's Lymphoma

OD-Optical Density

PARP-Poly ADP Ribose Polymerase

PBS-Phosphate Buffer Saline

PCR-Polymerase Chain Reaction

PE- Paper Electrophoresis

PET- Positron Emission Tomography

PMSF- Phenyl Methyl Sulfonyl Fluoride

POD-Peroxidase

qPCR-Quantitative Polymerase Chain Reaction

RIA- Radio Immuno Assay

RNA-RiboNucleic Acid

RPMI 1640- Roswell Park Memorial Institute 1640

RT-PCR- Reverse Transcriptase Polymerase Chain Reaction

SDS-Sodium Dodecyl Sulphate

SPECT- Single Photon Emission Computed Tomography

SSTR-Somatostatin Receptor

TCA-Tri Chloro Aceticacid

## LIST OF FIGURES

S.No.	Figure No.	Figure Legends	Page No.
1.	1.1	Penetration range of alpha ( ), beta ( ) or gamma ( ) rays	4
2.	1.2	Types of fragmented antibody	15
3.	1.3	Nomenclature of antibody used in the therapy	16
4.	1.4	Mechanism of Doxorubicin binding with DNA	23
5.	2.1	Effect of different ionizing radiations on DNA damage	31
6.	2.2	Flow chart of experimental plan	36
7.	2.3a	Effect of number of washing on non specific cell bound activity of Na <sup>131</sup> I in Raji cells	40
8.	2.3b	Na <sup>131</sup> I radioactivity associated with Raji cells after 3 <sup>rd</sup> wash	41
9.	2.3c	Na <sup>131</sup> I radioactivity associated with U937 cells after 3 <sup>rd</sup> wash	42
10.	2.3d	Na <sup>131</sup> I radioactivity associated with MCF-7 cells after 3 <sup>rd</sup> wash	42
11.	2.3e	Na <sup>131</sup> I radioactivity associated with A431 cells	43

		after 3 <sup>rd</sup> wash	
12.	2.4	Estimation of cell toxicity in A431, MCF-7, U937 and Raji cell lines induced by NaI, Na <sup>131</sup> I and gamma radiation (0.4 Gy) by trypan blue dye uptake	44
13.	2.5	Estimation of DNA fragmentation in A431, MCF-7, U937 and Raji cell lines treated with NaI, Na <sup>131</sup> I and gamma radiation (0.4 Gy)	45
14.	2.6	Estimation of PARP cleavage in A431, MCF-7, U937 and Raji cell lines treated with NaI, Na <sup>131</sup> I and gamma radiation (0.4 Gy)	46
15.	2.7a	Expression of <i>BAX</i> gene in Raji cells at 30 and 240 min after irradiation	47
16.	2.7b	Expression of <i>P21</i> gene in Raji cells at 30 and 240 min after irradiation	48
17.	2.7c	Expression of <i>RAD51</i> gene in Raji cells at 30 and 240 min after irradiation	48
18.	2.8	Schematic representation of effect of high LET (Na <sup>131</sup> I) and low LET (γ-rays) radiation on Raji cells	53
19.	3.1	Mechanism of action of anti CD20 mAbs	56

20.	3.2	Flow chart of experimental plan	63
21.	3.3	Schematic representation of membrane stripping	65
22.	3.4a	Schematic representation of TCA precipitation	66
23.	3.4b	Schematic representation of paper electrophoresis	67
24.	3.5	Flow cytometric analysis of CD20 receptor in U937 and Raji cells	70
25.	3.6a	PD10 column elution profile of $^{131}\text{I}$ -rituximab	71
26.	3.6b	HPLC pattern of cold rituximab, $^{131}\text{I}$ , reaction mixture with free iodide and purified $^{131}\text{I}$ -rituximab	72
27.	3.7	Radioactivity counts in Raji cells incubated with $^{131}\text{I}$ -rituximab after four washes	73
28.	3.8	Radioactivity counts in Raji cells incubated with $^{131}\text{I}$ -rituximab with two amount of FCS	74
29.	3.9a	Percent cell binding in Raji and U937 cell lines	75
30.	3.9b	Percent inhibition of $^{131}\text{I}$ -rituximab in Raji cells after incubation of cold rituximab	76
31.	3.10a	Percent cell binding in Raji cells	77
32.	3.10b	Average radioactivity counts in per million Raji cells	77

33.	3.11a	Distribution of $^{131}\text{I}$ -rituximab on cell membrane and cytoplasm in Raji cells at different incubation period	78
34.	3.11b	Morphology of membrane stripped Raji cells	79
35.	3.12a	Distribution of $^{131}\text{I}$ -rituximab on cells and cell supernatant	80
36.	3.12b	Percentage of radioactivity count in TCA precipitate and supernatant	81
37.	3.12c	Percentage of radioactivity count in supernatant by paper electrophoresis	82
38.	3.13	Percentage of LDH release in supernatants after $^{131}\text{I}$ -rituximab treatment of Raji cells	83
39.	3.14	Apoptotic DNA enrichment in Raji cells upon exposure of $^{131}\text{I}$ -rituximab	84
40.	3.15	Expression of apoptosis related proteins upon exposure of $^{131}\text{I}$ -rituximab in Raji cell	85
41.	4.1	Flow chart of experimental plan	94
42.	4.2	Estimation of percent cell proliferation by MTT assay of Raji cells treated with doxorubicin for 6 h	97
43.	4.3	Estimation of cell death in Raji cells treated with	98



		doxorubicin in combination with $^{131}\text{I}$ -rituximab determined by trypan blue dye	
44.	4.4a	Estimation of apoptotic DNA fragmentation in Raji cells treated with doxorubicin in combination with $^{131}\text{I}$ -rituximab	99
45.	4.4b	Fold change in apoptotic DNA fragmentation of Raji cells as a ratio of enrichment factor	100
46.	4.5a	Estimation of PARP cleavage in Raji cells treated with doxorubicin in combination with $^{131}\text{I}$ -rituximab	101
47.	4.5b	Fold change in PARP cleavage of Raji cells as a ratio of enrichment factor	102
48.	4.6a	Expression of apoptotic proteins in Raji cells treated with doxorubicin in combination with $^{131}\text{I}$ -rituximab	103
49.	4.6b	Ratio of intensity of expression of apoptotic proteins by Western blotting with respect to the beta actin (loading control)	103
50.	4.6c	Expression of MAPK proteins in Raji cells treated with doxorubicin in combination with $^{131}\text{I}$ -rituximab	105

51.	4.6d	Ratio of intensity of expression of MAPK proteins by Western blotting with respect to the beta actin (loading control)	105
52.	4.7	Schematic diagram of signaling associated with $^{131}\text{I}$ -rituximab and combinatorial treatments	109
53.	5.1	Schematic of cell signaling pathways induced in Raji cells by $\gamma$ -rays, $^{131}\text{I}$ , rituximab, $^{131}\text{I}$ -rituximab and doxorubicin in combination with $^{131}\text{I}$ -rituximab	114

**LIST OF TABLES**

<b>S.No.</b>	<b>Table No.</b>	<b>Table Legends</b>	<b>Page No.</b>
1.	1.1	Radionuclides commonly used for therapy ( $\alpha$ / $\beta$ / Auger)	10
2.	1.2	Selected radiolabeled mAbs approved and currently undergoing clinical trials for the treatment of cancer	18

# CHAPTER 1

## INTRODUCTION

## 1.1 PREAMBLE

In the ancient scriptures of India dating back thousands of years, the words ‘Anu’ and ‘Paramanu’, which are the Sanskrit terms for the ‘smallest particle’ and ‘atom’ respectively have been mentioned. Ancient India sage “Kanad” coined the term “Anu” the smallest particle and ‘Paramanu’ is described in Brahma Samhita (written 5000 years before) Chapter 5 Verse 35 (Bhaktisiddhanta, 1932). This Sanskrit verse is as follows-

*eko 'py asau racayitum jagad-anda-kotim,yac chaktir asti jasad-anda-caya yad-antah*

*andantara-stha-paramanu-chayantara-stham,govindam adi-purusham tam aham bhajami.*

*(He is an undifferentiated entity as there is no distinction between potency and the possessor thereof. In His work of creation of millions of worlds, His potency remains inseparable. All the universes exist in Him and He is present in His fullness in every one of the atoms that are scattered throughout the universe, at one and the same time. Such is the primeval Lord whom I adore.)*

Later, Greeks predicted the existence of the atom around 500 BC. They named the predicted particle 'atomos' meaning "indivisible" and have taken credit to coin the term.

Centuries later, in 1803, John Dalton (1766-1844) introduced the term ‘atom’ which is accepted by the modern day scientists. But the area of atomic sciences remained under dark until the end of the nineteenth century, when a series of genius discoveries opened the avenue of nuclear science of the twentieth century.

## 1.2 HISTORY OF RADIATION AND RADIONUCLIDES

Wilhelm Conrad Roentgen’s "photograph of his wife's hand" (an image of her fingers’ bones including the wedding ring) was an epoch discovery, which opened the world of

unseen 'mysterious rays'. Roentgen's discovery of "mysterious rays", later known as X-rays, paved the path for a new avenue of application in health care namely, non-invasive imaging of internal organs of the body.

In March 1896, Antoine Henri Becquerel, while working with the phenomena of fluorescence and phosphorescence, made an accidental but remarkable discovery. He wrapped the photographic plates and put them away in a dark drawer along with some crystals containing uranium. Much to his surprise, the plates got exposed. Later it led to the conclusion that some kind of radiation was emanating from the crystals. Through the use of an electroscope, Becquerel had noted that uranium emanations could turn air into a conductor of electricity. But, Marie Curie (1898) reasoned that a very active but unknown substance must exist within the pitchblende. The extensive work of Marie Curie resulted in the identification and separation of two new elements from pitchblende, namely 'Polonium' (named in honor of Marie's native country Poland) and Radium (to mean 'Rays'). Curie, Pierre Curie and Becquerel won the prestigious Nobel Prize in 1903 in chemistry for the discovery of phenomenon of radioactivity and new radioactive elements.

Ernest Rutherford's (1911) experimentation wherein, he bombarded thin gold foils with the positively charged  $\alpha$ -particles and concluded that in an atom there would be a lot of empty space, so that all the particles passed through the foil undisturbed. A very small number of  $\alpha$ -particles "bounced back" almost at  $180^\circ$ , which showed that the atom must be made of a heavy central positive nucleus.

In 1934, the artificial production of radioactivity was reported by Irene-Joliot-Curie and Frederick Joliot, which won them the Nobel Prize in 1935. However, artificial

production of radioisotopes initiated by bombarding with alpha particles and later with neutrons resulted in production of many radioisotopes. The pioneering work of George Hevesy (1943) opens an avenue for radiotracer applications in industry and biology. The work of Becquerel, the Curies, Rutherford, Hevesy and others, made modern medical and scientific research more than a dream with many applications of radioisotopes in science, industry and healthcare.

The radioactive isotopes of an element are generally unstable in nuclear configurations, which attain stability by re-configuring the nucleus. During this process energetic radiations such as alpha (  $\alpha$  ), beta (  $\beta$  ) or gamma (  $\gamma$  ) rays are emitted resulting in an isotope of a different element. The penetration ranges of these radiations are depicted in Fig. 1.1.

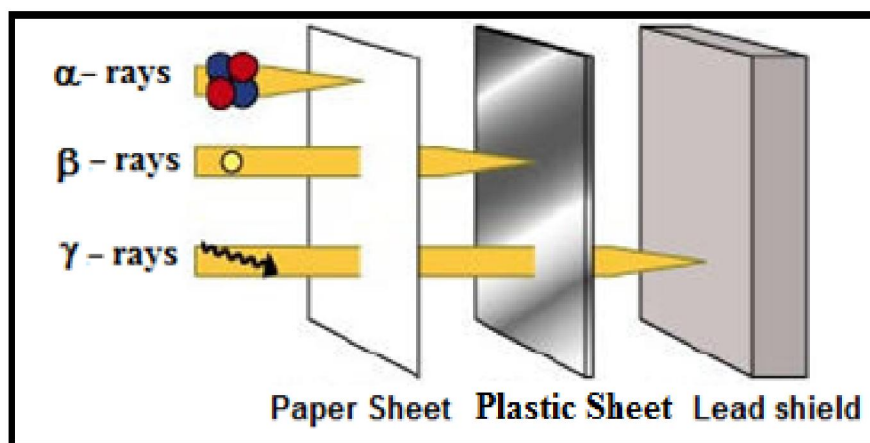


**Figure 1.1** Penetration range of alpha (  $\alpha$  ), beta (  $\beta$  ) or gamma (  $\gamma$  ) rays

### 1.3 PRODUCTION OF RADIOISOTOPES

Most of the radioisotopes used in medicine, biology, industry and other applications are artificially produced. The stable nuclides can be transformed into the radioactive isotopes of the same or different element through nuclear reactions. This nuclear reaction can be

achieved by bombarding the target nuclide with a projectile either a neutron or a charged particle (such as proton, deuteron, etc.). The major facilities for producing artificial radioisotopes are nuclear reactors and charged particle accelerators (cyclotrons). Although, cyclotron was the first route for production of radioisotope, most of the radioisotopes used in different applications are currently being produced in the nuclear reactors. The reactors offer the large volume irradiation and thus enabling economically viable production of various radionuclides.

In nuclear reactor, radioisotopes are produced by exposing target materials to the neutron flux for an appropriate period of time. Radioisotopes are produced in the reactor through different routes such as  $(n, \gamma)$ ,  $(n, \beta^-)$ ,  $(n, p)$ ,  $(n, \alpha)$  and  $(n, f)$ , which are generally neutron rich and mostly decay by beta emission and at times associated with gamma emission. The rates of production of radionuclides are determined by the neutron flux, abundance of the target nuclide and the activation cross-section for the desired reaction.

In accelerators, energetic charged particles such as proton (p), deuteron (d), alpha ( $\alpha$ ),  $^3\text{He}^{2+}$  etc are used as projectiles to bombard the target nuclides. Resulting radionuclides are rich in positive charge (neutron deficient) and most often decay through positron emission ( $\beta^+$ ) or electron capture. The need for high current and the sophisticated technology of accelerator, makes cyclotron produced radioisotopes more expensive than the reactor produced radioisotopes.

#### 1.4 APPLICATION OF RADIONUCLIDES IN HEALTHCARE

Application of radioisotopes in health care began with therapy using  $^{131}\text{I}$  (Hertz et al. 1940). But, over the past several decades, different radioisotopes have been used both for diagnostic as well as therapeutic purposes. Brief descriptions of these are given below.



**1.4.1 In-vitro use of radionuclides: competitive radioligand assay**

The major in-vitro uses of radionuclides in health care are as radiotracer applications, such as RIA and IRMA. These techniques are used to quantitatively estimate hormones, cancer related antigens, secretory proteins, toxins, drugs etc. in biological samples such as blood, urine etc. RIA also called as competitive radioligand assay, is a very sensitive and specific technique developed by Rosalyn Yalow and Solomon Aaron Berson (Yalow et al. 1960). Around the same period Ekins and Slater (Ekins et al. 1960) also described the method of estimation of total exchangeable sodium and potassium in human. In this method, radioisotope ( $^{131}\text{I}$ ,  $^{125}\text{I}$ , tritium etc.) labeled molecules are used as tracer to estimate analytes/metabolites in blood and other body fluids. IRMA is an extension of RIA with higher sensitivity as well as specificity, due to the use of a pair of specific antibodies. Despite the high sensitivity and specificity, these assays are very simple, easy to perform and inexpensive.

**1.4.2 In-vivo use of radionuclides: diagnosis, therapy and bone pain palliation**

The use of radioactive preparations, either orally or as an injectable product has been established since more than seven decades. This field is known as nuclear medicine where radionuclides are widely used for the diagnosis as well as treatment of joint pain, bone pain and various cancers. The radioactive preparations (drugs and specific molecules tagged with radionuclide) used in nuclear medicine are known as radiopharmaceuticals. These are akin to pharmaceuticals as they are internally administered in the patients. However, there are differences compared to the regular pharmaceuticals due to their short shelf lives. In the case of therapy, the efficacy is reliant on both chemical as well as physical nature of the radiopharmaceuticals. In the past, the

carrier molecules were chosen based on the specificity and bio-chemical behavior so that it can localize in the desired target lesion/organ. Some examples of this approach are antibodies and peptides for targeting antigen or receptor on diseased tissue, colloids and lipophilic molecules for imaging liver and hydrophilic molecules for imaging kidney functions. Hence, the carrier molecules should be chosen with great care for quick localization at the target sites and amenable to radiolabeling for stable (kinetic and thermodynamic) preparations. However, the physical half-life of the radioisotope is a critical parameter to be considered in the design of a radiopharmaceutical. In-vivo diagnostics, therapeutic and bone pain palliation applications of radiopharmaceuticals are described as below.

#### 1.4.2.1 Diagnostic radiopharmaceuticals

Radionuclides that emit electromagnetic radiations such as  $\gamma$  or X-rays, deposit their energy over a long range, have comparatively shorter half life and do not emit particulate radiations are suitable for diagnostic applications. The invention of gamma camera by Anger in 1957 was an important milestone that accelerated the growth of diagnostic nuclear medicine. The gamma cameras that are capable of reconstructing 3-D images from acquired data of attenuated single energy photons are called SPECT. Several radionuclides such as  $^{99m}\text{Tc}$ ,  $^{67}\text{Ga}$ ,  $^{81m}\text{Kr}$ ,  $^{82}\text{Rb}$ ,  $^{111}\text{In}$ ,  $^{123}\text{I}$ ,  $^{133}\text{Xe}$  and  $^{201}\text{Tl}$  that emit gamma rays with single energy are suitable for SPECT imaging. However, the commercial availability of  $^{99}\text{Mo}$ - $^{99m}\text{Tc}$  generators and a variety of kits for preparation of  $^{99m}\text{Tc}$ -radiopharmaceuticals to image several organs of the body, made  $^{99m}\text{Tc}$  the “work-horse” of diagnostic nuclear medicine. The use of  $^{99m}\text{Tc}$  continues to this day, although the use of positron emitters, especially Fluorine-18, has increased enormously in the past

10-15 years. The positrons when emitted, immediately combine with electrons and annihilate each other resulting in the emission of two 511 keV photons in opposite (at 180° apart) directions. The two photons akin to gamma rays emitted simultaneously in opposite directions are recorded in a co-incidence manner to construct very good quality image with high resolution. Such imaging is known as PET, which also gives a 3-dimensional image even more resolved than SPECT. Although the concept of PET imaging existed since the 1950's, positron imaging made an entry into the clinics in the 1970's with the synthesis of  $^{18}\text{F}$ -FDG at the Brookhaven National Laboratory, USA. PET imaging advanced with the development of BGO scintillation detectors in a circular array with coincidence circuits designed to specifically detect the 511 keV photons emitted in opposite directions along with proper computations. There are two kinds of diagnostic imaging that can be possible with PET and SPECT. (a) Static imaging for obtaining anatomy/ morphology of tissues/organs and (b) dynamic imaging for detecting functions of tissues/organs. Diagnostic radiopharmaceuticals are used in very low concentrations ( $10^{-6}$ - $10^{-8}$  M), to image the morphology as well as the functions of the organs and are not intended to have any pharmacological effects.

#### 1.4.2.2 Therapeutic Radiopharmaceuticals

Therapeutic radiopharmaceuticals are molecules designed to deliver therapeutic doses of ionizing radiation to the diseased sites. The success of therapy depends on deposition of high concentration of radionuclide in diseased target site over an adequate time span to cause complete destruction of the cancerous cells. The effective range and LET of radionuclides depend on the type of the particle as well as the energy. The size of the tumor, intra-tumoral distribution of the radiopharmaceutical, pharmacokinetics of the

tracer are the major factors that would influence the type of radionuclide desirable for effective therapy. Although, particulate emissions are responsible for therapeutic efficacy, concomitant emission of (a small percentage) gamma rays with energy in the diagnostically useful range are useful in imaging/localization/dosimetry of the therapeutic radiopharmaceutical in patients. Radioisotopes which emit particulate radiations viz.  $\alpha$  or  $\beta$  or auger electron, and deposit their energy within a small range are suitable for therapeutic applications. They are also categorized based on the chemical nature, namely (i) simple chemical form (e.g. Iodine-131 as iodide for thyroid imaging and treatment of thyroid cancers; Strontium-89 chloride and  $^{32}\text{P}$ -sodium orthophosphate for skeletal pain palliation), (ii) labeled molecule, when a carrier molecule is radiolabeled and are target specific (e.g. antibodies, peptides or small targeting molecules etc. used in treatment of several cancers). Some radiolabeled molecule localizes owing to the size {(e.g.  $^{90}\text{Y}$ - glass microsphere of 20–30  $\mu\text{m}$  and  $^{90}\text{Y}$ - resin microsphere of 20–40  $\mu\text{m}$  in size, obtained US, FDA approval in year 2002 and 2000 respectively)} and used for the therapy of hepatic cancer. Table 1.1 enlists commonly used beta emitting therapeutic radionuclides in healthcare.

#### 1.4.2.3 Radiopharmaceuticals for bone pain palliation

Many malignant tumors especially prostate, breast and lung cancers in advanced stages get metastasized in bone. Bone metastasis is very painful and usually treated with analgesics drugs and radiolabeled phosphonates. Initially inorganic phosphate ( $^{32}\text{P}$ ) and  $^{89}\text{SrCl}_2$  were used in bone pain management, which mimics calcium and localizes in bone. However, it delivers ablation dose to bone marrow and causes hematological toxicity. Better agents are still being explored, that can selectively deliver effective dose

to skeletal lesions and minimize bone marrow suppression. In this effort combination of different radionuclides and carriers are reported, which include  $^{186}\text{Re}$ -HEDP (hydroxyl ethylene diphosphonate),  $^{153}\text{Sm}$ -EDTMP (ethylenediamine tetramethylene phosphonic acid),  $^{117\text{m}}\text{Sn}$ -DTPA (diethylene triaminepenta acetic acid) (Finlay et al. 2005 & Lewington 2005).  $^{153}\text{Sm}$ -EDTMP is a FDA approved bone pain palliative agent that is routinely used world over.

The average clinical response time for radiopharmaceuticals based on bone pain palliation is normally between 7 and 14 days, however, effectiveness may be seen as late as 4 weeks after treatment.

**Table 1.1** Beta emitting radionuclides commonly used for therapy

S. No.	Radionuclides	$t_{1/2}$ (h)	Diagnosis ( / +)	Therapy ( / /Auger)	Avg Range (mm)	E (avg) (keV)	E (keV)	Production
1.	$^{166}\text{Ho}$	26.8		- EC	2.43 <0.02	665.7	80.6 1379.4	$^{166}\text{Dy}/^{166}\text{Ho}$ generator
2.	$^{124}\text{I}$	100.22	+	+ EC	3.25 <0.02	830.5	602.7	$^{124}\text{Te}(p, n)^{124}\text{I}$
3.	$^{125}\text{I}$	1443.4		EC	<0.02	-	35.49	$^{124}\text{Xe}(n, \gamma)^{125}\text{Xe}/^{125}\text{I}$
4.	$^{131}\text{I}$	192.96		-	0.36	181.7	364.5	$^{131}\text{Te}(n, \gamma)^{131}\text{I}$
5.	$^{177}\text{Lu}$	161.04		- EC	0.22 <0.02	133	208.4 113.0	$^{176}\text{Lu}(n, \gamma)^{177}\text{Lu}$
6.	$^{188}\text{Re}$	16.98		- EC	2.91 <0.02	764.2	155 633.1	$^{185}\text{W}/^{188}\text{Re}$ generator $^{187}\text{Re}(n, \gamma)^{188}\text{Re}$
7.	$^{153}\text{Sm}$	46.27		-	0.5	223.6	103.2	$^{152}\text{Sm}(n, \gamma)^{153}\text{Sm}$
8.	$^{90}\text{Y}$	64.08	-	-	3.78	934.8	-	$^{90}\text{Sr}/^{90}\text{Y}$ generator
9.	$^{32}\text{P}$	342.72	-	-	2.3	694.7	-	$^{31}\text{P}(n, \gamma)^{32}\text{P}$ $^{32}\text{S}(n, p)^{32}\text{P}$
10.	$^{89}\text{Sr}$	29128.32	-	-	-	1491	-	$^{235}\text{U}(n, f)^{89}\text{Sr}$

## **1.5 CANCER AND THERAPEUTIC MODALITIES**

### **1.5.1 Cancer**

Cancer is medically known as a group of diseases of unregulated cell growths which are clinically benign and metastatic in nature. Benign tumors do not invade neighboring tissues while malignant tumors do invade nearby tissues and spread throughout the body via lymphatic system and/or bloodstream. There are over 200 different known cancers that affect human life. The causes of cancer are diverse, complex and only partially understood. However, the risk of cancer increases, due to many factors including tobacco use, dietary factors, infections, exposure to radiation, lack of physical activity, obesity and environmental pollutants.

#### **Classification of cancer**

Cancers are classified in various ways but one of the most acceptable and commonly used nomenclatures are based on the origin of the tumor. These types are as follows

- 1. Carcinoma:** These cancers are derived from epithelial cells which includes cancer of breast, prostate, lung, pancreas, and colon.
- 2. Sarcoma:** Sarcoma is a cancer of connective tissue origin i.e. bone, cartilage, fat and nerve, which develop from cells originating in mesenchymal cells outside the bone marrow.
- 3. Lymphoma and leukemia:** This class of cancer arises from hematopoietic (blood-forming) cells.
- 4. Germ cell tumor:** These cancers are derived from pluripotent cells of the testicle and ovary.

**5. Blastoma:** Such cancers derived from immature "precursor" cells or embryonic tissue and more common in children.

Cancers are generally named using -carcinoma, -sarcoma or -blastoma as a suffix while benign tumors are named using -omas a suffix, with the tissue of origin as the root. For example cancers of the liver parenchyma arising from epithelial cells is called hepatocarcinoma, while benign tumor of smooth muscle cells is called a leiomyoma. However, some types of cancer use the -noma suffix, examples including melanoma and seminoma.

### 1.5.2 Non- Hodgkin's lymphoma (NHL)

NHL is a clinically heterogeneous group of hematological malignancies arising from B, T or NK-lymphoid cells. It differs from the Hodgkin's lymphoma due to the absence of multinucleated Reed–Sternberg cells. It is eleventh most common cause of cancer incidence (Balkrishna 2008) and ranks 5<sup>th</sup> in cancer mortality (Bonavida 2007). For clinical purpose, NHL has been classified into three categories viz. low, intermediate and high grade malignancies. More than 90 % of NHL originates from the B-cells only. Most of human B-cell-lineage malignancies express a large number of CD20 (33-37 kDa) proteins (Anderson *et al.* 1984, Nadler *et al.* 1981, Beers *et al.* 2010). Hence, CD20 is considered to be an attractive and one of the possible targets for the treatment of NHL (Multani *et al.* 1998, Kunala *et al.* 2001). CD20 is a glycosylated phosphoprotein expressed on the surface of B-cells, encoded by the *MS4A1* gene in human. CD20 has no known natural ligand however, it helps in optimal T cell- independent antibody response and calcium channel in the cell membrane (Cragg *et al.* 2005, Kuijpers *et al.* 2010).

### **1.5.3 Therapeutic modalities of cancer**

There are various therapeutic modalities available for cancer which are employed alone or in combination depending on the type, location and grade of the cancer. These are summarized as below.

#### **1.5.3.1 Surgery**

Surgery is the primary modality of treatment of most solid cancers, aimed to remove entire cancerous tissue. It is typically prescribed after the definitive diagnosis and tumor biopsies.

#### **1.5.3.2 External beam radiotherapy**

Radiation is one of the modalities for treatment of cancers due to its ability to control cancer growth by damaging the DNA and thus leading to cell death. The biological effect is caused by direct and indirect effect of ionization radiation. Cancer cells are generally less differentiated and divide faster in an uncontrolled way than the normal cells. They have a diminished ability to repair sub-lethal damage due to which they are more susceptible to radiation damage. External beam radiotherapy is the medical use of ionizing radiation, using  $^{60}\text{Co}$  or  $^{137}\text{Cs}$  radionuclides as a radiation source to treat cancerous growth (Steel et al.1987, Bracey et al. 1995). It has evolved over the past decades to sophistication where very precise dose of radiation can be delivered to the tumor volume, with minimal damage to the surrounding healthy tissues. In cancer therapy ‘gamma knife’ are also used in which several beams of gamma rays are focused on the tumor tissue from different angles, so that the tumor receives the maximum dose.



**1.5.3.3 Brachytherapy**

Brachytherapy means ‘therapy in contact or close proximity’. In brachytherapy, the radiation source in the form of wire or beads or a mould is placed in contact with the tumor either interstitially (breast and prostate cancers) or as intracavitary (uterine cancers) or as a covering mould (Gerbaulet et al. 2005). Since radiation sources are precisely placed at the site of the cancerous tissues, it delivers high doses of localized radiation and concurrently reduces the probability of unnecessary damage to surrounding healthy tissues (Gerbaulet et al. 2005, Stewart et al. 2007). Traditionally, brachytherapy is to administer using high energy gamma emitters such as Gold-198, Iridium-92, Cesium-137 or Cobalt-60, which are metallic and can be prepared in the form of wires or seeds. The use of Iodine-125 in the form of immobilized rice sized capsules for treating certain types of ocular carcinomas and prostate cancers have been well established. In the recent past, customized patches embedded with high energy beta particles (such as Phosphorus-32) has been shown to be very effective in treating skin cancers especially basal cell carcinoma. This modality is ideal for patients with skin cancers that are difficult to operate at multiple lesions.

**1.5.3.4 Immunotherapy**

Immunotherapy is another mode of therapy where antibodies are used for the cancer therapy. The history of immunotherapy started after the invention of ‘hybridoma’ technology to produce ‘monoclonal’ antibodies (Kohler et al 1975). OKT3 was the first therapeutic murine monoclonal antibody against anti-CD3 used for treatment in 1986. However, OKT3 induced severe HAMA response in patients. To reduce the immunogenicity of murine antibodies in humans, chimeric antibodies with mouse

variable regions and human constant regions were constructed by genetic engineering (Morrison *et al.* 1984). In 1994, Reo Pro, a chimeric Fab, was introduced as the second therapeutic antibody. Since then, several chimeric antibodies have been clinically used. Although chimeric antibodies were less immunogenic than murine MAbs, human anti-chimeric antibody responses have been also observed. To further minimize the mouse component of antibodies, humanized antibodies were constructed by protein engineering (Jones *et al.* 1996, Dall'Acqua *et al.* 2005). Zenapax is the first humanized antibody that was marketed in 1997 (Tsurushita *et al.* 2005).

One major disadvantage with the antibodies for therapy is the large size (MW 150000 Da), owing to which it takes a long time to reach and accumulate in the target tissues. Efforts have been made to reduce the size by using antibody fragments containing the Fab region alone, but the success of using such fragments is yet to be realized in a big way. Fig. 1.2 and 1.3 describes different types of antibodies and nomenclature of antibodies used in the therapy.

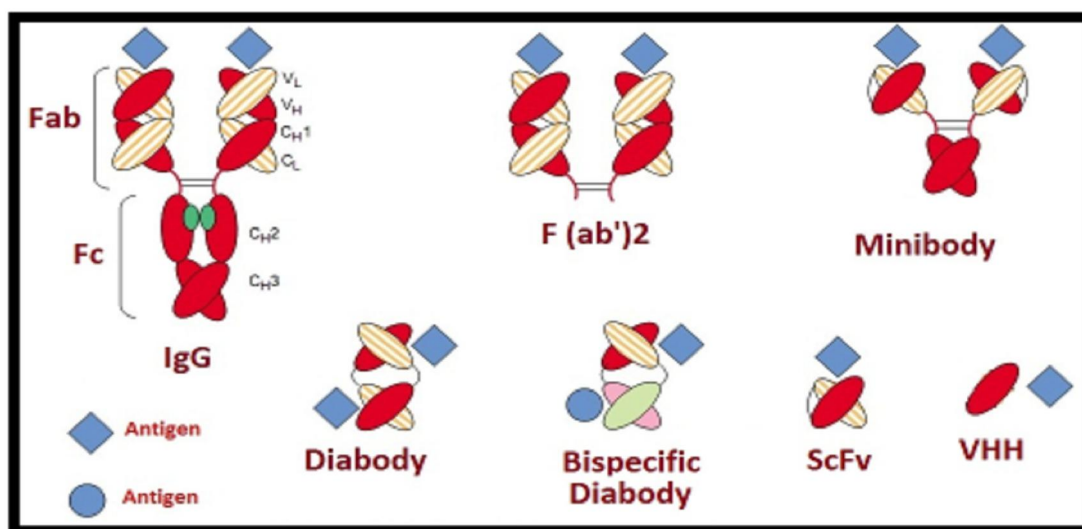
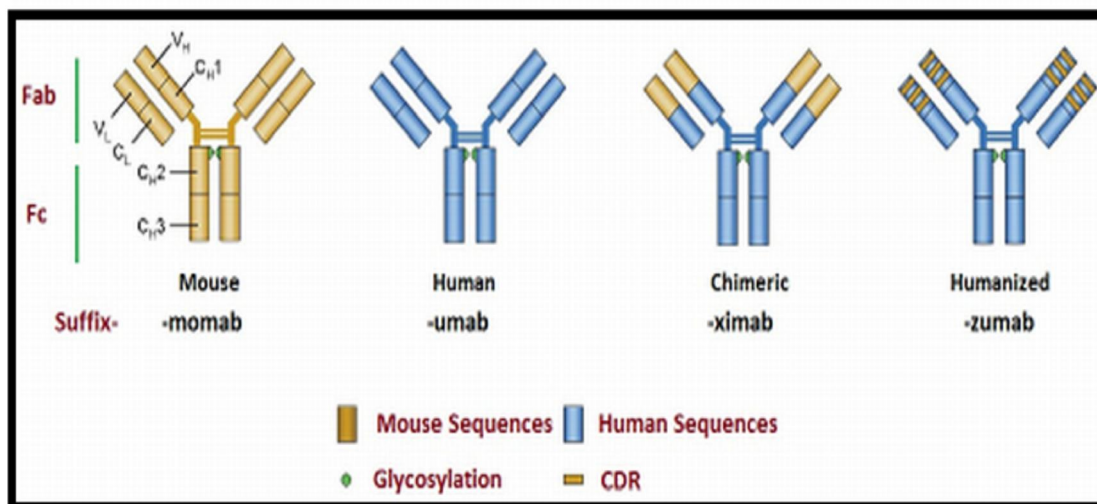


Figure 1.2 Types of fragmented antibody (Adapted from Presta, 2003)



**Figure 1.3** Nomenclature of antibody used in the therapy (Adapted from Kim et al. 2005)

#### 1.5.3.5 Radionuclide therapy (RNT)

RNT is one of the rapidly growing areas of nuclear medicine, which deals with the therapeutic radiopharmaceuticals. In RNT, specific biomolecules which target the diseased tissues act as cargo for loading of therapeutic radionuclides and delivering cytotoxic dose of radiation emitted from same at diseased site. RNT target diseases at the molecular level and affecting the gross diseased tissue. Mechanism of tumor targeting varied depending on the localization of unique antigen of tumor cells. These unique tumor antigens are either localized on cell membrane or inside the cell (cytoplasm based). Depending on their locations therapeutic effectiveness may be varied. Radiopharmaceuticals targeted to DNA are most potent and effective for therapy (Neshasteh-Riz et al. 1998, Morgenroth et al. 2011, Urashima et al. 2006).

##### 1.5.3.5.1 Radioimmunotherapy (RIT)

The strategy to use antibody for the targeted delivery of radionuclide enhances the therapeutic efficacy of the antibody. RIT came in realization after five years of the

invention of hybridoma technology. The first antibody was labeled with iodine -131 (DeNardo et al. 1980 & 1981). Later Carrasquillo et al. 1984, used the fragmented radiolabeled antibody for diagnosis and therapy of solid tumor. Antibodies have been used as targeted therapeutic agents to deliver adequate radiation dose to the targeted site when labeled with suitable radionuclides. In the past two decades antibodies which bind to cancer cell surface antigens/ receptors, have been extensively explored for the use as carrier molecules in targeted radiotherapy. This is primarily based on the promising results seen in therapy of several cancers with the monoclonal antibodies (e.g. Ibritumomab, tositumomab cetuximab etc.). These antibodies are radiolabeled and used for effective cancer therapy. Hence, radiolabeled antibodies emerge from “magic bullets” (Ehrlich 1960) to the “radioactive magic bullet” (Chamarthy et al. 2011) for the cancer therapy. FDA approved two radiolabeled anti CD20 mAbs [ $^{90}\text{Y}$ -labeled ibritumomab tiuxetan (Zevalin) in 2002 and  $^{131}\text{I}$ -labeled Bexxar in 2003] for the treatment of NHL, which was a landmark in the history of therapeutic radiolabeled mAbs development (Sharkey *et al.* 2005, Chinn *et al.* 1999). Radionuclides coupled to antibodies (Goldenberg 2003, Milenic *et al.* 2004, Govindan *et al.* 2005, Ng 2006, Pohlman et al. 2006, Boswell *et al.* 2007) are undergoing clinical trials for different cancers. The physical half-life of the radionuclide must be long enough so that a considerable fraction of the radiation dose can be delivered after tumor localization. Generally 24 to 48 hours are required for radiolabeled antibody for maximum uptake in targeted site. Some of the FDA approved radiolabeled antibodies and ongoing clinical trials are enlisted in Table 1.2.

**Table1.2** Selected radiolabeled mAbs, approved and currently undergoing clinical trials for the treatment of cancer (Adapted from, Milenic *et al.* 2004, Wilkins *et al.* 2006, Boswell *et al.* 2007, www.ClinicalTrials.gov).

S.No.	Sponsor/Institutes	Agent	Cancer indication	Approved/ Phase
1.	GlaxoSmithKline	<sup>131</sup> I-Tositumomab vs. ibritumomab tiuxetan	NHL	2003
2.	Biogen IDEC	<sup>90</sup> Y-Ibritumomab Tiuxetan Zevalin	NHL	2002
3.	Jonsson Comprehensive Cancer Center/NCI	<sup>90</sup> Y-HMFG1 (monoclonal antibody)	Ovarian Cancer, Primary Peritoneal Cavity Cancer	III
4.	Memorial Sloan-Kettering Cancer Center/NC	<sup>213</sup> Bi-M195 (humanized anti-CD33 mAb)	Advanced myeloid cancer	II
5.	Fred Hutchinson Cancer Research Center	<sup>131</sup> I-BC8 (mAb)	AML or Myelodysplastic syndromes	II
6.	Duke University/NCI	<sup>211</sup> At-81C6 (anti-tenascin chimeric mAb)	Primary/metastatic brain tumor	II
7.	Weill Medical College of Cornell/Columbia Univ.	<sup>177</sup> Lu-J591	Prostate cancer	II
8.	Immunomedics, Inc.	<sup>90</sup> Y-hLL2 (Epratuzumab)	NHL	II
9.	Nantes University Hospital, France	<sup>131</sup> I -bispecific antibody	Medullary Thyroid Neoplasms	II
10.	Glaxo Smith Kline	Tositumomab + <sup>131</sup> I- Tositumomab	Lymphoma, Non-Hodgkin	II
11.	Korea Cancer Center Hospital	<sup>131</sup> I-rituximab	Relapsed or Refractory Follicular Lymphoma or Mantle Cell Lymphoma	II
12.	Fred Hutchinson Cancer Research Center/University of Washington Cancer Consortium	<sup>131</sup> I-BC8 & DRUGS	AML	II

S.No.	Sponsor/Institutes	Agent	Cancer indication	Phase
13.	Philogen S.p.A. Italy/UK	$^{131}\text{I}$ -L19SIP &WBRT	Brain metastases	II
14.	Philogen S.p.A. Italy	$^{131}\text{I}$ -F16SIP	Tumor blood vessel	I/II
15.	Garden State Cancer Center at the Center for Molecular Medicine and Immunology/NCI	$^{111}\text{In}$ -hLL2 IgG/ $^{90}\text{Y}$ -epratuzumab	Leukemia & Lymphoma	I/II
16.	Immunomedics, Inc.	$^{90}\text{Y}$ -hMN14 (labetuzumab)	Pancreatic neoplasms	I/II
17.	National Cancer Institute (NCI)	$^{90}\text{Y}$ -Daclizumab (ANTI cd25) +drugs	Hodgkin disease & Hodgkin lymphoma	I/II
18.	Immunomedics, Inc.	$^{90}\text{Y}$ -PAM 4	Pancreatic cancer	I
19.	Ludwig Institute for Cancer Research	$^{131}\text{I}$ - A33 and capecitabine	Metastatic colorectal carcinoma	I
20.	NCI	$^{131}\text{I}$ -TNT-1/B	Glioblastoma	I
21.	Memorial Sloan Kettering Cancer Center/NCI	$^{131}\text{I}$ -8H9	CNS or leptomeningeal cancer	I
22.	Radbound University	IMP-288 labeled with $^{111}\text{In}$ and $^{177}\text{Lu}$	Colorectal neoplasms	I
23.	Memorial Sloan-Kettering Cancer Center/NCI	$^{131}\text{I}$ -8H9 (mAbs)	Brain and CNS tumors	I
24.	Memorial Sloan-Kettering Cancer Center/NCI	$^{131}\text{I}$ -3F8 (mAbs)	Neuroblastoma	I
25.	University of California, Davis/NCI	$^{111}\text{In}$ - Lym-1/ $^{90}\text{Y}$ - Lym-1	Lymphoma	I
26.	Radbound University	IMP-288 labeled with $^{111}\text{In}$ and $^{177}\text{Lu}$ & DRUG	Colorectal neoplasms	I
27.	Memorial Sloan-Kettering Cancer Center	$^{131}\text{I}$ -8H9/ $^{124}\text{I}$ -8H9	Peritoneal cancer	I
28.	Areva Med LLC	$^{212}\text{Pb}$ -TCMC-Trastuzumab	Breast, Peritoneal, Ovarian, Pancreatic & Stomach Neoplasms	I
29.	Centre René Gauducheau	$^{131}\text{I}$ -BB4 antibody	Multiple myeloma	I

#### 1.5.3.5.2 Peptide receptor radionuclide therapy (PRRT)

There are various receptors on cells whose natural ligands are peptides. Derivatives of these peptides may contain 3- 25 amino acids and possess high affinity for their receptors. Some of the receptors are over expressed in certain human cancers, offering the possibility to target these tumors with radiolabeled peptides. This is primarily based on the promising results seen in therapy of several cancers with the unlabeled peptides e.g. Octreotide in somatostatin receptor expressing neuroendocrine cancers. Neuroendocrine tumors including primary and metastases overexpress somatostatin receptors (sst1-sst5). The somatostatin analog DOTA-TOC, DOTA-NOC and DOTA-TATE labeled with radionuclides such as  $^{177}\text{Lu}$  and  $^{90}\text{Y}$  are currently under clinical trials. Several small radiolabeled peptide ligands (such as cyclic RGD, somatostatin, bombesin and neurotensin) are also in clinical trials for cancer therapy (Fani *et al.* 2012, Okarvi 2008, Jamous *et al.* 2013, Liu, 2009).

#### 1.5.3.6 Chemotherapy

Chemotherapy is another modality of cancer treatment using individual or combinations of drugs. These drugs have different mode of action and accordingly classified as

- 1. Alkylating agents-** Alkylating agents have the ability to alkylate proteins, RNA and DNA. This drug can form intrastrand or interstrand crosslink to the DNA strand following DNA damage during replication. This may leads to cell death or apoptosis. Alkylating agents will work at any phase of the cell cycle. Cisplatin, cyclophosphamide, carboplatin and oxaliplatin are common alkylating agents used for the cancer chemotherapy.
- 2. Anti-metabolites-** Antimetabolites are class of drugs that interfere with DNA and

RNA growth by substituting for the normal building blocks of RNA and DNA. These agents damage cells during the S phase of cell cycle. Commonly used anti-metabolites for cancer chemotherapy are anti-folates (methotrexate and pemetrexed), deoxynucleoside analogues (gemcitabine, decitabine, pentostatin etc.).

3. **Mitotic Inhibitor-** Mitotic inhibitor are microtubule inhibiting agents which block cell division by preventing microtubule function thus, preventing the cancer cells to completing the cell division (mitosis). They can stop mitosis or inhibit enzymes for making proteins needed for cell reproduction. These drugs work during the M phase of the cell cycle but can damage cells in all phases. Taxol, vincristine, vinblastine, vinorelbine, vindesine, paclitaxel etc. are commonly used mitotic inhibitors for the cancer chemotherapy.
4. **Topoisomerase inhibitors-** These drugs interfere with enzymes called topoisomerases, which help to separate the strands of DNA during replication. Topotecan and irinotecan (CPT-11) inhibit topoisomerase-I while, etoposide (VP-16) and teniposide inhibit topoisomerase-II. These drugs bind to their respective topoisomerase and resulted in DNA strand break during replication followed by cell death.
5. **Cytotoxic antibiotics or Anti-tumor antibiotics-** The cytotoxic antibiotics are varied group of drugs that have various mechanisms of action. The group includes- (a) **Anthracyclines-** Anthracyclines are anti-tumor antibiotics that interfere with enzymes involved in DNA replication. These drugs work in all phases of the cell cycle. Examples of anthracyclines include daunorubicin, doxorubicin, epirubicin, idarubicin etc. (b) **Other anti-tumor antibiotics** that are not anthracyclines include



actinomycin-D, bleomycin, mitomycin-C etc.

6. **Corticosteroids-** Steroids are natural hormones and hormone-like drugs that are useful in treating certain types of cancer (lymphoma, leukemia, and multiple myeloma), as well as other illnesses. These drugs are used to kill cancer cells or to slow their growth hence, considered as chemotherapy drugs. Prednisone, methylprednisolone (Solumedrol®), and dexamethasone (Decadron®) are commonly used corticosteroids used for cancer therapy.
7. **Miscellaneous chemotherapy drugs-** Some chemotherapy drugs act in slightly different ways and do not fit well into any of the other categories. L-asparaginase, which is an enzyme, and the proteasome inhibitor bortezomib.

Amongst the cytotoxic antibiotics or anti-tumor antibiotics doxorubicin is the oldest known since 1967. Doxorubicin (trade name Doxil; also known as hydroxy daunorubicin) is an anthracycline antibiotic closely related to the natural product daunomycin. It is commonly used in the treatment of a wide range of cancers, including hematological malignancies, many types of carcinoma and soft tissue sarcomas. The drug is administered intravenously as the hydrochloride salt and sold under different brand names Adriamycin PFS, Adriamycin RDF, or Rubex. Doxorubicin has exhibited high therapeutic efficacy against mouse and human tumors and also known to cause cardiotoxicity (Di Marco *et al.* 1969, Zhang *et al.* 2012). Till date, there are over 2,000 known analogs of doxorubicin and more than 500 of them had been evaluated in the screening program at the National Cancer Institute (NCI) (Weiss, 1992). Like other anthracycline, doxorubicin works by intercalation of DNA and inhibition of replication (Momparler *et al.* 1976). This inhibits the enzyme topoisomerase II by forming stable

complex, which relaxes supercoils in DNA, thereby stopping the process of replication (Fornari *et al.*1994). The crystal structures of doxorubicin DNA complex are shown in Fig. 1.4 (Pigram *et al.*1972. Frederick *et al.* 1990).

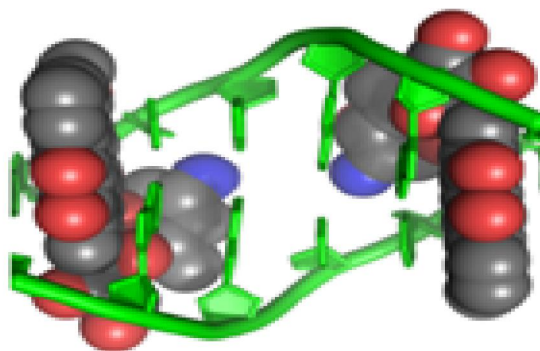


**Figure 1.4** Mechanism of doxorubicin binding with DNA (adapted from Pigram *et al.* 1972)

There are various chemotherapy protocols like CVP (cyclophosphamide, vincristine and prednisone), CHOP (cyclophosphamide, doxorubicin, vincristine and prednisone), MACOP-B (methotrexate, doxorubicin, cyclophosphamide, vincristine, prednisone and bleomycin) and Pro MACE-CytaBOM (cyclophosphamide, etoposide, cytarabine, vincristine, bleomycin, methotrexate and prednisone) are available for the treatment of cancers.

#### 1.5.3.6 Photodynamic therapy (PDT)

PDT is other treatment modalities of cancer which requires photosensitizer or photosensitizing drugs and a particular type of non toxic light. The basic principle of PDT is that photosensitizing drugs are administered to the patients so that it can accumulate in tumor site and non toxic rays are bombarded on the localized site. The photosensitizer absorbs the light and produces oxygen radical, which destroys nearby cancer cells. A wide array of photosensitizers for PDT exists. Several photosensitizers are commercially

available for clinical use, such as Allumera, Photofrin, Visudyne, Levulan, Foscan, Metvix, Hexvix, Cysview, and Laserphyrin (Dolmans et al. 2003).

### 1.5.3.7 Neutron Capture Therapy (NCT)

NCT is a noninvasive therapeutic modality for treating locally invasive malignant tumors such as primary brain tumors and recurrent head and neck cancers. In this case, the tumor localizing drug containing a non-radioactive isotope of  $^{10}\text{B}$  or  $^{157}\text{Gd}$  is administered which is irradiated with neutrons of low energy. The nuclear reaction is as follows:



In theory NCT is a highly selective type of radiation therapy that can selectively target the tumor at the cellular level without causing radiation damage to the adjacent normal cells and tissues. NCT can deliver 60–70 Gy doses to the tumor cells in one or two applications compared to 6–7 weeks for conventional external beam irradiation. The sodium borocaptate or BSH ( $\text{Na}_2\text{B}_{12}\text{H}_{11}\text{SH}$ ) and boron phenylalanine or BPA are two compounds of  $^{10}\text{B}$  used for therapy in brain tumor (Kankaanranta et al. 2012, Kawabata et al. 2009). The possible use of gadolinium-157 as a capture agent for NCT becomes interesting because of very high neutron capture cross section of 254,000 barns. Moreover, Gd-DTPA (gadopentetate dimeglumine Magnevist®) has been used routinely as contrast agents for magnetic resonance imaging (MRI) of brain tumors. The selective destruction of brain tumor (glioma) cells using  $^{157}\text{Gd}$  had been studied in patients (Yasui et al. 2008).

## 1.6 IODINE-131 BASED RADIOPHARMACEUTICALS

### 1.6.1 Iodine-131

In 1811, Bernard Courtois discovered natural iodine in water that was used to dissolve certain parts of seaweed ash. Radioiodine ( $^{131}\text{I}$ ) was discovered by Glenn T. Seaborg and John Livingood at the University of California, Berkeley in the late 1930's.  $^{131}\text{I}$  is one of the earliest known radionuclides used in therapy, particularly in thyroid cancer (Hertz et al. 1940). It also served as a diagnostic radionuclide, especially for thyroid imaging for several decades until  $^{99\text{m}}\text{Tc}$  took over.

### 1.6.2 Physical characteristics

$^{131}\text{I}$  decays by emission of beta, gamma as well as X-rays with a physical half life of 8.04 days (Kocher, 1981).  $^{131}\text{I}$  emits beta particles with maximum energies of 0.248 MeV (2.1 %) (  $\text{avg}$  0.0694), 0.334 MeV (7.4 %) (  $\text{avg}$  0.0966) and 0.606 MeV (89.3 %) (  $\text{avg}$  0.192), along with several energies of gamma rays [0.723 MeV (1.8 %), 0.637 MeV (7.3 %), 0.364 MeV (81.2 %), 0.284 MeV (6.1 %) and 0.080 MeV (2.6 %)] as well as X-Ray of 0.030 MeV (3.9 %). The maximum range of the beta particles from  $^{131}\text{I}$  in air is 165 cm (Kaplan, 1964), while in tissue the maximum range is 2.3 mm (Wheat et al. 2011). The unshielded exposure rate at 1 cm from a 1 mCi of  $^{131}\text{I}$  point source is 2.16 R/h, with half-value layer (HVL) for lead shielding of 2.3 mm.

### 1.6.3 Occupational Limits

For normal people, the annual limit of intake (ALI) of  $^{131}\text{I}$  is 30  $\mu\text{Ci}$  (1.1 MBq) for oral ingestion and 50  $\mu\text{Ci}$  (1.8 MBq) for inhalation. Derived air concentration (DAC) is  $2 \times 10^{-8} \mu\text{Ci/ml}$  (740 Bq/m<sup>3</sup>).

**1.6.4 Biological half life and metabolism**

The biological half-life of iodine in the human thyroid is expected to be an average quantity. In 1959, the International Commission on Radiological Protection recommended that the biological half-life of iodine should be 138 days, which was revised downwards in 1978 to a value of 120 days and again in 1989 to a value of 80 days (Kramer et al. 2002). In an adult, 30 % of the initial intake of iodine is taken up by the thyroid and 20 % goes to faecal excretion. The biological half life of  $^{131}\text{I}$  in blood and rest of the body are 0.25 and 12 days, respectively (Kramer et al. 2002).

**1.6.5 Therapeutic radiopharmaceuticals of Iodine -131**

In the area of therapy, Iodine-131 has been used since 1940 (Hertz et al. 1940) in the form of sodium iodide ( $\text{Na}^{131}\text{I}$ ), and is still continued to be used extensively although a large number of beta and alpha emitting radioisotopes have been available and used to varied extent. Despite the advent of several new radionuclides in the therapy,  $^{131}\text{I}$  continues to hold the place of the most widely used radionuclide in cancer therapy. The wider applications of  $^{131}\text{I}$  is due to its excellent physical properties, ease of production, wide availability at affordable costs and most importantly its simple labeling method and unique efficacy in treatment of thyroid cancers. The use of  $^{131}\text{I}$  for labeling antibodies and peptides have also attracted wide attention after Bexxar (which is  $^{131}\text{I}$  labeled monoclonal antibody used for treatment of NHL) and  $^{131}\text{I}$ -Lipiodol (hepatocarcinoma) became commercially available.  $^{131}\text{I}$  labeled antibody at various stages of development, and in advanced stages of clinical trials, are enlisted in Table 1.2.

**1.7 BIOLOGICAL EFFECTS OF RADIATION**

There are several biological effects that can result from exposure to ionizing radiation

which may have acute or delayed effects depending on the amount of exposure (Elgazzar et al. 2001). The nucleus is more radiosensitive than the cytoplasmic organelles of a cell (Ward, 1988). Upon exposure to radiation the events of cell death starts with DNA and membrane damage. DNA damage in due course of time get repaired, otherwise cell opts for apoptotic death. The principal mechanism by which cell death occurs is mainly through the apoptosis which is governed by extrinsic and intrinsic signaling pathways (Elmore 2007). Ionizing radiation stimulus induce signal transduction pathway (Friedman 1998), which results in cell death (Lei et al. 2001, Szumiel 1994) by means of apoptosis (Harms-Ringdahl et al. 1996). Ionizing radiation can cause mitochondrial membrane permeabilisation and release of cytochrome-c and other factors, which are generally blocked by anti apoptotic protein like bcl2 and bclxl (Cory et al. 2003). During apoptotic cell death, anti-apoptotic gene viz bcl2, bclxl, mcl etc. are downregulated. The dying cells are precisely framed by caspase (Degterev et al.2003), packaged into apoptotic bodies (Erwig et al. 2008) as a mechanism to avoid immune activation by means of necrosis (Darzynkiewicz et al. 1997). Several methods are available to detect apoptosis of which, characteristic DNA ladder by electrophoresis (Daniel et al. 1999), DNA fragmentation by ELISA method, flow cytometry, Western blotting and real time PCR are often used.

## 1.8 RATIONALE OF THE THESIS

Radioiodine ( $^{131}\text{I}$ ) is one of the oldest radionuclides to be used in radiopharmaceuticals and continues to have an unique place in therapy. Iodine is chemically amenable for incorporation into a variety of biological molecules through simple electrophilic substitution of iodine (as  $\text{I}^+$ ) in ortho and para positions in tyrosine, histidine and tryptophan moieties. Hence,  $^{131}\text{I}$  become a favorite radionuclide for labeling peptides,

proteins and other molecules containing such groups and fulfills the criteria of an ideal therapeutic radioisotope to a large extent. It has (a) relatively moderate half life of 8.02 days, (b) decays by emission of high energy of beta particles ( $E_{\max}$  0.606 MeV) capable of effectively destroying the cancer cells and (c) also emits gamma rays (364 keV, 81.2 %) suitable for imaging. Due to these properties several molecules labeled with  $^{131}\text{I}$  have been used for treating cancers such as  $^{131}\text{I}$ -lipiodol in liver cancers,  $^{131}\text{I}$ -tositumomab for NHL, and several  $^{131}\text{I}$  labeled antibodies are in various stages of development and clinical trials. Multi-modality treatment is common in cancer management of which radiolabeled mAb would be an appropriate agent for NHL management. In this context, rituximab with proven potential for treating NHL would be an ideal candidate for radioiodination with  $^{131}\text{I}$ . Additionally, exploration of use of a chemotherapeutic agent such as doxorubicin as a combinatorial approach would be further beneficial in NHL management. Biological effectiveness of radiolabeled rituximab and its combination with doxorubicin was evaluated in Raji cells, a CD20 positive human lymphoma cell line.

## 1.9 SCOPE AND OBJECTIVES OF THE THESIS

The scope of thesis is to evaluate the following aspects of radiopharmaceutical, particularly in the context of radioimmunotherapy in cancers:

Efficacy of  $\alpha$  radiation on different cell lines are known, however, efficacy of beta radiation is limited. Hence, comparative studies have been carried out with beta radiation emitted from  $^{131}\text{I}$  as the representative radionuclide and the equivalent dose of gamma radiation in human tumor cell lines of various origins.

Rituximab is chimeric monoclonal antibody available in clinics for the therapy of NHL. Rituximab itself can induce cell death but it can also induce resistance during

therapy. Hence, rituximab is conjugated to  $^{131}\text{I}$  considering that it may overcome the resistance and increase the cytotoxic effects. The detail mechanisms of internalization and subsequent toxicity of  $^{131}\text{I}$ -rituximab is not known, which may play significant role in efficacy of radiopharmaceuticals.

Doxorubicin is a commonly used chemotherapeutic agent, however, it exerts undesirable side effects and drug resistance at the doses applied to the patients. To minimize the dose of drug, it is imperative to combine it with other treatment modalities. Employing of  $^{131}\text{I}$ -rituximab in combination with doxorubicin can be one of the effective modes of cancer therapy.

Hence the thesis has following objectives:

1. Comparison of effect of beta radiation emitted from  $^{131}\text{I}$  with an equivalent dose of  $\beta$ -radiation in human cancer cells
2. Study on cellular internalization and mechanism of toxicity of  $^{131}\text{I}$ -rituximab in Raji cells
3. Study on effect of  $^{131}\text{I}$ -rituximab in combination with doxorubicin on Raji cells



## CHAPTER 2

# **Comparison of Effects of Beta Radiation Emitted from $^{131}\text{I}$ with an Equivalent Dose of -radiation on Human Cancer Cells**

## 2.1 INTRODUCTION

Effects of ionizing radiation on living cells are largely due to its interaction with constituent atoms of cells by the process of ionization. The radiation induced biological damage involves two mechanisms viz. direct and indirect effects. In direct effect, radiation interacts with the atoms of the biological targets of the cell. Since water is a major ingredient of biological system, radiation causes radiolysis of water. Thus primary radicals formed may interact with biomolecules and cause damage to the cells, collectively known as indirect effect of radiation. Direct effects are predominant in the case of high LET radiations such as alpha and neutron while indirect effects occurs mostly due to the low LET radiations like X-rays and  $\gamma$ -rays. Effect of low and high LET radiation is depicted in Fig.2.1.

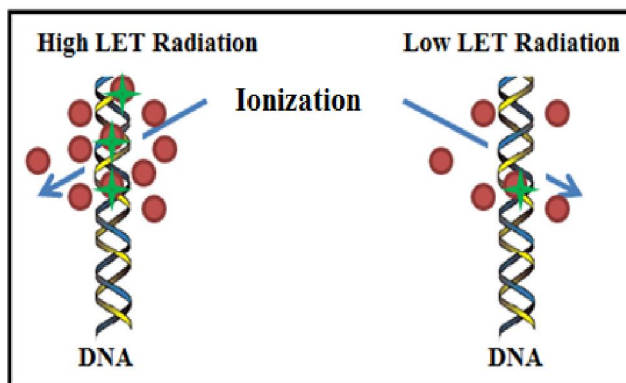


**Figure 2.1.**Effect of different ionizing radiations on DNA damage

The biological effects of radiation are either acute or delayed type (Elgazzar et al. 2001, Friedman, 1998). The initial events which start upon exposure to radiation are damage to DNA, membrane and other cellular targets. The DNA damages are either single strand breaks or double strand breaks. Depending on the severity of DNA damage, there is cell cycle arrest by involvement of *P53* and *P21*. The *P21* gene is under the transcriptional control of *P53* that arrest cell cycle or induces apoptosis or

cell senescence (El-Diery et al. 1993).

Radioiodine ( $^{131}\text{I}$ ) is used in therapy of thyroid disorders (Hertz 1940, Boelaert et al. 2003, Biersack et al. 2005). It emits beta (0.606 MeV), gamma (0.364 MeV) and X-rays (0.030 MeV). The beta radiation emitted from radioiodine is useful in therapy while its  $\gamma$ -radiation is used for diagnosis. The effect of  $\gamma$  and X-rays emitted from  $^{131}\text{I}$  in therapy is insignificant because most of these escape from the target site without much damage to the target (cancer) cells. On the other hand, the beta radiation deposits their energy within a short distance in tissue and cause cell death. The mechanisms of cell death induced by  $\beta$ - radiation emitted from radionuclides are not well known. Hence, with an aim to understand the mechanism of damage, tumor cells of various tissue origins were irradiated with beta radiation emitted from  $^{131}\text{I}$ , with a total dose of  $\sim 0.4$  Gy. Several parameters such as cell toxicity, apoptosis, DNA damage and expression of proapoptotic genes were evaluated in irradiated cancer cells and these effects were compared with that produced by an equivalent dose of radiation (0.4 Gy).

X-rays or  $\gamma$ -rays irradiation has limitation during cancer therapy because tumor of different origin shows difference in radiosensitivity. This can be due to difference in their p53 status, antioxidant and hypoxic level of tumor tissue. Since, comparatively high LET radiations overcome most of these limitations, current studies have been carried out with beta radiation and compared the effects with radiation.

## 2.2 SCOPE AND OBJECTIVES OF THE CHAPTER

$^{131}\text{I}$  has been widely used in cancer therapy and continues to be more due to the simple procedure of labeling of biomolecules with iodine. However, the details of

mechanism of cell death induced by beta radiation emitted from  $^{131}\text{I}$  in tumor cells are not well understood. In this chapter, the efficacy of beta radiation was compared with  $\gamma$ -radiation. For this study, tumor cells of various tissue origins were irradiated with beta radiation and with an equivalent dose of  $\gamma$  radiation. The magnitudes of cell death and expression of DNA damage and apoptosis related genes were evaluated in  $\gamma$  as well as  $\beta$  irradiated cancer cells.

## 2.3 MATERIALS AND METHODS

### 2.3.1 Chemicals and reagents

Unless otherwise stated chemicals and kits for assays were purchased from Sigma Chemical Inc. (St. Louis, MO, USA). Cleaved PARP ELISA kit and 'In-Situ' Cell Death Detection ELISA kit<sup>PLUS</sup> were purchased from Abcam, Tokyo, Japan and Roche Diagnostics GmbH (Indianapolis, IN, USA), respectively. PerfectPure RNA Cultured Cell Kit and Masterscript kits were procured from 5 PRIME Inc. Gaithersburg, MD, USA. Iodine-131 ( $\text{Na}^{131}\text{I}$ ) was obtained from Radiochemicals Section, Isotope Production & Applications Division, Bhabha Atomic Research Centre, Mumbai, India. All other reagents used were of cell culture grade. Radioactivity was measured either in pre-calibrated isotope dose calibrator (Curiementor-3, PTW-Freiburg, Germany) or in NaI(Tl) gamma counter (GRS-301, Pla Electro Appliances Pvt. Ltd. Mumbai, India)

### 2.3.2 Cell culture

Raji (human Burkitt lymphoma), U937 (human histiocytic lymphoma), MCF-7 (human breast adenocarcinoma) and A431 (human skin carcinoma) cell lines were obtained from the National Center for Cell Sciences (NCCS), Pune, India. Raji and U937 cells were cultured in RPMI-1640, while MCF-7 and A431 cells were cultured in DMEM, supplemented with 10 % serum (Invitrogen Carlsbad, CA) and antibiotic/antimycotic solution. All cell cultures were maintained at 37 °C in humidified incubator with 5 %  $\text{CO}_2$ . Adherent cells (MCF-7 and A431) were harvested after trypsinization in subsequent experiments.

### 2.3.3 Cell binding studies of $^{131}\text{I}$ in tumor cells

Raji cells ( $1 \times 10^6$ ) were incubated with varying amounts of radioactivity of  $\text{Na}^{131}\text{I}$

(0.037, 0.37, 1.85, and 3.7 MBq) and incubated for 2 h at 37 °C. The cells were washed four times with PBS and the radioactivity associated with cells after each wash was measured in gamma counter NaI(Tl). Thus, the optimum numbers of washing steps required were determined for further experiments.

### 2.3.4. Irradiation of tumor cells and dosimetry

Raji, U937, MCF-7 and A431 cells ( $0.5 \times 10^6$ ) were plated in 6 well plates and cultured overnight. These cells were incubated with 1.85 MBq of  $\text{Na}^{131}\text{I}$  for 2 h. In another set, equivalent amount of NaI with similar chemical composition was added as control to all the cell lines and incubated for 2 h at 37 °C. After completion of incubation, the cells were washed thrice with PBS and further incubated upto 24 h at 37 °C in complete media. The cells were harvested and used for further experiments. Dose delivered by  $\text{Na}^{131}\text{I}$  was calculated assuming that the energy deposited in the cells by the beta particles was 100 % while dose received was negligible by gamma radiation. Dose delivered by 1.85 MBq of  $\text{Na}^{131}\text{I}$  was calculated by following equation (Sood et al. 2000, Goddu et al. 1994, Friesen et al. 2003).

Absorbed Dose rate ( $\text{Gy s}^{-1}$ ) -

$$\{A (\text{Bq}) \times E (\text{MeV}) / W (\text{g}) \times T (\text{s})\} \times 1.6 \times 10^{-13} (\text{J/MeV}) \times 10^3 (\text{g/Kg})$$

$$= 1.6 \times 10^{-10} A \times E \text{ Gy/s}$$

{Where A-Radioactivity in Bq, E-Energy of particle in MeV per disintegration, W-Wt of tissue or sample, T- time of incubation (residence time) in second, and Bq in dps (disintegration per second)}

For gamma radiation, Raji, U937, MCF-7 and A431 cells ( $0.5 \times 10^6$ ) were plated in 6 well plates, cultured overnight and irradiated with gamma radiation of  $^{60}\text{Co}$  radiotherapy unit (Bhabhatron-II, Panacea medical technology, Bangalore, India) (dose 0.4 Gy; dose rate 0.4 Gy/min) which is equivalent to dose delivered by 1.85

MBq of  $\text{Na}^{131}\text{I}$  for 2 h. These irradiated cells were incubated at 37 °C in humidified incubator with 5 %  $\text{CO}_2$  upto 24 h.

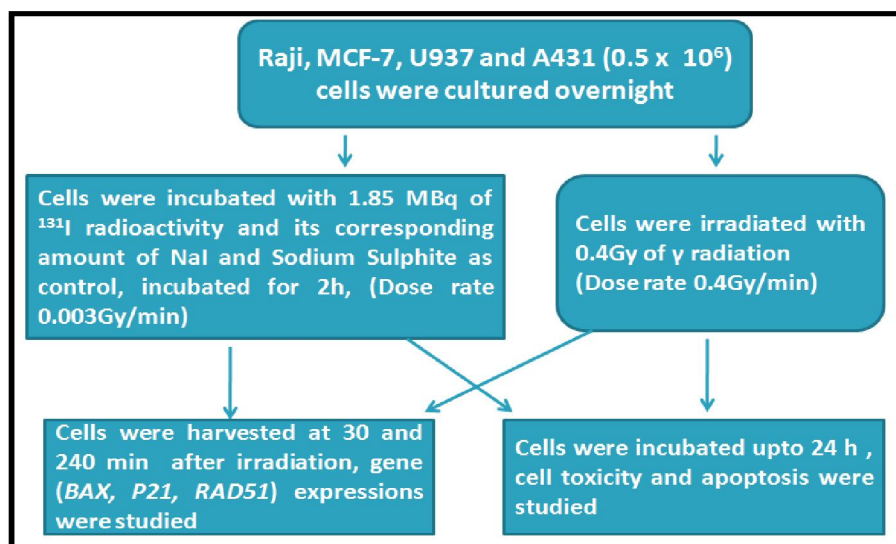


**Figure 2.2** Flow chart of experimental plan

### 2.3.5 Study of effect of $\text{Na}^{131}\text{I}$ and $\gamma$ -radiation on cell toxicity

Three sets of tumor cells (Raji, U937, MCF-7 and A431) were treated with (i)  $\text{Na}^{131}\text{I}$  (1.85 MBq for 2 h), (ii) equivalent concentration of NaI for 2 h as vehicle control and (iii)  $\gamma$ -radiation (0.4 Gy). Cells were harvested after 24 h. Magnitudes of cell death in control and treated cells were determined by trypan blue method (Kumar et al. 2013a). In brief, the cells were mixed with equal volume of 0.4 % w/v trypan blue dye and observed under bright field microscope. Living cells exclude dyes, while dead cells take up the dyes which were counted using a haemocytometer. Percent cell death was calculated as the ratio of dead cells to the total cells multiplied by 100.

### 2.3.6 Study of effect of $\text{Na}^{131}\text{I}$ and $\gamma$ -radiation on apoptotic DNA fragmentation

For determination of apoptosis, DNA fragmentation study was carried out using “In-Situ Cell Death Detection ELISA Kit<sup>plus</sup>” according to the protocol mentioned in kit. During apoptosis, the fragmented nuclear DNA and histone exudes to cytoplasm,

which can be detected by ELISA method. Briefly, Na<sup>131</sup>I, NaI and gamma radiation treated/irradiated tumor cells (Raji, U937, MCF-7 and A431) were harvested after 24 h of incubation, from which  $1 \times 10^5$  cells were lysed in cell lysis buffer for 30 min and centrifuged at  $20,000 \times g$  for 10 min. The supernatant was carefully transferred to fresh tubes. The supernatant was diluted to 1:10 and 20  $\mu$ L of this solution was added into streptavidin coated microplate. Anti-histone biotin and anti DNA-POD antibody were mixed just before use in the ratio of 1:1 (v/v) from which 80  $\mu$ L was added in each well and the plate was kept on shaker for 2 h. Thereafter, the wells were washed thrice with buffer provided with the kit and incubated with the substrate solution for 20 min. The color developed was quantified by spectrophotometer at 405 nm. DNA fragmentation was expressed as EF, which is the ratio of ODs of treated and control samples.

### 2.3.7 Study of effect of Na<sup>131</sup>I and gamma radiation on PARP cleavage in tumor cells

PARP protein is the hall mark of induction of apoptotic cell death and hence was studied to estimate the extent of apoptosis. Determination of PARP cleavage was carried out according to the protocol described in 'cleaved PARP human ELISA' kit. During apoptosis, the native PARP proteins (113 kDa) cleave into 89 and 24 kDa protein fragments. The 89 kDa proteins are detected by ELISA method and are indicative of the extent of apoptosis. Briefly, Na<sup>131</sup>I, NaI and radiation treated/irradiated tumor cells (Raji, U937, MCF-7 and A431) were harvested after 24 h of incubation, lysed in cell lysis buffer for 45 min and centrifuged at  $20,000 \times g$  for 20 min. The supernatant protein was carefully transferred to fresh tubes and stored at -80°C until analysis. Protein concentration in the samples was quantified by Bio-Rad Protein Assay (Bio-Rad Lab Inc, Hercules CA, USA). The cell lysate (containing 60



µg of protein) was added in anti-PARP coated ELISA plate and incubated for 2 h with gentle shaking. Thereafter, the wells were washed twice with the buffer (provided with kit) and incubated with detector antibody for one hour. The wells were again washed twice with the buffer and incubated with HRP labeled antibody for one hour. The wells were finally washed thrice with buffer and incubated with substrate for 20 min. The reaction was stopped by addition of 1N HCl and the absorbance was measured at 450 nm. PARP cleavage was expressed as EF which is the ratio of ODs of treated to control samples.

### **2.3.8 Study of effect of Na<sup>131</sup>I and gamma irradiation on expression of genes using Real Time PCR**

#### **Total RNA Isolation**

Raji cells were incubated with 1.85 MBq of Na<sup>131</sup>I for 2 h, washed thrice and further incubated upto 4 h. Another set of cells were identically incubated with non-radioactive NaI, as vehicle control. Likewise, cells were irradiated with 0.4 Gy of radiation and incubated under similar conditions in complete media. Total RNA was isolated from the control and irradiated cells, following protocol provided with 'PerfectPure RNA Cultured Cell Kit'. Briefly, cells were harvested at 30 and 240 min after completion of irradiation and lysed by addition of 400 µL of cell lysis buffer. The cell lysis was completed by repeated pipetting. Lysate was transferred on column tube and centrifuged at 13000 rpm for 1 min followed by washing with wash buffer. Subsequently, DNase was added and incubated for 10 min and washed twice with DNase wash buffer. The column was again washed twice with wash-2 buffer. The RNA was eluted by addition of elution buffer followed by centrifugation at 13000 rpm for a minute. The quality and quantity of the RNA was determined by spectrophotometer (JASCO V-530 UV/VIS) ( $A_{280}/A_{260} > 1.8$ ). RNA was stored either

at -20 °C for immediate use or kept at -80 °C ( in small aliquots) for longer storage.

### Real Time PCR

The cDNA synthesis was carried out following the procedure described in the Masterscript Kit. Briefly, for each sample, reverse transcriptase enzymes, dNTPs mix, oligo (dT)<sub>18</sub> primer, Reverse Transcriptase buffer and 0.5 µg of RNA from the sample, were mixed and subjected to one step PCR amplification at 55 °C for 60 min. Then, cDNA samples were subjected to PCR amplification using sequence-specific forward and reverse primers {*ACTIN* (F-gatcattgctcctctgagc, R-aaagccatgccaatctcatc), *BAX* (F- gctgttgggctggatccaag, R-tcagcccatcttctccaga), *P21* (F-cctcatcccgtgttctccttt, R- gtaccaccagcggacaagt) and *RAD51* (F- atcatcgcccatgcatcaacacc, R- agtctttggcatctcccactccat)} using SYBR green master mix (Jayakumar et al. 2012). The PCR reactions were composed of 10× SYBR green PCR mix with 5 µL of twice-diluted (1:2) cDNA templates, 1 µL each of the forward and the reverse primers (0.5 µM), and 3 µL of PCR-grade water in a 20 µL reaction mixture. The above reaction mixtures were amplified with a denaturation step at 95 °C for 5 min and 40 cycles of amplification including 95 °C for 15 s, 58 °C for 20 s and 72 °C for 20 s, followed by a melting curve analysis on a Rotor Gene 3000 (Corbett Life Science, Australia). The specificity of the respective amplicons was confirmed from the melting curve analysis. The threshold cycle values obtained from the runs were used for calculating the fold change in gene expression using REST-384 version 2 software (Pfaffl et al. 2002), where relative expression is compared to the untreated control cells.

### 2.3.9 Statistical analysis

Unless mentioned, the results are mean ± SD of at least three independent experiments, where t-test was used to compare control and irradiated samples. Significance level was determined by considering *p* values below 0.05.

## 2.4. RESULTS

### 2.4.1 Cell binding studies of tumor cells with $\text{Na}^{131}\text{I}$

In order to minimize non specific cell binding, the number of washing during cell binding assay was optimized. Raji cells ( $1 \times 10^6$ ) were incubated with 0.037-3.7 MBq

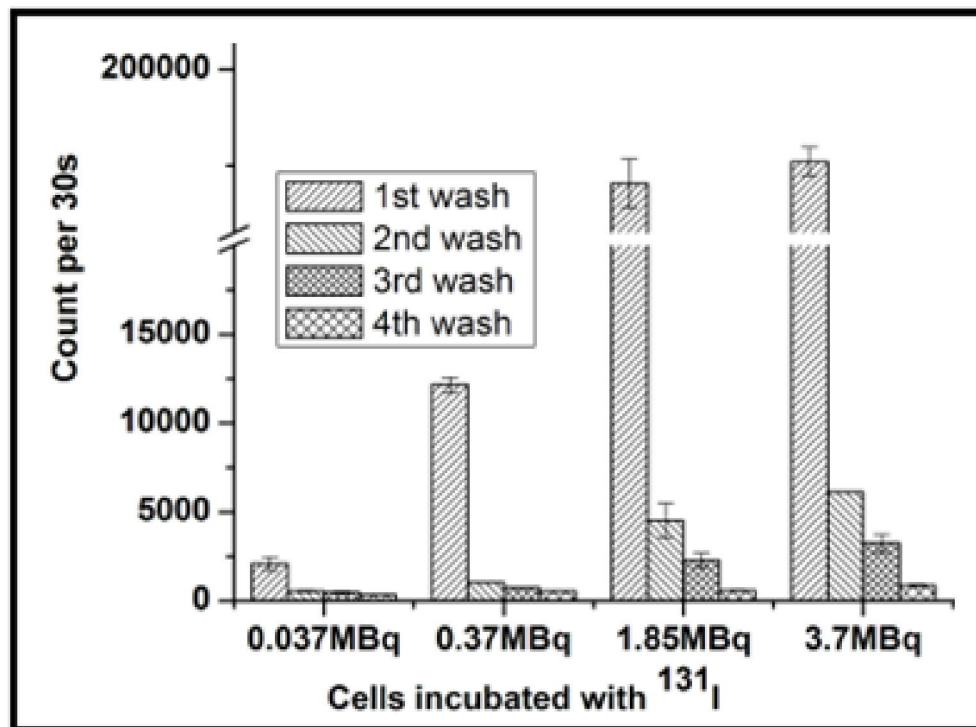


**Figure 2.3a** Effect of number of washing on non specific cell bound radioactivity of  $\text{Na}^{131}\text{I}$  in Raji cells

radioactivity of  $\text{Na}^{131}\text{I}$  (2 h at  $37^\circ\text{C}$ ), followed by repeated washing and centrifugation ( $1400 \times g$ , 5 min). Associated radioactivity counts in cells were measured after each wash (Fig 2.3a). It was found that after the second wash, most of the radioactivity from the cells was washed out. The third and subsequent wash did not have any impact on removal of nonspecific cell bound radioactivity at lower amounts of  $\text{Na}^{131}\text{I}$  incubation viz. 0.037 and 0.37 MBq. However, it was found that in cells incubated with higher radioactivity of  $\text{Na}^{131}\text{I}$  ( $>1.85$  MBq), the radioactivity counts decreased

significantly after 2<sup>nd</sup> wash followed by marginal decrease after 3<sup>rd</sup> and 4<sup>th</sup> wash. Hence, a minimum three washing steps were selected for further experiments.

In order to estimate the radioactivity associated with the cells, tumor cells ( $1 \times 10^6$  cells) of various origin were incubated with 0.037-3.7 MBq radioactivity of  $\text{Na}^{131}\text{I}$  for 2 h at 37 °C. The associated radioactivity in the cells was measured after 3<sup>rd</sup> wash. It was found that cell associated radioactivity of Raji cells (Fig. 2.3b), U937 (Fig. 2.3c), MCF-7 (Fig. 2.3d) and A431 (Fig. 2.3e) increased with the increase in amount of  $\text{Na}^{131}\text{I}$  radioactivity. However, the percent of  $\text{Na}^{131}\text{I}$  radioactivity associated with cells were less than 0.02 % in all the tumor cells, with no significant difference amongst the cell lines. For further experiments, 1.85 MBq of  $\text{Na}^{131}\text{I}$  was chosen which provides suitable dose, dose rate and the permissible radioactivity for safe handling during experiments.

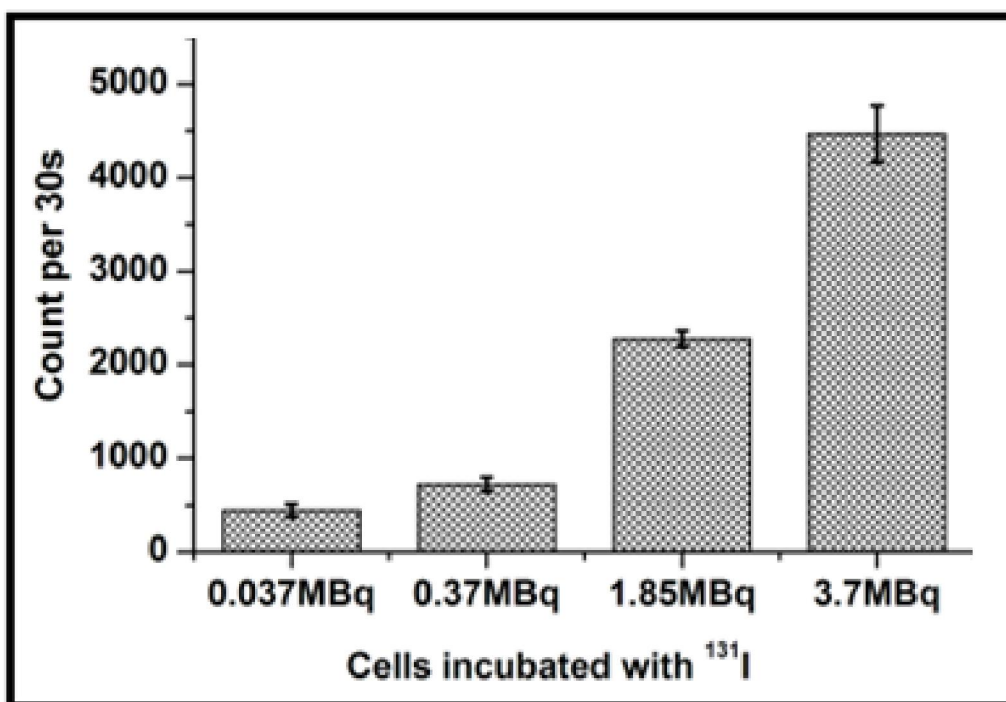


**Figure 2.3b**  $\text{Na}^{131}\text{I}$  radioactivity associated with Raji cells after 3<sup>rd</sup> wash

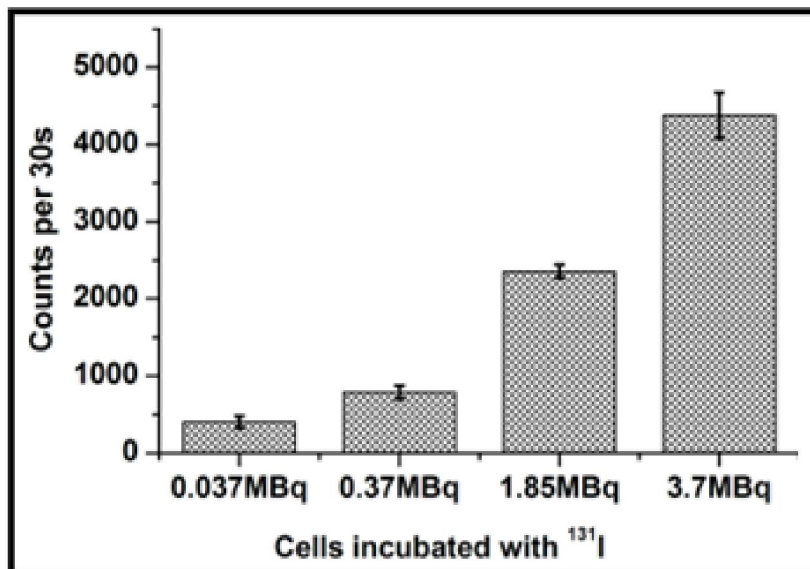


Figure 2.3c Na<sup>131</sup>I radioactivity associated with U937 cells after 3<sup>rd</sup> wash

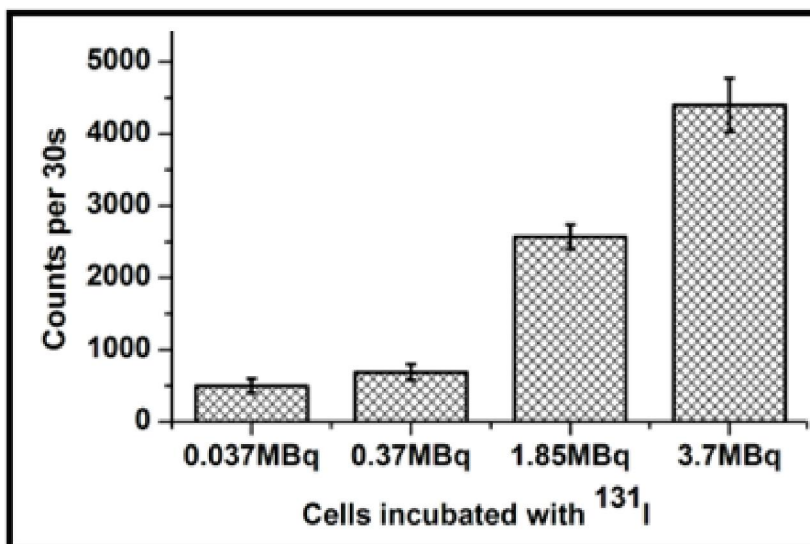
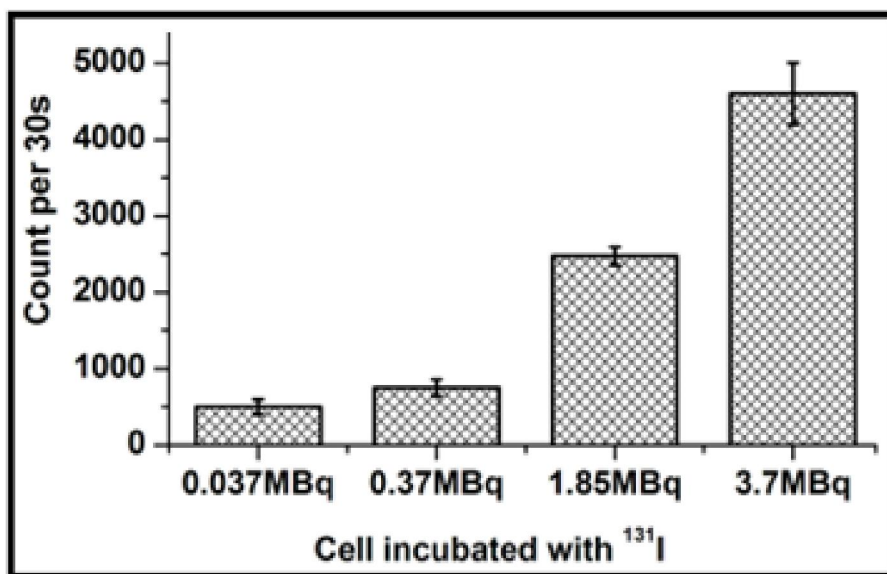


Figure 2.3d Na<sup>131</sup>I radioactivity associated with MCF-7 cells after 3<sup>rd</sup> wash



**Figure 2.3e**  $\text{Na}^{131}\text{I}$  radioactivity associated with A431 cells after 3<sup>rd</sup> wash

#### 2.4.2 Calculation of radiation dose to the cells after $\text{Na}^{131}\text{I}$ treatment

Radiation dose delivered by  $\text{Na}^{131}\text{I}$  to the cells was calculated using the values for energy of avg of  $\text{Na}^{131}\text{I}$  as 0.1815 MeV, residence time of 7200s (2 h) and radioactivity as 1.85 MBq (as mentioned in section 2.3.4). These values correspond to an absorbed dose (Gy) of  $1.6 \times 10^{-10} \text{ A} \times \text{E Gy s}^{-1} = 1.6 \times 10^{-10} \times 1.85 \times 10^6 \times 0.1815 \times 7200 = 0.38 \text{ Gy}$ . The dose rate for  $\text{Na}^{131}\text{I}$  was calculated as 0.003 Gy/min.

#### 2.4.3. Effect of $\text{Na}^{131}\text{I}$ and gamma irradiation on cell toxicity in tumor cells

The cell toxicity to Raji, U937, MCF-7 and A431 cells was assessed by trypan blue dye (Fig. 2.4). The results indicated that NaI does not have any significant effect on cell toxicity upto 24 h, in all the cell lines used in the study. Compared to unirradiated/vehicle control, irradiated cells ( $\text{Na}^{131}\text{I}$  and radiation) showed increase in cell toxicity and the magnitude of cell death varied with the tumor cell line. It was interesting to observe that in majority of cell lines, the extent of cell death by  $\text{Na}^{131}\text{I}$  was higher than in those with 0.4 Gy of gamma irradiation. Cell toxicity induced by

$\text{Na}^{131}\text{I}$  were significantly ( $p < 0.05$ ) higher, compared to the equivalent dose of radiation in the cell lines namely, Raji, U937 and MCF-7 except A431. Amongst the cell lines used in the study, only Raji cells showed maximum cell toxicity (16 %) induced by  $\text{Na}^{131}\text{I}$  while it was ~ 10 % with 0.4 Gy of radiation ( $p < 0.05$ ).

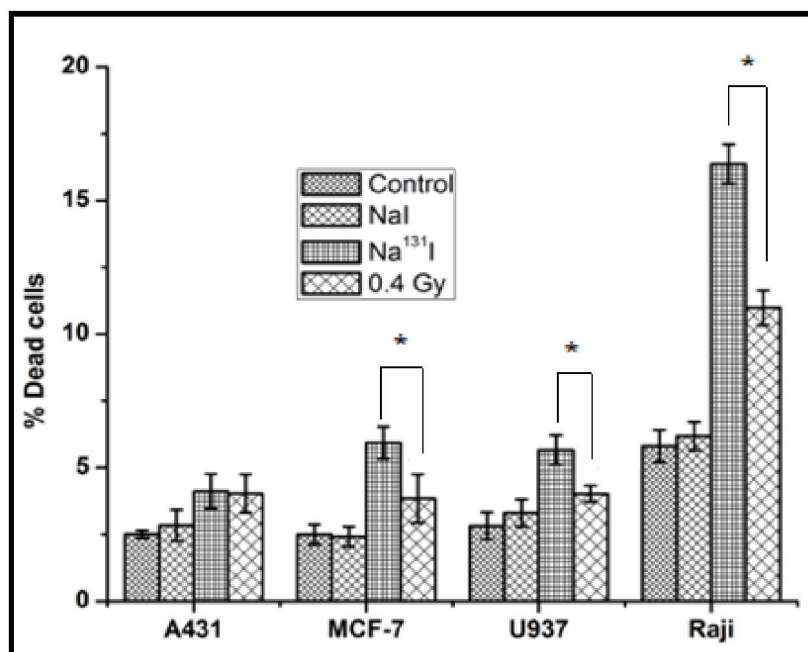


**Figure 2.4** Estimation of cell toxicity in A431, MCF-7, U937 and Raji cell lines induced by NaI,  $\text{Na}^{131}\text{I}$  and gamma radiation (0.4 Gy) by trypan blue dye uptake (where \* is significant within group with  $p < 0.05$  and  $n = 3$ .)

#### 2.4.4. Effect of radiation from $\text{Na}^{131}\text{I}$ and gamma irradiation on induction of apoptotic cell death

In order to investigate the mechanism of cell death in Raji, U937, MCF-7 and A431 cells against irradiation with  $\text{Na}^{131}\text{I}$  and gamma radiation, the magnitude of apoptotic DNA fragmentation was studied by In-Situ Cell Death Detection ELISA method. It was observed that in comparison with the control group, the effect of NaI was not significant on DNA fragmentation upto 24 h (Fig.2.5). However, the DNA fragmentation induced by beta radiation was significantly higher ( $p < 0.05$ ) compared



to gamma radiation (0.4 Gy) in all cell lines (A431, MCF-7, U937 and Raji). It was found that in Na<sup>131</sup>I treated cells, the EF of DNA fragmentation was in the order of 1.8 to 2.4 and the maximum effect was observed in the Raji cell line. The EF of DNA fragmentation by the gamma radiation in all the cell lines was close to the control cells.

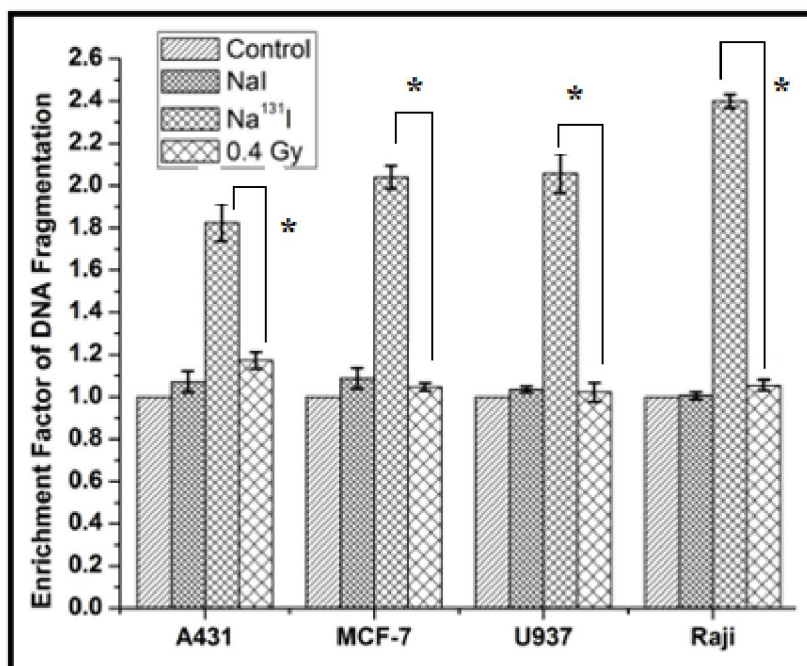


**Figure 2.5** Estimation of DNA fragmentation in A431, MCF-7, U937 and Raji cell lines treated with NaI, Na<sup>131</sup>I and gamma radiation (0.4 Gy) (where \* is significant within group, with  $p < 0.05$  and  $n = 3$ .)

#### 2.4.5 Effect of radiation from Na<sup>131</sup>I and gamma radiation on induction of PARP cleavage

The extent of apoptosis was also estimated in terms of PARP cleavage by ELISA method in Raji, U937, MCF-7 and A431 cells against irradiation with Na<sup>131</sup>I and radiation. It was also found that there is no significant difference in the extent of PARP cleavage between the control and the NaI treated cells (Fig. 2.6). However, the



irradiated cells exhibited significant PARP cleavage. The extent of PARP cleavage was significantly higher in  $\text{Na}^{131}\text{I}$  treated cells compared to the irradiated cells ( $p < 0.05$ ). MCF-7 and Raji cell lines exhibited higher EF of PARP cleavage in comparison to A431 and U937 cells. In A431, the effect of  $\text{Na}^{131}\text{I}$  as well as gamma radiation was minimum in terms of induction of PARP cleavage.

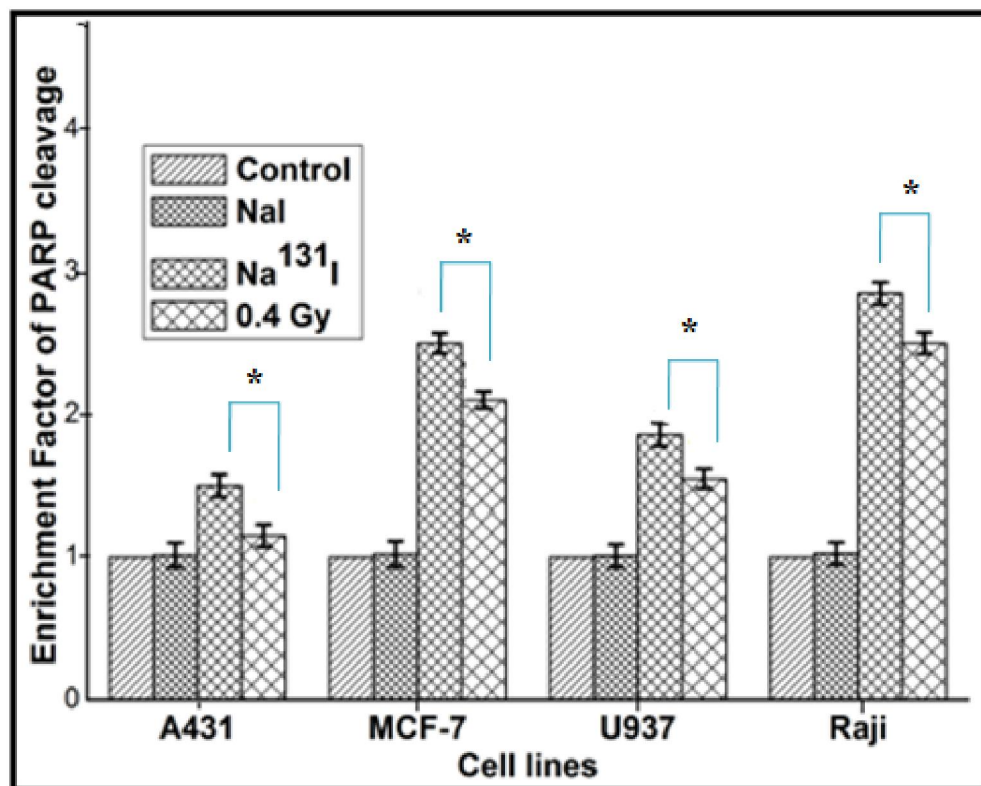


**Figure 2.6** Estimation of PARP cleavage in A431, MCF-7, U937 and Raji cell lines treated with NaI,  $\text{Na}^{131}\text{I}$  and gamma radiation (0.4 Gy). (where \* is significant within group, with  $p < 0.05$  and  $n = 3$ .)

#### 2.4.6 Expression of *BAX*, *P21* and *RAD51* genes in Raji cell line

Since, Raji cells showed maximum cell toxicity and apoptosis compared to the other cell lines, it was of interest to study further the expression of genes in this cell line. A study was carried out to evaluate expression of DNA damage and apoptosis related genes after 30 and 240 min of treatment of the cells with  $\text{Na}^{131}\text{I}$  and radiation.

Expression of *BAX*, *P21* and *RAD51* genes was analyzed by real time PCR. It was found that *BAX* gene is upregulated from 30 min to 4 h ( $p < 0.05$ ). (Fig. 2.7a) in both,  $\text{Na}^{131}\text{I}$  and irradiated Raji cells. However, no significant change in *BAX* expression was observed between  $\text{Na}^{131}\text{I}$  and gamma treated Raji cells for a particular time of incubation. At 30 min of incubation, it was observed that the *P21* expression (Fig. 2.7b) was much higher for 0.4 Gy from gamma radiation compared to  $\text{Na}^{131}\text{I}$  but decreased subsequently at 4 h. However, in case of  $\text{Na}^{131}\text{I}$ , *P21* expression increased from 30 min to 4 h ( $p < 0.05$ ). *RAD51* gene expression was found to remain unaffected with time for  $\text{Na}^{131}\text{I}$  irradiated cells. On the other hand, in gamma irradiated cells, the *RAD51* expression (Fig. 2.7c) was high at 30 min, but decreased after 4 h ( $p < 0.01$ ). It was also seen from the graph that the relative expression of any particular gene induced by  $\text{NaI}$  was less than one.

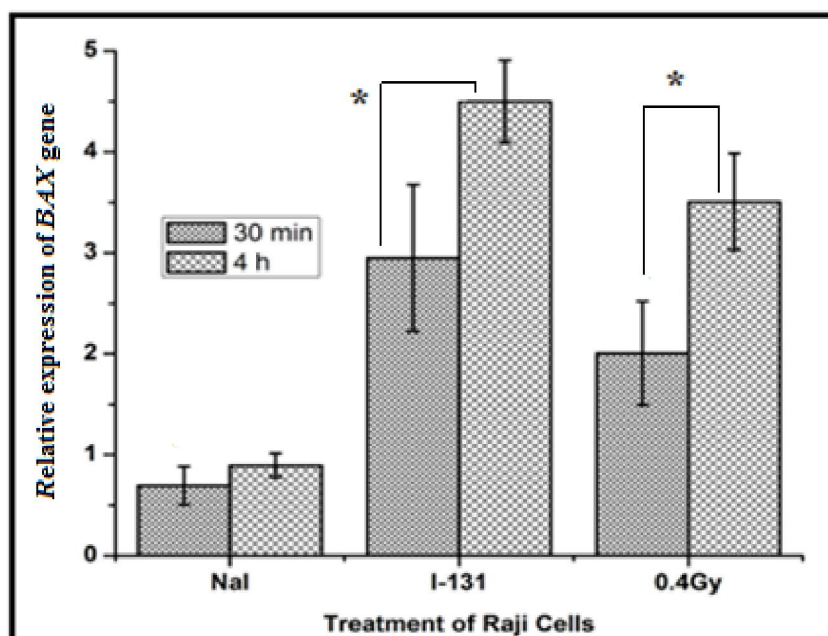


**Figure 2.7a** Expression of *BAX* gene in Raji cells at 30 and 240 min after irradiation (where

\* is significant within group, with  $p < 0.05$  and  $n=3$ )

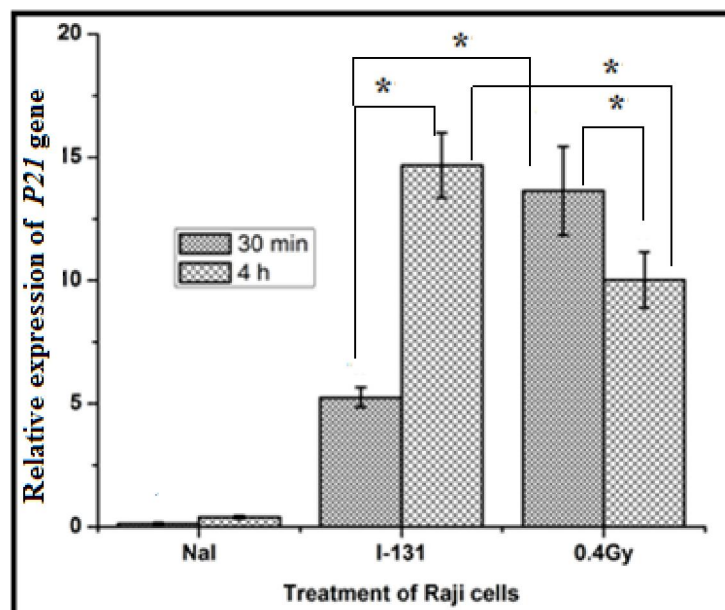


**Figure 2.7b** Expression of *P21* gene in Raji cells at 30 and 240 min after irradiation (\* is significant within/between group, with  $p < 0.05$  and  $n = 3$ .)

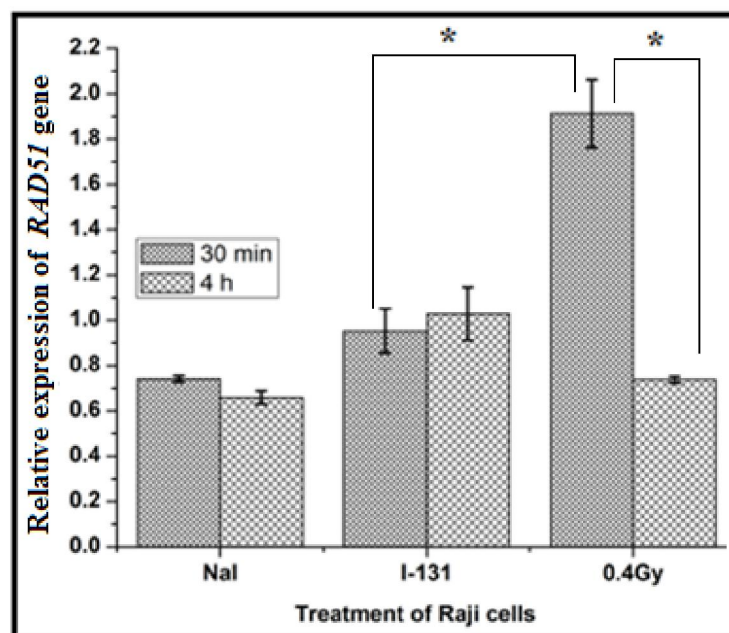


**Figure 2.7c** Expression of *RAD51* gene in Raji cells at 30 and 240 min after irradiation (where \* is significant within/between group, with  $p < 0.05$  and  $n = 3$ .)

## 2.5 DISCUSSION

The effect of radiation on living systems depends on the nature of radiation. Particulate radiations such as electrons mainly cause direct effect while non particulate radiation causes indirect effect through the radiolysis of water. Hence, it was interesting to study the effect of beta radiation emitted from  $\text{Na}^{131}\text{I}$  and compare it to the equivalent dose of radiation by  $^{60}\text{Co}$ . For this study, different cell lines of various tissue origins were irradiated with beta as well as radiation and a number of cellular and molecular parameters were assessed.

Initial experiments were performed to standardize the number of washing steps required to remove any non-specific cell bound radioactivity of  $\text{Na}^{131}\text{I}$ , and to measure the cell binding. Predictably, it was found that at lower radioactive concentration of  $\text{Na}^{131}\text{I}$ , a single wash was sufficient to remove the loosely bound radioactivity, while at higher concentrations more number of washes were required (Fig. 2.3a). Although the cell associated  $\text{Na}^{131}\text{I}$  radioactivity increased with the increase in amount of radioactivity, the cell bound radioactive fractions were less than 0.02 % in all the cell lines. This small amount of cell associated radioactivity is perhaps due to non-specifically bound radioactivity which may be adsorbed on cell surface. Active uptake/binding of  $\text{Na}^{131}\text{I}$  is not expected because cellular uptake of iodine needs sodium iodide symporter (NIS) which is known to be present/functional in the differentiated thyroid cancer, lactating breast, salivary gland etc. (Willhauck et al. 2008, Harun-Or-Rashid et al. 2010 and Spitzweg et al. 1998). Hence the dose received by the beta counterpart of radiation from  $\text{Na}^{131}\text{I}$  to tumor cells is mainly from outside of the cellular environment or close to the cell surface.

Magnitudes of cell deaths estimated after 24 h post exposure to radiation were found to be dependent on the type of tumor and radiation (Fig.2.4). Among the cell

lines studied, A431 cancer cells were found to be the most radioresistant cell line while, MCF-7 and U937 were moderately radiosensitive to  $\gamma$  radiation as well as beta radiation ( $\text{Na}^{131}\text{I}$ ). As expected, Raji cell line which has lymphoma origin was found to be the most radiosensitive among the cell lines studied (O'Connor et al. 1993 and Meijer et al. 2001).

Apoptosis study was carried out by estimation of DNA fragmentation and PARP cleavage by ELISA method. It was found that beta radiation causes significantly higher DNA fragmentation and PARP cleavage than gamma radiation. The magnitude of apoptosis determined by DNA fragmentation and PARP cleavage also showed that Raji cell lines are more radiosensitive than the other cell lines. The beta radiation ( $\text{Na}^{131}\text{I}$ ) caused more apoptosis than the corresponding amount of gamma radiation (0.4 Gy) suggesting that the apoptotic cell death induced by radiation is dependent on nature of irradiation (Friesen et al 2003, Lim et al. 2006, Eriksson et.al. 2008, Meng et al. 2012). These results are in agreement with the previous study showing that auger electron is a more potent inducer of apoptosis than the corresponding dose of  $\gamma$  radiation (Urashima et al. 2006). In all the cell lines used in the studies, beta irradiation from ( $\text{Na}^{131}\text{I}$ ) caused higher cell death and apoptosis compared to the equivalent dose of 0.4 Gy of  $\gamma$  radiation. In typical radiobiological studies where effects of very low dose rate radiations get attenuated, in our studies beta irradiation (0.003 Gy/min for 2h while 0.4 Gy/min of  $\gamma$  - radiation) caused more cell death/apoptosis than the corresponding  $\gamma$  radiation even at very low dose rate. Hence, these results indicate that beta emitters ( $\text{Na}^{131}\text{I}$ ) caused more cell death compared to the 0.4 Gy of  $\gamma$  radiation, which again was dependent on tumor types.

The differential pattern of dead cells estimated by trypan blue dye uptake

studies and apoptosis by ELISA method was observed in different tumor cell lines. Such difference in observation may be associated due to the sensitivity of different techniques and the method of estimation. The trypan blue dye exclusion assay is less sensitive to detect membrane alterations at advanced stage of cell death (Pandey et al. 2003 & Skoog et al. 1997). The magnitude of apoptosis estimation by DNA fragmentation and PARP cleavage are dissimilar. This may be due to beta radiation causing DNA strand breaks (non apoptotic DNA fragmentation) other than the apoptotic DNA fragmentations. This non apoptotic DNA fragments can be detected by this ELISA method which are difficult to differentiate and hence, resulted in increase of EF values.

*P21* is a cell cycle regulatory protein expressed early during the cellular stress with the involvement of *P53* (Mirzayans et al. 2012). *P21* expression increases from 30 min to 4 h in  $\text{Na}^{131}\text{I}$  treatment, whereas it decrease from 30 min to 4 h in radiation treatment. This initial higher expression of *P21* induced by radiation could be due to the higher dose rate of radiation (0.4 Gy/min) compared to the lower dose rate of  $\text{Na}^{131}\text{I}$  (0.003 Gy/min). However, the cumulative radiation effect of  $\text{Na}^{131}\text{I}$  was more due to low dose rate and the particulate nature of radiation, due to which its expression may be increased after 4 h. This is in agreement with the previous report that high LET particulate radiation has pronounced effect on cell cycle delay compared to the low LET radiation (Hu et al. 2014 & Fournier et al. 2004)

*RAD51* gene is involved in the homologous recombination repair of DSB (Peter et al. 1998, Khanna et al. 2001, Karran 2000, Schieler et al. 2013). It was found that after 4 h, *RAD51* expression drastically reduced in gamma ray treatment while there was no change in  $\text{Na}^{131}\text{I}$  treated cells. This might be because homologous recombination repair of DNA damage does not occur after damage due to beta

radiation. Homologous recombination repairs DNA before the cell enters mitosis (M phase). It occurs during and shortly after DNA replication, in the S and G2 phases of the cell cycle, when sister chromatids are more easily available, hence it is predominant in low dose rate irradiation (Schipler et al. 2013). Due to the particulate nature of beta irradiation, DNA damage was severe and hence the cell is unable to attain S/G2 phase for the repair through homologous recombination. While in the gamma irradiation DNA damages were less and hence cells bypass the DNA damage and reach the S/G2 phase for the repair through homologous recombination.

It was found that expression of *BAX* in Raji cells increased from 30 min to 4 h in  $\text{Na}^{131}\text{I}$  and radiation, however, there was no significant difference observed between  $\text{Na}^{131}\text{I}$  and radiation. This may be because *BAX* is a late pro-apoptotic marker than the DNA damage (Cory et al. 2003) and hence its expression was not pronounced within 4 h of cells treatment.

All the various parameters studied are presented in schematic representation (Fig 2.8), and indicated that radiation from  $\text{Na}^{131}\text{I}$  is not only potent in induction of cell toxicity and apoptosis compared to radiation but it follows different mechanism of cell death. *RAD51* and *P21* have a major role in discriminating the effect of  $\text{Na}^{131}\text{I}$  and gamma radiation, and detailed mechanisms need to be investigated.

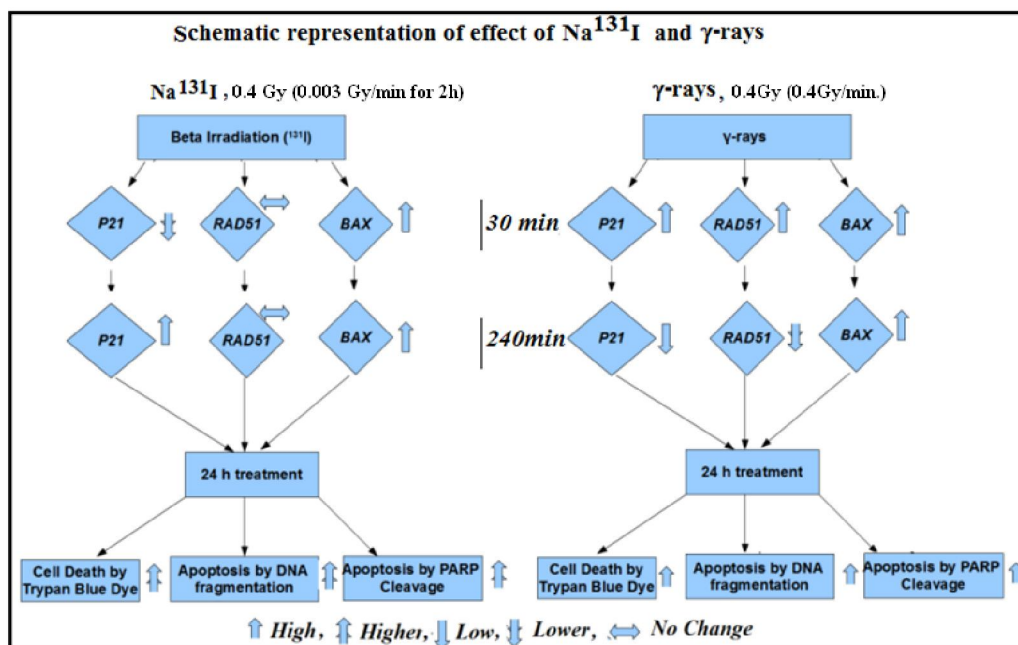


**Figure 2.8** Schematic representation of effect of Na<sup>131</sup>I and  $\gamma$  irradiation on Raji cells.



## CHAPTER 3

# **Studies on Cellular Internalization and Mechanism of Toxicity of <sup>131</sup>I-rituximab in Raji Cells**

### 3.1 INTRODUCTION

NHL is a clinically heterogeneous group of hematological malignancies arising from B, T or NK -lymphoid cells and the 11<sup>th</sup> most common cause of cancer incidence (Balkrishna 2008), and holds the 5<sup>th</sup> rank in cancer mortality (Bonavida et al 2007). Survival rate of NHL patients varies depending on the lymphoma type, stage, age of the patient etc. It has been reported that the estimated new cases and deaths from NHL in the United States in 2013 are 69,740 and 19,020, respectively (www.cancer.gov). Most of the B-cell malignant tumor cells such as NHL express a high number of CD20 receptors, making it one of the possible targets for therapy for such cancer (Anderson et al.1984).

#### **Antibody against CD20**

Over the past two decades, scientists have put in a lot of efforts to develop anti-CD20 mAbs for treatment of NHL, resulting in various successful products. There are several anti CD20 antibodies available commercially (tositumomab, ibritumomab, epratuzumab and rituximab). Moreover various newer mAbs (ofatumumab, ocrelizumab, velutuzumab, obinutuzumab etc.) targeting other tumor antigens are being explored for treating haematological malignancies (Olazoglu et al. 2010, Boswell et al. 2007, Castillo et al. 2008, Lim et al. 2010), and thus increasing the choice of immunotherapy in oncology (Corinna et al. 2010). The in-vitro studies comparing two isotope-matched anti-CD20 mAbs, 1F5 and B1 (tositumomab) demonstrated that all anti-CD20 mAbs are not the same (Beers et al. 2010). Functionally, anti CD20 mAbs have been divided into two types, termed as type I and II. Type I (rituximab-like) mAbs induce CD20 to redistribute into large detergent resistant microdomains (rafts), whereas type II (tositumomumab like)

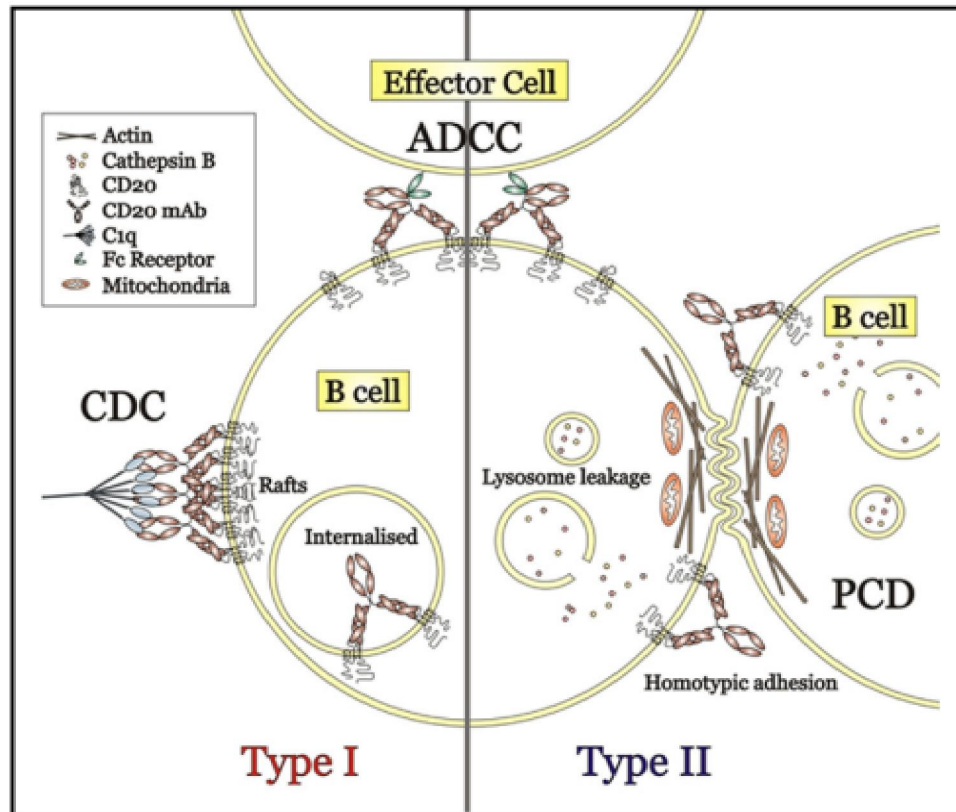


**Figure 3.1** Mechanism of action of anti CD20 mAbs (Adapted from Beers et al. 2010)

mAbs do not. Importantly, this redistribution by type I mAb has an impact on binding properties and effectors functions that control the therapeutic success of anti-CD20 mAb by internalization. The majority of anti CD20 mAbs generated to date are type I (Lim et al, 2010) and they display a remarkable ability to elicit CDC. The binding of anti CD20 antibody to the CD20 receptor is the first step in the elicitation of its biological function. It induces cell death through ADCC, CDC, direct cell killing or through apoptosis pathways (Fig 3.1) (Reff et al 1994, Meertan et al. 2006, Zhou et al. 2008, Weiner 2010, Stel et al. 2007, Deans et al. 2002). In ADCC, antibodies bind to Fc receptors on the surface of effector cells such as natural killer cells and macrophages, and trigger phagocytosis or lysis of the targeted cells/antigen. In CDC, antibodies kill the targeted cells by triggering the complement cascade.

**Rituximab**

Rituximab (trade name Rituxan & MAbThera) is a 144 kDa chimeric mouse/human monoclonal antibody consisting of a glycosylated IgG1 kappa immunoglobulin of murine light and heavy chain variable regions (Fab), and human kappa and gamma-1 constant regions (Fc domain). It is produced using recombinant DNA technology in Chinese Hamster Ovary cells and has antitumor activity in various types of NHL (Boye *et al.* 2003, Plosker *et al.* 2003, Lim *et al.* 2010, Olazoglu *et al.* 2010). Rituximab was approved by FDA in 1997 for use in humans for immunotherapy. Among the various available anti CD20 antibody, rituximab is easily available immunotherapeutic agent for NHL, and also devoid of HAMA response. Although rituximab is immunotherapeutic, it induces cell death by various mechanisms in B-cell lymphoma (Fig. 3.1). In clinical situation, large amounts of antibodies (250-375 mg/m<sup>2</sup>) have to be administered for effective therapy. Furthermore, it has been found that rituximab induces resistance in immunotherapy (Smith, 2003, Scott *et al.* 2008). However, if antibody is radiolabeled and used in radioimmunotherapy, the amount of antibody needed is only 4 mg (40 mCi/100kg BW), as seen in the case of Bexxar. Tagging the antibody with a lethal payload such as a particulate radiation emitting radionuclide, enables selective targeting of tumor and destroying it. In such a case, associated resistance may not be observed. Attempts to label rituximab with various beta emitting radionuclides viz. <sup>131</sup>I, <sup>177</sup>Lu and <sup>90</sup>Y (Kang *et al.* 2013, McQuillan *et al.* 2014, Forrer *et al.* 2013, Thakral *et al.* 2014, Gholipour *et al.* 2014,) and alpha emitting radionuclides viz. <sup>213</sup>Bi and <sup>211</sup>At (Vandenbuleke *et al.* 2003, Aurlen *et al.* 200) has been reported, which are at various stages of clinical trials (Table 1.3). However, <sup>131</sup>I, the oldest radionuclides is preferred for several reasons. The simple

method of radiolabeling, less steric hindrance of molecules after radiolabeling, easy availability of  $^{131}\text{I}$  made it ( $^{131}\text{I}$ ) more amenable for wider use in the clinics. The effect of radioiodination on the biological properties of rituximab (Tran et al. 2011) and biodistribution/ kinetics of  $^{131}\text{I}$ -labelled anti-CD20 (Scheidhauer et al. 2002) are reported in NHL patients.  $^{131}\text{I}$ -rituximab showed patients specific stable biodistribution and tissue kinetics (Antonescu et al. 2005), with an adequate radiological safety for administration of the outpatient treatment for NHL (Calais et al. 2012). There are various reports of radioimmunotherapy using  $^{131}\text{I}$ -rituximab for NHL patients (Rao et al. 2005, Bienert et al. 2005, Kersten 2011) and relapsed indolent NHL patients (Leahy et al. 2006, 2011). However, the detailed mechanism regarding the fate of antibody internalization and underlying mechanism of cell toxicity are limited in literature. Hence, this study is an attempt to understand the mechanism of action of  $^{131}\text{I}$ -rituximab in Raji cells.

### 3.2 SCOPE AND OBJECTIVE OF THE CHAPTER

Wide clinical use of monoclonal anti-CD20 antibody of murine origin has a major challenge as these may trigger HAMA response in patients. Both the radioimmunotherapeutic anti-CD20 agents viz. Bexxar and Zevalin suffer from this limitation. Hence, a chimeric monoclonal antibody like rituximab has emerged as a promising therapeutic agent, and may exhibit better therapeutic efficacy. Rituximab itself induces cell killing in various ways (Fig 3.1). Its efficacy could be further enhanced with the incorporation of therapeutic radionuclides such as  $^{131}\text{I}$ . Evaluations of  $^{131}\text{I}$ -rituximab induced cytotoxicity in cancer cells are limited in literature (Wei et al. 2006 and 2009). Cytotoxic efficacy is also governed by the fate of  $^{131}\text{I}$ -rituximab after internalization in tumor cells. Hence, this study is of importance.

In Chapter 2, it was seen that beta radiation from  $^{131}\text{I}$  has higher cytotoxicity than  $\alpha$ -radiation in tumor cells, and among the various cancer cell lines studied, Raji cells were the most susceptible. Hence, in the next step selective targeting of  $^{131}\text{I}$  was carried out by radiolabeling of rituximab, a CD20 specific antibody. The efficacy of  $^{131}\text{I}$ -rituximab was studied in tumor cells expressing CD20 receptors. The aim was to study cellular localization/stability of  $^{131}\text{I}$ -rituximab bound to CD20 receptor and the molecular mechanism underlying the cytotoxicity in human lymphoma cells (Raji cells, CD20 positive).

### **3.3 MATERIALS AND METHODS**

#### **3.3.1 Reagents**

In-Situ Cell Death Detection ELISA kit' and BM chemiluminescence kit were purchased from Roche Diagnostics GmbH. FITC labeled human anti CD20 monoclonal antibody were procured from Invitrogen Carlsbad, CA, USA. PD10 column and hyperfilm (X-ray film) were purchased from GE Healthcare, Amersham, UK. Non-fat milk protein and primary antibody were purchased from Cell Signaling Technology, Danvers, MA, USA. All other reagents used were of cell culture grade.

#### **3.3.2 Cell culture**

Raji and U937 cell lines were obtained from the National Center for Cell Sciences (NCCS) Pune, India, and were cultured in RPMI-1640, supplemented with 10 % serum (Invitrogen) and antibiotic/antimycotic solution. All cultures were maintained at 37 °C in a humidified 5 % CO<sub>2</sub> incubator.

#### **3.3.3 Characterization of CD20 receptor by flow cytometry**

To ascertain the expression of CD20 receptor in Raji and U937 cells, flow cytometry was carried out. Cells were grown in six well plates, fixed in 2 % formaldehyde and stained with 5 µL FITC labeled mouse mAb to the human CD20 receptor in staining buffer (100 µL of 2 % serum in PBS) for one hour. Cells were washed twice with staining buffer. Fluorescence intensity of cells was recorded in Partec flow cytometry system (Partec GmbH, Munster, and Germany) and data was analyzed with Flowjo software (Tree Star, Inc., Ashland, OR).

### 3.3.4 Radiolabeling (Iodination) of rituximab with $^{131}\text{I}$

Rituximab was radioiodinated using the Iodogen method (Fraker et al. 1978). Rituximab (100  $\mu\text{g}$ ),  $\text{Na}^{131}\text{I}$  (~1 mCi, theoretical specific activity- 125Ci/mg) and 100  $\mu\text{L}$  of 0.5 M phosphate buffer, pH 7.5 were taken in an iodogen (1  $\mu\text{g}$ ) coated tube and mixed for ~10 min. The reaction was stopped by transferring the reaction mixture to a new glass vial.

### 3.3.5 Characterization of $^{131}\text{I}$ -rituximab

#### Column chromatography for purification

The reaction mixture was purified on PD10 Sephadex column using phosphate buffer (0.05 M, pH 7.6) as the eluent. Briefly, PD10 column was equilibrated with phosphate buffer and the reaction mixture was added on top of the column filter. The column was eluted with phosphate buffer and nearly 25 fractions (1 mL each) were collected in tubes. The radioactivity in the fractions was monitored by taking 5  $\mu\text{L}$  of each fraction and measuring it in a NaI(Tl) counter.

#### HPLC method for determination of yield and purity

The labeling yield and radiochemical purity were determined by HPLC (JASCO with Ray test radiation detector GmbH, Germany) in TSK gel column (Tosoh Bioscience, PA USA) in isocratic mode using 0.05 M phosphate buffer, pH 6.8 as the mobile phase. About 10  $\mu\text{L}$  of rituximab,  $\text{Na}^{131}\text{I}$ , reaction mixture and purified fraction of  $^{131}\text{I}$ -rituximab were injected separately and the HPLC patterns were recorded in both radioactivity as well as UV channel. The rituximab peak followed through the UV signals was used for identification of the radiolabeled rituximab and to ascertain the purity of  $^{131}\text{I}$ -rituximab. The radioactivity peak for  $\text{Na}^{131}\text{I}$  was used to identify the unlabeled free



iodide ( $\text{Na}^{131}\text{I}$ ) in the reaction mixture. The labeling yield was calculated as the percent of radioactivity in the  $^{131}\text{I}$ -rituximab peak in the HPLC profile of the reaction mixture.

### 3.3.6 Determination of specificity and interference of FCS on cell binding of $^{131}\text{I}$ -rituximab

In order to estimate the extent of binding,  $1 \times 10^6$  cells of U937 (CD20 negative) and Raji (CD20 positive) were incubated for 2 h with  $^{131}\text{I}$ -rituximab (0.037 MBq) at 37 °C. The cells were washed thrice with PBS and radioactivity was measured in NaI(Tl) counter. Cell binding was expressed as percent cell binding, calculated as (radioactivity count rate associated with cell/total tracer radioactivity count rate)  $\times 100$ .

To determine the extent of interference of FCS, cell binding was performed in culture media containing 1 % and 10 % FCS. Raji cells ( $1 \times 10^6$ ) were incubated for 2 h with  $^{131}\text{I}$ -rituximab (0.037 MBq) at 37 °C. Cells were washed thrice with PBS and radioactivity was measured in NaI(Tl) counter.

### 3.3.7 Study of competitive inhibition of $^{131}\text{I}$ -rituximab with rituximab in Raji cells

Competitive inhibition studies were carried out in Raji cells to demonstrate the specificity of  $^{131}\text{I}$ -rituximab retention towards the CD20 receptor. Raji cells ( $1 \times 10^6$ ) were incubated for 2 h at 37°C with 0.037 MBq of  $^{131}\text{I}$ -rituximab along with different amounts of rituximab (0.1-100  $\mu\text{g}$ ). The cells were washed with PBS and radioactivity was measured in NaI(Tl) counter. Percent cell binding inhibition was calculated as  $\{[1 - (\% \text{ cell binding in presence of rituximab} / \% \text{ cell binding in absence of rituximab})] \times 100\}$ .

### 3.3.8 Standardization of incubation time and concentration of $^{131}\text{I}$ -rituximab for optimal cell binding in Raji cells

To assess the minimum number of washing required to remove the nonspecific cell binding of the radiolabeled antibody, Raji cells ( $1 \times 10^6$ ) were incubated for 2 h with  $^{131}\text{I}$ -rituximab (0.037, 0.37, 1.85 and 3.7 MBq) at 37 °C. The cells were washed four times with PBS and after every wash the radioactivity associated with the cells was measured using NaI(Tl) counter.

To standardize the optimal concentration of  $^{131}\text{I}$ -rituximab and time of incubation for maximum cell binding, Raji cells ( $1 \times 10^6$ ) were incubated with varying amounts of  $^{131}\text{I}$ -rituximab (0.037, 0.37, 1.85 and 3.7 MBq) for 30 min., 2 and 6 h at 37 °C. The cells were washed thrice with PBS and the radioactivity associated with cells was measured in gamma counter NaI(Tl). Cell binding was calculated as described earlier.

### 3.3.9 Cell irradiation and dosimetry of $^{131}\text{I}$ -rituximab

The optimum concentration of  $^{131}\text{I}$ -rituximab and time of incubation were 1.85 MBq and 2 h, respectively. In further experiments, Raji cells ( $1 \times 10^6$ ) were mixed with

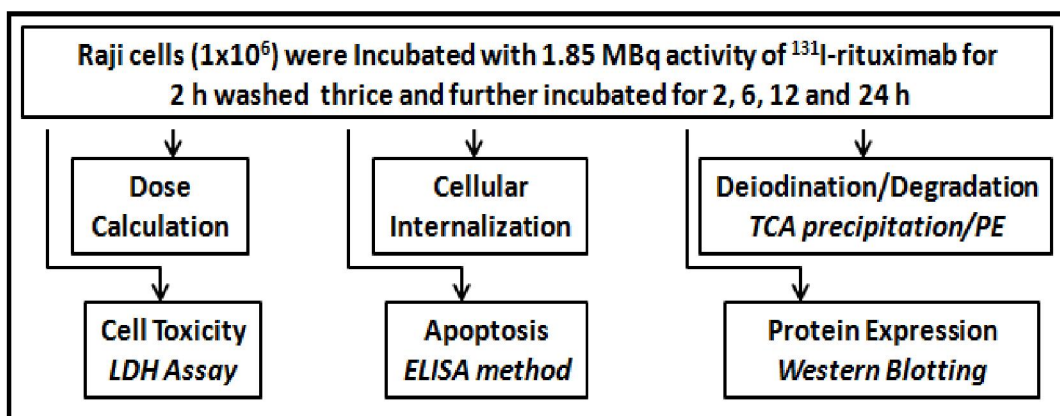
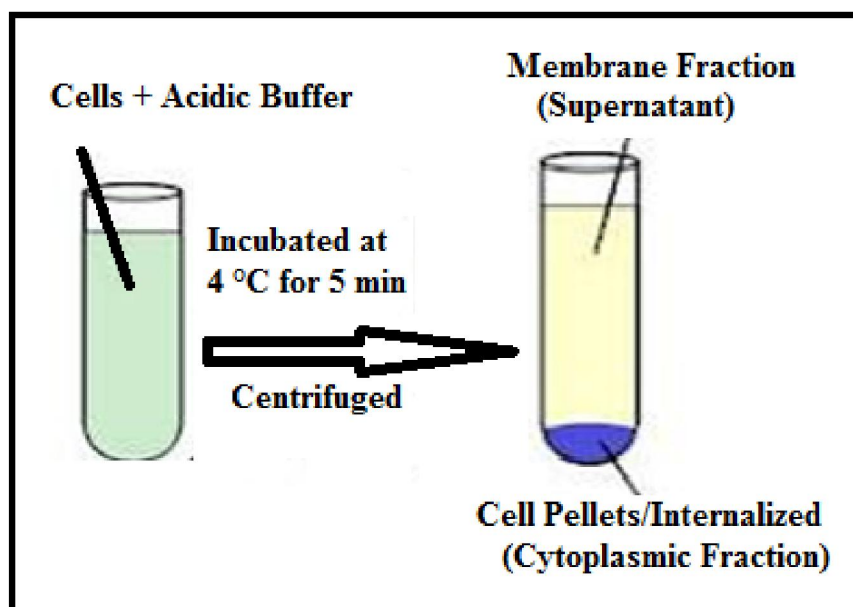


Figure 3.2 Flow chart of experimental plan

1.85 MBq of  $^{131}\text{I}$ -rituximab and incubated for 2 h. Raji cells were harvested after 2h, washed thrice with PBS and incubated for 2, 6 12 and 24 h. The fraction of  $^{131}\text{I}$ -rituximab that were bound to the CD20 of Raji cells after washing continuously irradiated Raji cells and contributes towards the increase in total absorbed dose with the increase of time of incubation (as mentioned in Section 2.3.4).

### 3.3.10 Study of cellular internalization of $^{131}\text{I}$ -rituximab in Raji cells by membrane stripping

The binding of  $^{131}\text{I}$ -rituximab to the CD20 is similar to the antigen-antibody binding and comprised of several hydrogen bonds. At acidic pH, these hydrogen bonds are disrupted and the CD20 receptor bound  $^{131}\text{I}$ -rituximab gets detached. This principle is used in membrane stripping, wherein acidic pH is used to separate the membrane bound radiolabeled antibody, which can then be quantified by measuring radioactivity in the supernatant fraction. The radioactivity in cell pellets represents the  $^{131}\text{I}$ -rituximab that is internalized in the cells. In this set of experiments, the Raji cells ( $1 \times 10^6$ ) were harvested after 2, 6, 12 and 24 h of treatments and treated with acidic buffer (200 mM sodium acetate in 500 mM of sodium chloride pH 2.5 for 5 min. at 4 °C) followed by centrifugation (1400  $\times$ g; 5 min.) (Fig.3.3). Cell pellets were washed twice with the acidic buffer and the supernatant were pooled to measure the total radioactivity stripped from the cell membrane. Cell pellets were lysed in 1 N NaOH and the radioactivity internalized in the cells was measured in a NaI(Tl) counter. Percent distribution of  $^{131}\text{I}$ -rituximab, either in supernatant fraction (membrane bound) or cell pellets fraction (cytoplasm or internalized) was calculated as following: {Radioactivity in either supernatant or cell pellets / [total radioactivity (supernatant + cell pellets)]  $\times$  100}.



**Figure 3.3** Schematic representation of membrane stripping

### 3.3.11 Estimation of degradation and deiodination of $^{131}\text{I}$ -rituximab in Raji cells

This experiment was carried out to estimate the degradation/deiodination of  $^{131}\text{I}$ -rituximab in due course of incubation after cell binding assay. Raji cells ( $1 \times 10^6$ ) were treated with  $^{131}\text{I}$ -rituximab for 2 h at 37 °C followed by washing and incubation, as detailed in the earlier experiments. Cells were harvested at different time periods (2, 6, 12 and 24 h) and supernatant culture media were collected by centrifugation (1400×g; 5 min.). Radioactivity in supernatant and cell pellets was determined by using NaI(Tl) counter. Supernatant was used to estimate deiodination or degradation of  $^{131}\text{I}$ -rituximab by TCA precipitation and paper electrophoresis method, as described below:

#### TCA precipitation

For TCA precipitation (Fig 3.4a), 500  $\mu\text{L}$  of supernatant media was mixed with 2 mg of immunoglobulin (as carrier) in ice cold 10 % trichloroacetic acid (TCA). The mixture

was vortexed followed by centrifugation at  $10,000 \times g$  for 10 min. The supernatant was carefully transferred and pellets were dissolved in 1mL of 2 N NaOH. The radioactivity in both fractions was measured using NaI(Tl) counter and the percentage radioactivity in both fractions was calculated as following:  $\{ \text{Radioactivity in either supernatant or protein pellets} / [\text{total radioactivity (supernatant + protein pellets)}] \} \times 100$ .

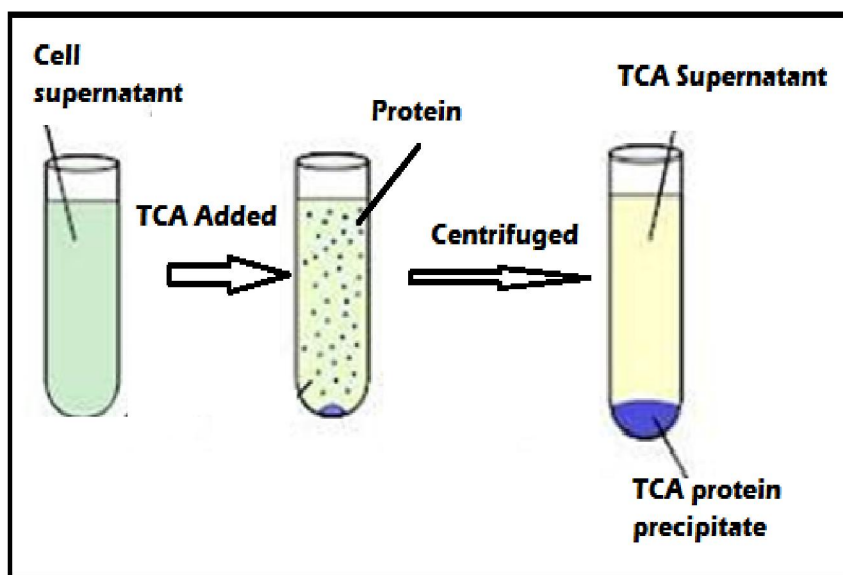


**Figure 3.4a** Schematic representation of TCA precipitation method

### Paper electrophoresis

For paper electrophoresis (Fig 3.4b), Whatman paper strip (30 ×1 cm) was soaked in 0.025 M phosphate buffer pH 7.6 and left in air for a few minutes to allow the excess buffer to evaporate so that the sample can be applied on the paper without spreading. Cell supernatants (20  $\mu$ L) from each time point were spotted on separate paper strips at the centre and electrophoresis was carried out at 245 V for an hour. The paper strip was dried, cut into 1 cm pieces and the radioactivity in each piece was counted in NaI(Tl) counter.

$^{131}\text{I}$ -rituximab and  $\text{Na}^{131}\text{I}$  were used as control samples to ascertain that the radiolabeled

antibody stays at the point of application and to note the position of migration of iodide species towards the anode. Percent radioactivity retained either at the point of application or migrated as iodide species was calculated as  $\{\text{Radioactivity in either point of spotting or point of radioiodide} / [\text{total radioactivity}] \times 100$ .

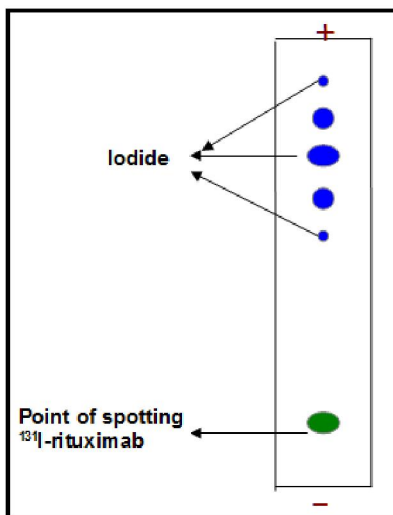


**Figure 3.4b** Schematic representation of paper electrophoresis

### 3.3.12 Estimation of cell toxicity by lactate dehydrogenase assay

Raji cells ( $1 \times 10^6$ ) were treated with  $^{131}\text{I}$ -rituximab (1.85 MBq) or an equivalent amount of rituximab (as vehicle control) in complete medium in culture conditions for 2 h, followed by washing of cells (as mentioned earlier) and further incubation. After completion of different time periods of incubation, cells were centrifuged and the supernatant culture medium was collected to estimate the release of LDH. The release of LDH is an index of cell death. The LDH assay was carried out according to the protocol described in the kit. In brief, LDH assay mixture was prepared freshly before use by mixing equal volume of LDH assay substrate, cofactor and dye. The reaction mixture was added alongwith culture media (2:1, v/v) in 96 well plates. They were mixed well and

covered with aluminum foil to protect from light and incubated for 25 min at room temperature. The reaction was terminated by adding 1/10<sup>th</sup> volume of 1 N HCl and the absorbance was measured at 490 nm. The percent release of LDH was calculated as [(OD of treated sample/ OD of control sample) × 100].

### **3.3.13 Estimation of apoptotic DNA fragmentation**

For determination of magnitude of apoptosis, DNA fragmentation study was carried out according to protocol described in In-Situ Cell Death Detection ELISA kit. Raji cells were harvested after completion of treatment followed by incubation and nearly 1×10<sup>5</sup> cells were lysed using lysis buffer for 30 min and centrifuged to 20,000 × g for 10 min. Supernatant was carefully transferred to new tubes. ELISA plate was coated overnight at 4 °C with anti-histone antibody followed by incubation of 100 µL of cell lysate for 90 min. Thereafter, the wells were washed thrice with buffer (provided with kit) and incubated with anti-DNA-HRP antibody for 90 min. The wells were again washed thrice with buffer and subsequently incubated with substrate solution for 20 min. The color obtained was quantified at 405 nm. DNA fragmentation was expressed as EF which is the ratio of OD of treated to control sample.

### **3.3.14 Study of expression of apoptotic proteins by Western blotting**

Raji cells were harvested after completion of treatment followed by incubation and lysed in cellLytic<sup>TM</sup> cell lysis buffer (Sigma) and protease inhibitor cocktail (Sigma). The protein concentration in samples was estimated by Bio-Rad Protein assay. Protein (50 µg) was loaded on 10 % and 15 % SDS PAGE gel for PARP and p53 proteins respectively, and the electrophoresis was carried out. The protein was transferred onto nitrocellulose

membrane by electroblotting. Membrane blocking was carried out using 5 % non-fat milk protein followed by incubation (1.5 h) with primary antibodies for PARP, p53 and beta-actin. The membrane was washed with Tris buffer saline with Tween 20 (0.1 %) followed by treatment with secondary antibody. The membrane was incubated with BM luminescent reagents followed by exposure to Hyper-film, which was processed and developed by Kodak developer and fixer solution.

### **3.3.15 Statistical analysis**

Unless mentioned, the results are mean  $\pm$  SD of at least three independent experiments, where t-test was used to compare control and irradiated samples. Significance level was determined by considering  $p$  values below 0.05.



### 3.4. RESULTS

#### 3.4.1 Magnitude of CD20 receptor expression in Raji and U937 cell line

In order to establish the magnitudes of CD20 expression in Raji and U937 cell lines, cells were labeled with FITC-CD20 antibody, followed by flow cytometry. The results of the flow cytometry experiments (Fig.3.5) suggest that the percentage of FITC positive cells for the CD20 antigen were  $69.4 \pm 1.2$  % for Raji cells whereas for U937 it was only  $3.5 \pm 0.376$  %.

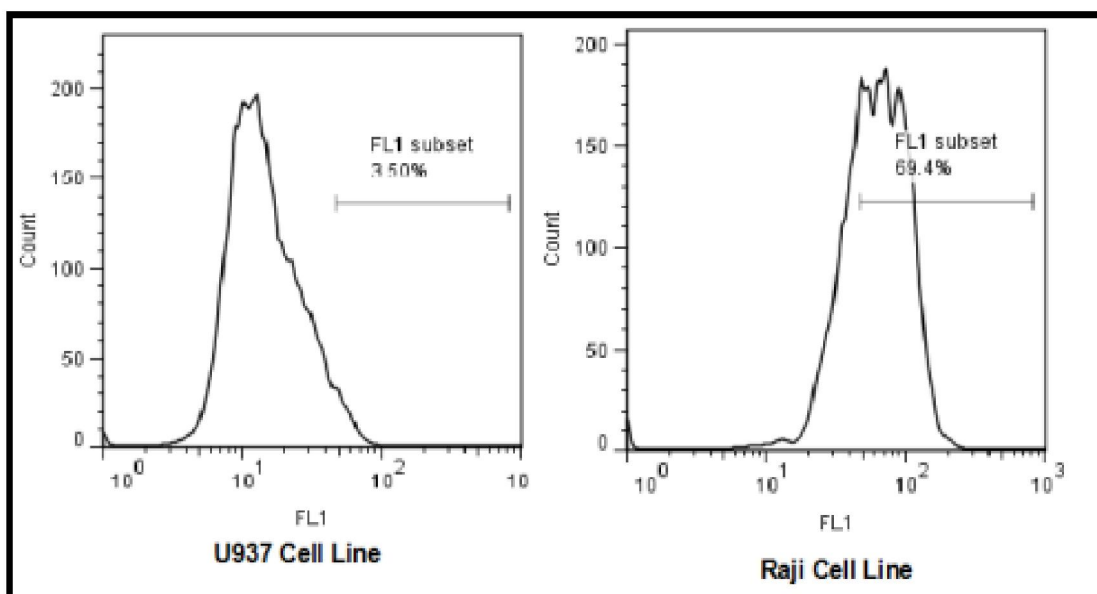


**Figure 3.5** Flow cytometry analysis of CD20 receptor in U937 and Raji cells

#### 3.4.2 Radiolabeling and characterization of <sup>131</sup>I-rituximab

Rituximab was labeled with radioiodine (<sup>131</sup>I) by the iodogen method. The radioiodination yield was >90 %, as determined by HPLC. The PD10 column elution profile is shown in Fig 3.6a. In PD10 column, bigger molecules are eluted earlier than the smaller molecules. The <sup>131</sup>I-rituximab eluted in the third and fourth fraction while free

iodide was eluted in the 10<sup>th</sup> fraction onward. The radiochemical purity of  $^{131}\text{I}$ -rituximab was >99 % determined by HPLC after PD10 column purification. Specific activity of  $^{131}\text{I}$ -rituximab obtained was 0.30-0.35 MBq/ $\mu\text{g}$ . HPLC pattern of rituximab,  $^{131}\text{I}$ , reaction mixture and purified fraction of  $^{131}\text{I}$ -rituximab are depicted in Fig 3.6b. It was found that rituximab and radioiodide were eluted at 15 and 22 minutes, respectively. In the reaction mixture, a few small peaks were seen which was eluted earlier than 15 minutes, were perhaps the aggregates of  $^{131}\text{I}$ -rituximab. Similar peaks are also seen in the UV profile of the rituximab. However, these small peaks were not visible in purified fraction of  $^{131}\text{I}$ -rituximab.

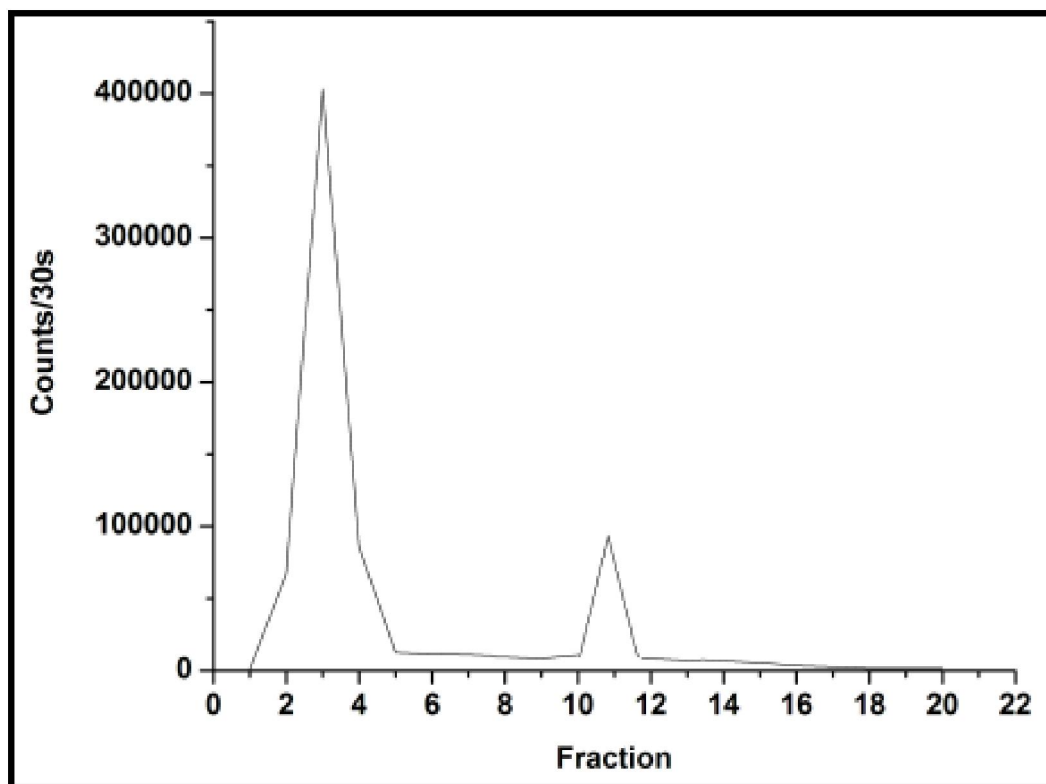


**Fig 3.6a** PD10 column elution profile of  $^{131}\text{I}$ -rituximab

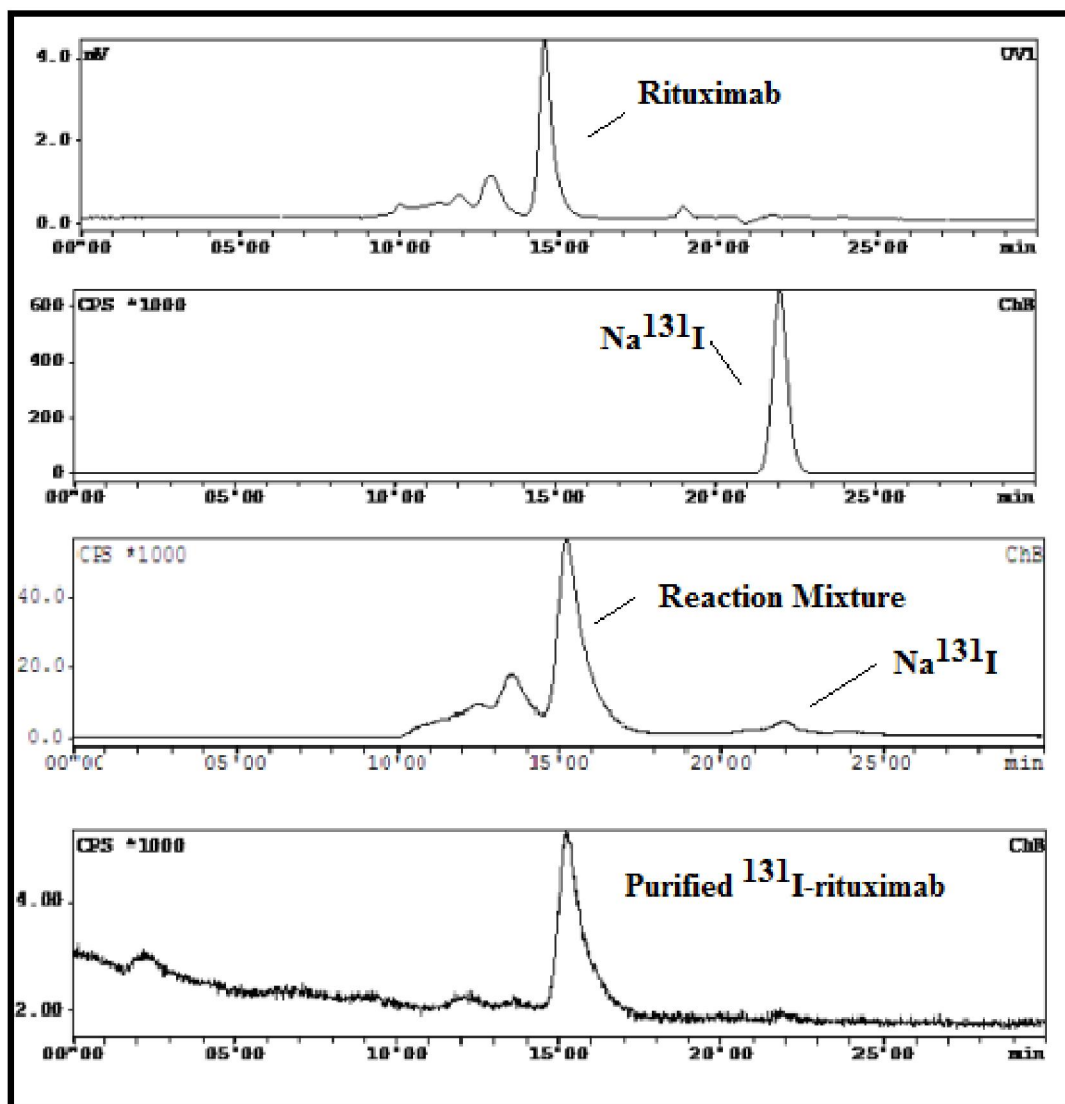


**Fig. 3.6b** HPLC pattern of rituximab, <sup>131</sup>I, reaction mixture with free iodide and purified fraction of <sup>131</sup>I-rituximab

### 3.4.3 Dosimetry of beta irradiation of <sup>131</sup>I-rituximab treated Raji cells

The total dose delivered was calculated which was 0.38 Gy during 2 h incubation period. These cells containing residual <sup>131</sup>I-rituximab radioactivity, were further incubated for 2, 6 12 and 24 h, and contributes the theoretical absorbed dose of 0.01, 0.02, 0.04 and 0.08Gy respectively. Hence, the cumulative dose received by cells during incubation

period of 2h followed by additional 2, 6 12 and 24 h, were 0.39, 0.40, 0.42 and 0.46 Gy respectively.

#### 3.4.4 Standardization of incubation time and concentration of $^{131}\text{I}$ -rituximab for optimal cell binding in Raji cells

The initial sets of experiments were carried out to determine the minimum number of washing steps required to minimize the nonspecific cell binding. It involved incubation of Raji cells ( $1 \times 10^6$ ) for 2 h with different amounts of  $^{131}\text{I}$ -rituximab (0.037, 0.37, 1.85 and 3.7 MBq) at 37 °C. The cells were washed four times with PBS and radioactivity after each washing step was measured in NaI(Tl) counter. It was found that there is no significant difference in radioactivity counts after third and fourth washings (Fig. 3.7), indicating that three washings were adequate to remove the non-specifically bound  $^{131}\text{I}$ -rituximab. Hence unless stated, further experiments were carried out with three washings in PBS after treatment of  $^{131}\text{I}$ -rituximab.

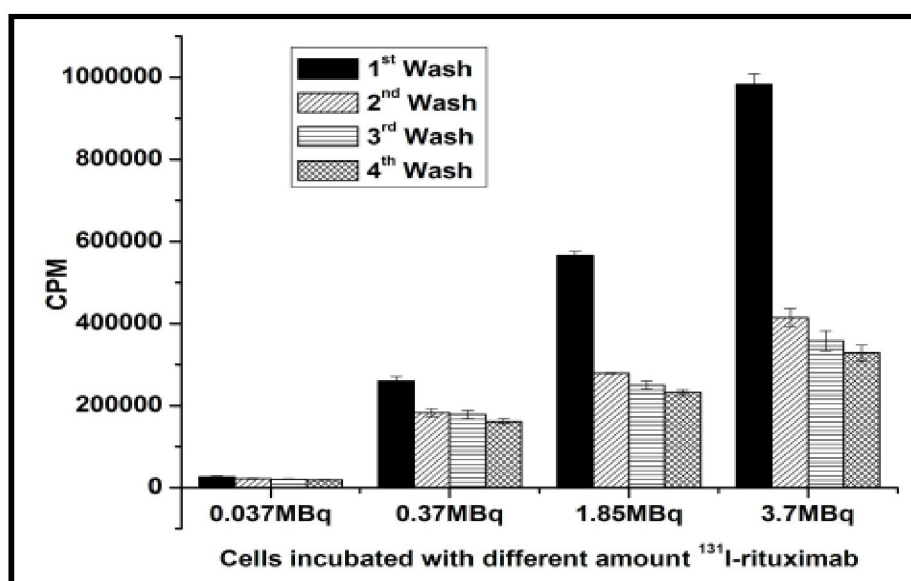


**Figure 3.7** Radioactivity counts in Raji cells incubated with  $^{131}\text{I}$ -rituximab after four washes

### 3.4.5 Effect of FCS on cell binding

Generally, cell binding experiments are carried out in 1 % FCS. In this experiment, cell binding studies were carried out at 37 °C for 2 h and further incubated for 24 h. Hence, it was necessary to maintain the optimum FCS concentration (10 %) for optimal cell growth due to long incubation of treated cells during the experiments. To find any change occurred in cell binding, the experiment was carried out in 1% and 10 % FCS concentration in culture media. The lowest concentration of  $^{131}\text{I}$ -rituximab (0.037 MBq) was chosen and incubated for 2 h with the cells containing 1 % and 10 % FCS. It was found that the average radioactivity counts per million cells were almost similar in both cases, namely 1 and 10 % FCS (Fig. 3.8). Hence all experiments were carried out at 10 % FCS containing media to maintain the optimum culture condition for the growth of cells.

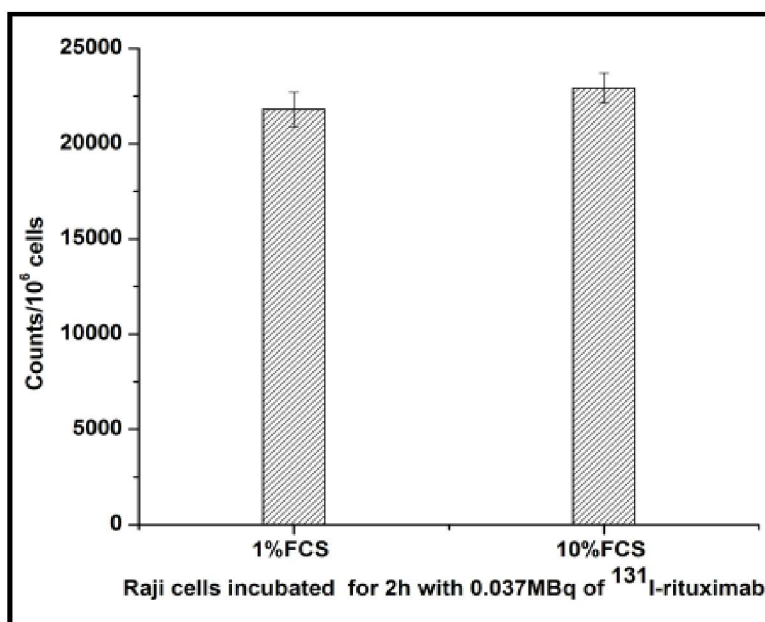


**Figure 3.8** Radioactivity counts in Raji cells incubated with  $^{131}\text{I}$ -rituximab with two different amount of FCS

### 3.4.6 Study of antibody specificity and competitive cell binding inhibition in Raji cells

In order to establish the functional CD20 receptor expression in Raji and U937 cell lines, cell binding experiments were carried with  $^{131}\text{I}$ -rituximab (0.037 MBq; incubation 2 h). These results depicted in Fig 3.9a, showed that compared to Raji cells (~12 % binding), the U937 cells exhibited very low binding (<0.5 %), confirming the specificity of  $^{131}\text{I}$ -rituximab to Raji tumor cells with CD20 receptors.

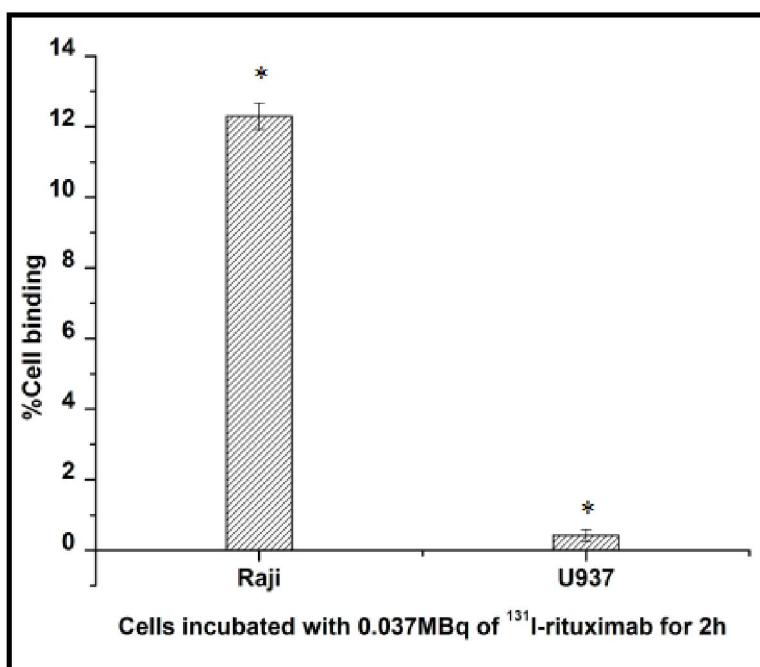


**Figure 3.9a** Percent cell binding in Raji and U937 cell line (where \* is significant with  $p < 0.05$  and  $n=3$ ).

To demonstrate the unaltered specificity of antibody (rituximab) after labeling with  $^{131}\text{I}$  ( $^{131}\text{I}$ -rituximab), competitive binding inhibition study was performed in presence of rituximab. The results of binding of  $^{131}\text{I}$ -rituximab (0.037 MBq) with Raji cells in the presence of increasing concentrations of rituximab (0.1-100  $\mu\text{g}$ ) for 2 h, were shown in

Fig. 3.9b. It was found that with increase in concentration of rituximab, the binding of the radiolabeled rituximab decreased, which attained saturation (~90 % inhibition) at 50  $\mu\text{g}$  or higher concentration of rituximab. These results suggest that the immunoreactivity of rituximab was retained after labeling with  $^{131}\text{I}$ .

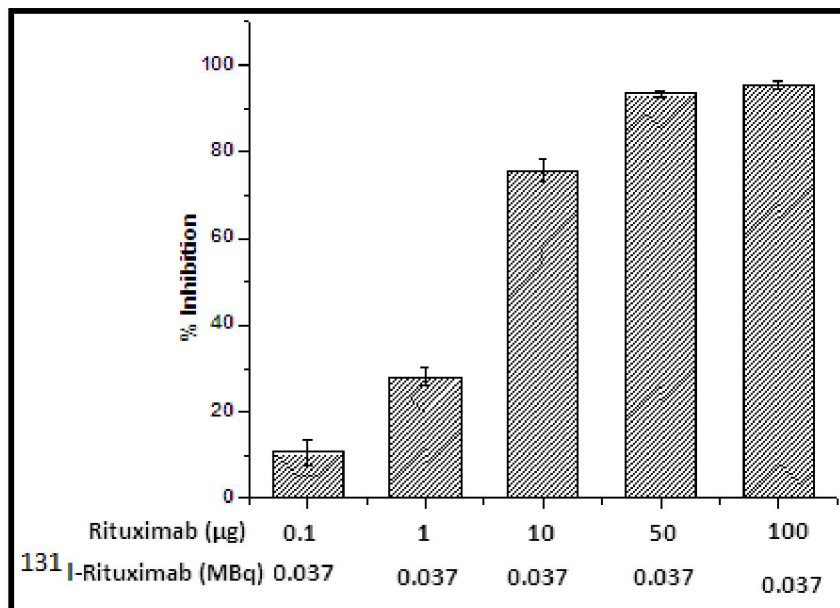


**Figure 3.9b.** Percent inhibition of  $^{131}\text{I}$ -rituximab in Raji cells after incubation of rituximab

#### 3.4.7 Optimization of time of incubation and concentration of $^{131}\text{I}$ -rituximab for treatment of Raji cells

It was found that, 2 h time period is optimum for obtaining maximum cell binding (Fig. 3.10a). The maximum radioactivity per million cells was observed for 2 h incubation irrespective of the amount of  $^{131}\text{I}$ -rituximab used (Fig. 3.10b). However, saturation of the cell bound radioactivity of  $^{131}\text{I}$ -rituximab was observed at 1.85 and 3.7 MBq per million cells. Hence, 1.85 MBq of  $^{131}\text{I}$ -rituximab and 2 h time period of incubation were considered for further experiments.

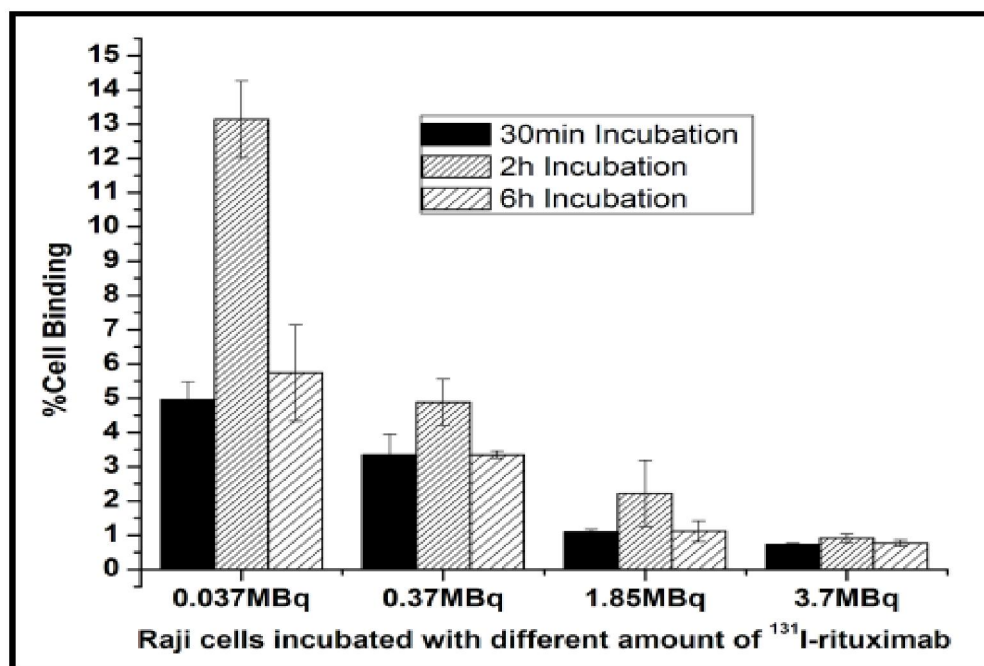


Figure 3.10a Percent cell binding in Raji cells

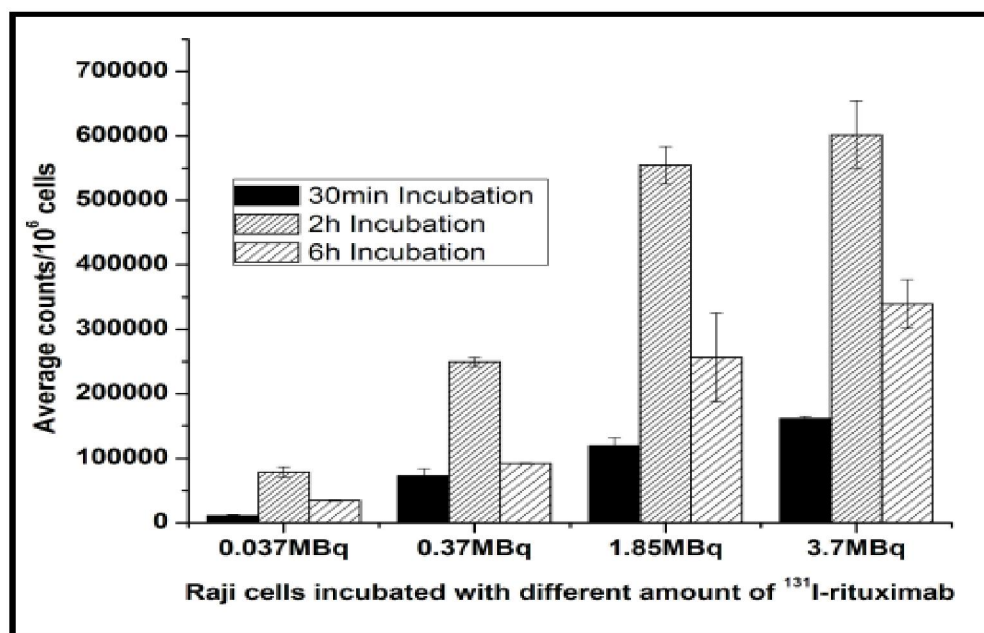
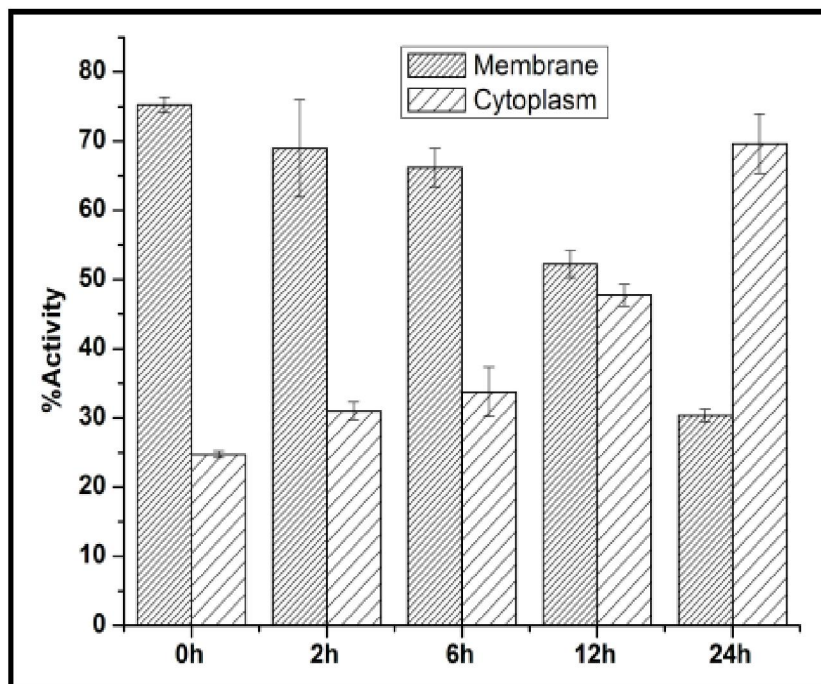


Figure 3.10b Average radioactivity counts per million of Raji cells



### 3.4.8 Study of cellular internalization of $^{131}\text{I}$ -rituximab in Raji cells

In order to study whether the  $^{131}\text{I}$ -rituximab bound to tumor cells was internalized into cytoplasm or remains membrane bound, the treated Raji cells (1.85 MBq, 2 h) were washed and again incubated for 24 h. The membrane stripping was carried out at 2, 6, 12 and 24 h. It was observed that upto 6 h, major fraction (~70 % of total radioactivity associated with cells) was membrane bound whereas at 24 h, the membrane bound radioactivity decreased to ~30 % (Fig. 3.11a). In accordance, the cytoplasmic fraction was lower at 6 h which increased significantly at 24 h of incubation. To verify, whether the membrane stripped Raji cells retained the morphology after acidic wash, cells were observed under microscope. It was found that there were no difference in the morphology of treated and control cells (Fig. 3.11b).



**Figure 3.11a** Distribution of  $^{131}\text{I}$ -rituximab on cell membrane and cytoplasm in Raji cells at different incubation period

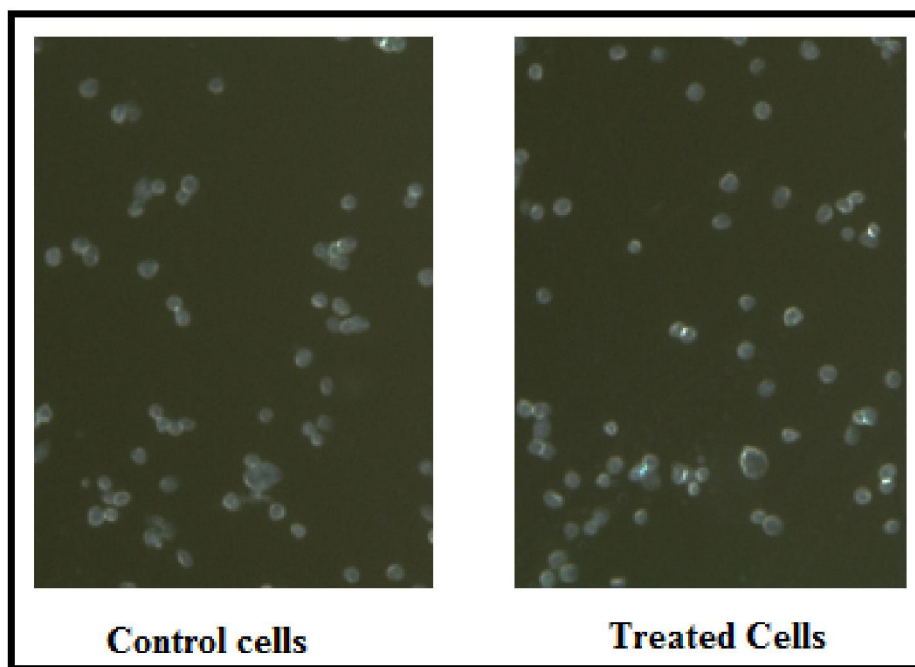


**Figure 3.11b** Morphology of membrane stripped Raji cells

#### 3.4.9 Study of stability of $^{131}\text{I}$ -rituximab and its deiodination/degradation in Raji cells

On increase of time of incubation of Raji cells with  $^{131}\text{I}$ -rituximab, beyond 2 h, the total cell bound radioactivity decreased, as shown in the Fig. 3.10b. Hence, to investigate the stability of  $^{131}\text{I}$ -rituximab bound with CD20 receptors in Raji cells during 2-24 h of incubation, radioactivity was determined in culture medium (supernatant) and cell pellets at various time intervals. The results are depicted in Fig. 3.12a and it can be seen that radioactivity in supernatant increased from  $59.85 \pm 1.55$  % at 2 h to  $83.82 \pm 1.51$  % at 24 h incubation period, while the radioactivity associated with cells decreased from  $40.15 \pm 0.37$  % at 2 h to  $16.17 \pm 0.12$  % at 24 h of incubation, indicating that on longer periods of incubation than 2 h, the fraction of  $^{131}\text{I}$ -rituximab associated with Raji cells declines.

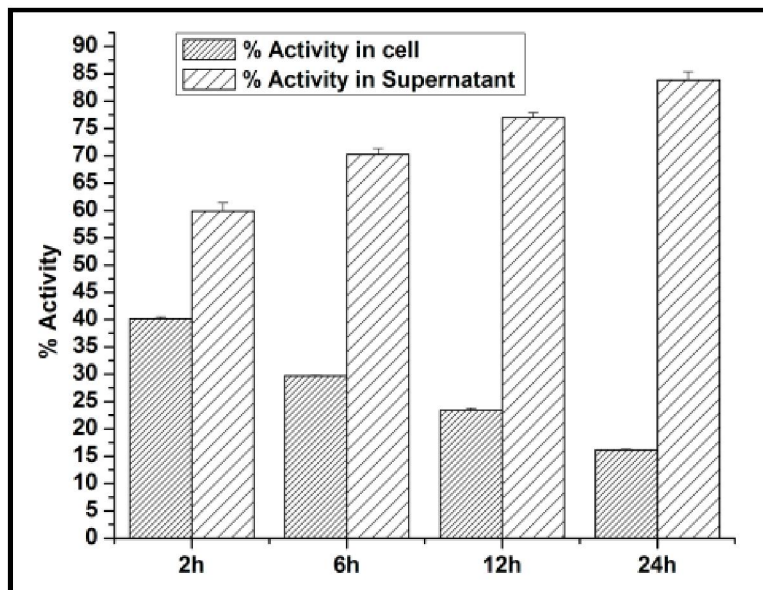


**Figure 3.12a** Distribution of  $^{131}\text{I}$ -rituximab on cells and cell supernatant

The change in radioactivity in cell bound fraction during course of incubation as above observations may be due to three reasons either independently or in combination: (i) detachment of  $^{131}\text{I}$ -rituximab from the cells surface; (ii) degradation of  $^{131}\text{I}$ -rituximab and (iii) deiodination of  $^{131}\text{I}$ -rituximab. Hence, to find the changes in radioactivity in cell bound fraction during the course of incubation, the following experiments were performed. The supernatant culture media of  $^{131}\text{I}$ -rituximab treated Raji cells (treated followed by washing and incubation) was obtained after different incubation periods. The magnitude of degradation/deiodination of  $^{131}\text{I}$ -rituximab was estimated in these culture media by TCA precipitation (Fig. 3.12b). It was found that the radioactivity associated with TCA precipitate was almost constant (90-95 %) up to 12 h incubation period, which decreased to ~75 % at 24 h (Fig. 3.12b), indicating that up to 12 h the  $^{131}\text{I}$  was associated with the antibody and the deiodination or degradation was slowly increased to an extent of 20-25 % in the next 12 h.

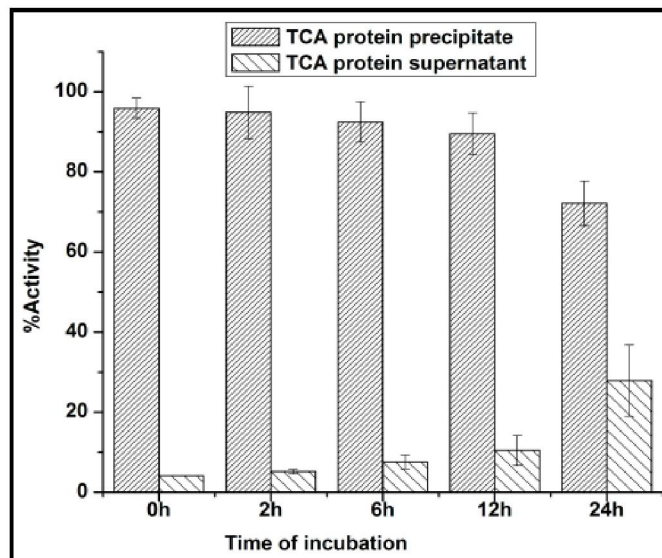


**Figure 3.12b** Percentage of radioactivity count in TCA precipitate and supernatant

In accordance, the radioactivity in supernatant fraction (of TCA precipitate) was nearly the same for up to 12 h (5-12 %), which increased to ~ 25 %, at 24 h. The observation from TCA precipitation method was further corroborated by paper electrophoresis method, whose results are depicted in Fig. 3.12c. It was found that the radioactivity associated with the point of spotting remains high (~90-95 %) for up to 6 h, which subsequently decreased to 75-80 % at longer time of incubation (12 and 24 h). However, the radioactivity in iodide zone, which represents free iodide, showed only ~10 % even at 24 h time point. This indicates that, at longer time period of incubation,  $^{131}\text{I}$ -rituximab perhaps gets detached from the CD20 receptor, degrade to small fragments due to auto radiolysis of  $^{131}\text{I}$ -rituximab and also get deiodinated. The smaller fragments may not be precipitated by TCA and hence in TCA supernatant at 24 h time point, ~24 % radioactivity was estimated, which may be due to free iodide ( $\text{Na}^{131}\text{I}$ ) and smaller fragments of  $^{131}\text{I}$ -rituximab.

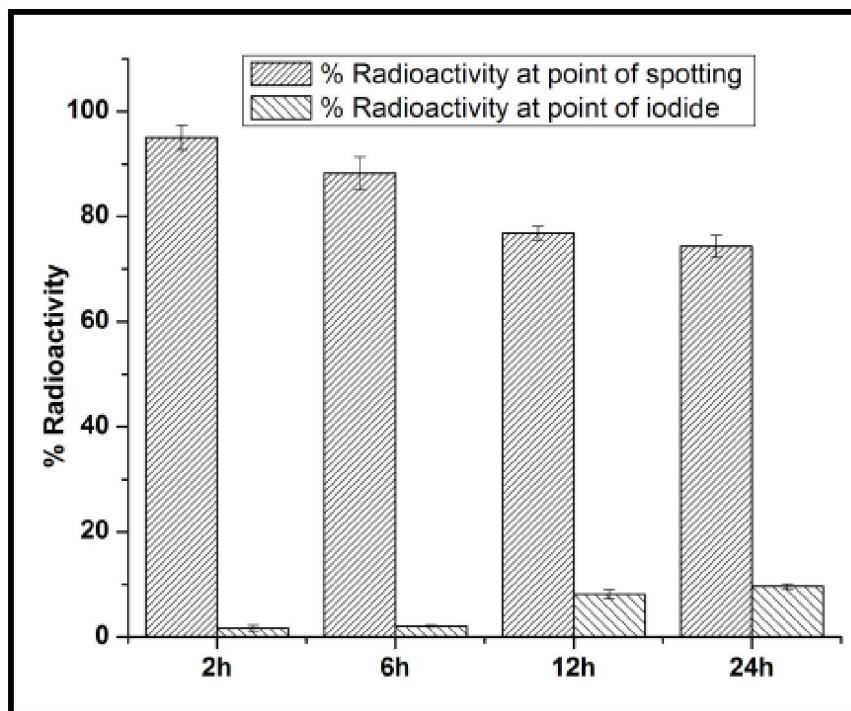


**Figure 3.12c** Percentage of radioactivity count in supernatant by paper electrophoresis

#### 3.4.10. Effect of $^{131}\text{I}$ -rituximab on cell toxicity in Raji cells

LDH gets released from the cells when the cell membrane is damaged and hence serves as a marker of cell toxicity. Raji cells treated with 1.85 MBq radioactivity of  $^{131}\text{I}$ -rituximab were assessed for cell toxicity by LDH assay after different incubation periods (2, 6, 12 and 24 h). Fig. 3.13 depicts the results of the cell toxicity expressed as percent LDH release, both for the  $^{131}\text{I}$ -rituximab as well as the vehicle control using an equivalent concentration (5  $\mu\text{g}$ ) of rituximab. It was observed that the cells treated with rituximab followed by incubation, showed increase in LDH release (1.5-3 fold) depending on the increase in duration of incubation. However, the extent of cell toxicity in  $^{131}\text{I}$ -rituximab treated cells was observed to be significantly higher than those observed

for unlabeled rituximab. An increase of 3-7.5 fold in LDH release was observed with radiolabeled antibody while in the case of unlabeled antibody it was 1-5-3 fold. These studies suggest that  $^{131}\text{I}$ -rituximab has additional therapeutic effect and causes cytotoxicity in Raji cells than the rituximab.

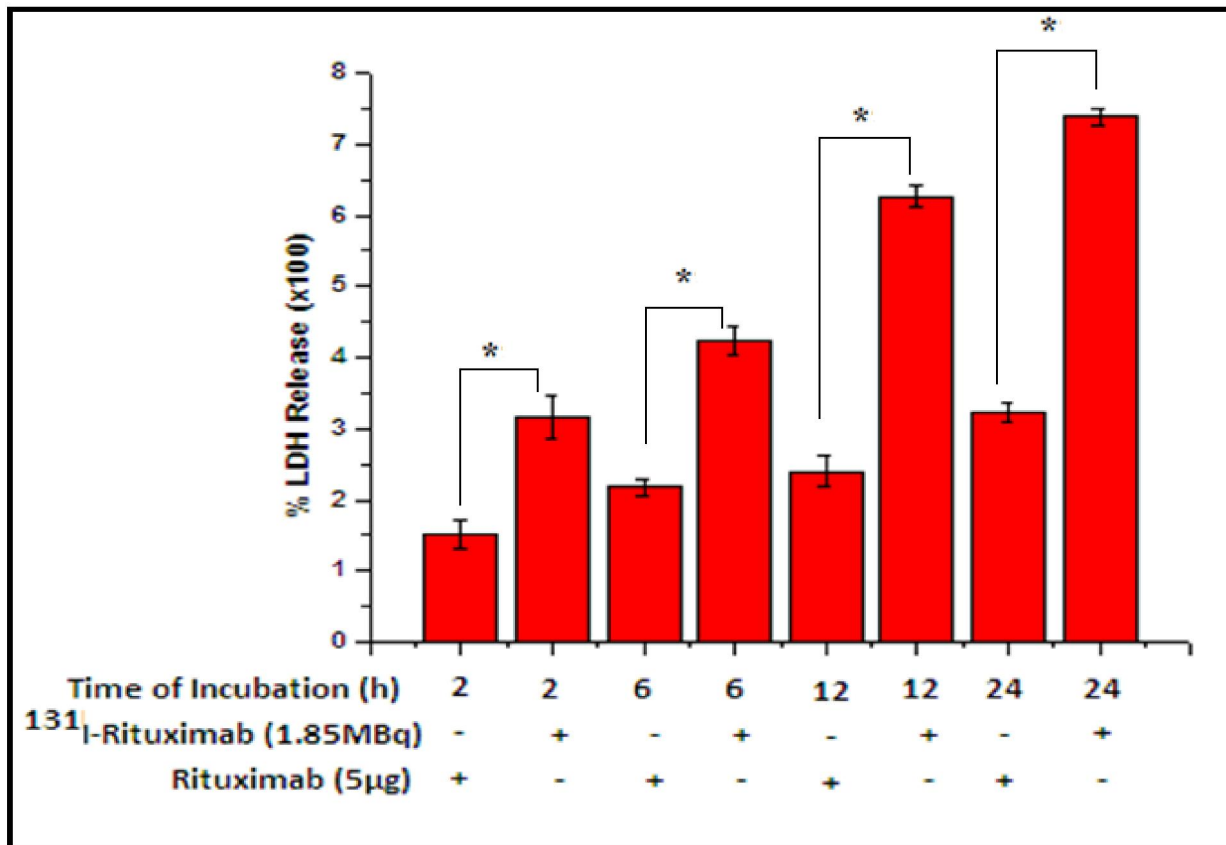


**Figure 3.13** Percentage of LDH release in supernatant after  $^{131}\text{I}$ -rituximab treatment of Raji cells.

( $^{131}\text{I}$ -rituximab treatment is significantly higher than the corresponding control.

Where \* p 0.05 and n=3).

#### 3.4.11. Effect of $^{131}\text{I}$ -rituximab on induction of apoptosis

In order to elucidate, the underlying mechanism and mode of cell death in Raji cells after  $^{131}\text{I}$ -rituximab treatment, magnitude of apoptosis was determined by in-situ cell death detection ELISA method. The results showed in Fig. 3.14, indicate that the enrichment

factor of Raji cells treated with rituximab was increased from ~1.5 fold at 2 h to ~4 fold at 24 h, whereas in Raji cells treated with  $^{131}\text{I}$ -rituximab increased from ~1.5 fold at 2 h to ~25 fold at 24 h. This clearly indicates that the radiation has positive impact on induction of apoptosis in comparison with the rituximab alone.

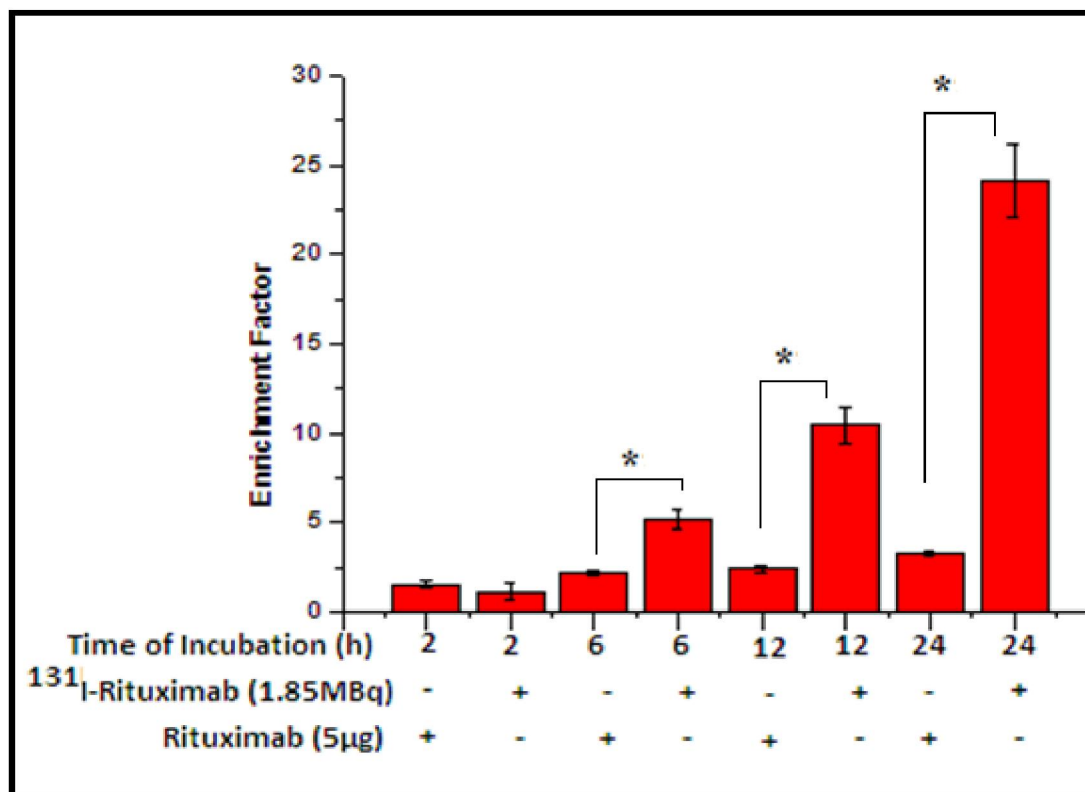


**Figure 3.14.** Apoptotic DNA enrichment factor in Raji cells upon exposure of  $^{131}\text{I}$ - rituximab.

( $^{131}\text{I}$ -rituximab treatment is significantly higher than the corresponding control after 6 h of treatment. Where \* p 0.05 and n=3).

#### 3.4.12. Effect of $^{131}\text{I}$ -rituximab on expression of proteins associated with DNA damage and apoptosis

The role of DNA damage and apoptotic proteins in induction of apoptotic death was studied in Raji cells (p53 wild type) after  $^{131}\text{I}$ -rituximab treatment. The results depicted in



Fig. 3.15, show that P53, a marker of DNA damage, was upregulated after 6 h and downregulated at 12 and 24 h in Raji cells treated with  $^{131}\text{I}$ -rituximab. PARP, which gets cleaved during apoptosis, showed a cleaved fraction(s) at 6 h, which was maximum at 24 h of  $^{131}\text{I}$ -rituximab treatment. Compared to  $^{131}\text{I}$ -rituximab treated cells, the cells treated with rituximab showed lower expression of p53 and cleavage of PARP at different time points.

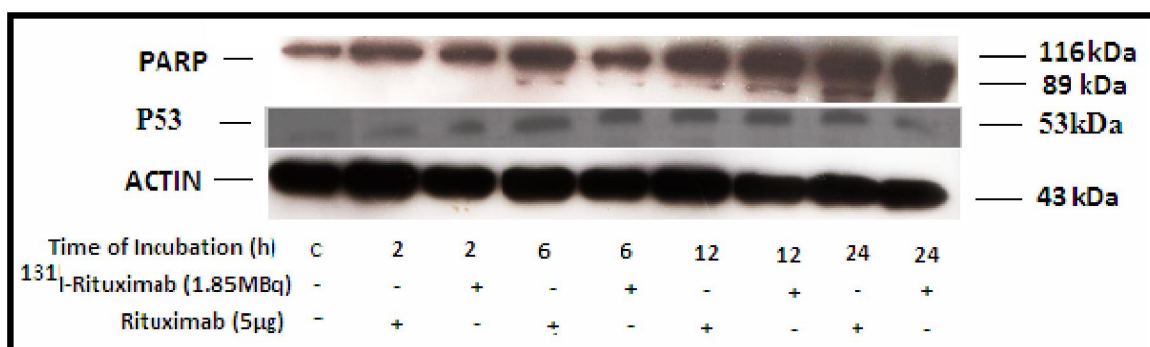


**Figure 3.15** Expression of apoptosis related proteins upon exposure due to  $^{131}\text{I}$ -rituximab in Raji cell



### 3.5.DISCUSSION

The aim of the present study was to investigate the internalization of  $^{131}\text{I}$ -rituximab to understand the fate of radiolabeled antibody and the mechanism of cytotoxicity in Raji cells. Iodogen method for radiolabeling of rituximab with  $^{131}\text{I}$  resulted in >90 % yields. On purification, it was possible to obtain radiolabeled antibody with >99 % radiochemical purity which was observed by HPLC analyses. Under the conditions of studies wherein,  $^{131}\text{I}$ -rituximab was used at a specific activity of 0.30-0.35 MBq/ $\mu\text{g}$ , The dose received by Raji cells were 46 cGy, which are comparatively lower than the prescribed dose limit of Bexxar and Zevalin i.e. 70 cGy (Baechler et al. 2010). The specific binding of  $^{131}\text{I}$ -rituximab to CD20 positive tumor cell line, in agreement with previous studies (Wei et al. 2006 and 2009) and the very low level of binding of  $^{131}\text{I}$ -rituximab to CD20 negative U937 cells (<0.5 %) indicate good specificity of  $^{131}\text{I}$ -rituximab. This is an important attribute desirable for a potential radiopharmaceutical. The instability of  $^{131}\text{I}$ -rituximab bound with Raji cells with incubation time, reported in this thesis can be attributed to deiodination and degradation of radiopharmaceuticals. It has been reported that the stability of antibodies labeled with radioisotopes ( $^{125}\text{I}$ ,  $^{188}\text{Re}$ ,  $^{111}\text{In}$ ) was evaluated up to 7 days for deiodination and degradation study (Shih et al. 1994), which occurred over longer period of time (7days,  $^{125}\text{I}$ ) than in this study (24 h,  $^{131}\text{I}$ ). The difference may be due to much higher energy of the beta particles emanating from  $^{131}\text{I}$  as well as the difference in type of cancer and its associated radiosensitivity. Cellular internalization study showed that radioactivity retained in tumor cells decreased with the time of incubation and concomitantly its degraded/deiodinated products in supernatant increased with incubation time as estimated

by TCA precipitation and paper electrophoresis. The difference (15 %) in the degraded  $^{131}\text{I}$ -rituximab radioactivity observed at 24 h between TCA precipitation and paper chromatography methods could be due to the small molecular weight fragmented  $^{131}\text{I}$ -rituximab, which are not precipitated by the TCA and therefore remains in the TCA supernatant.

Cellular toxicity caused by  $^{131}\text{I}$ -rituximab treatment was higher, compared to the rituximab. Rituximab is known to cause cytotoxicity in tumor cells involving cellular signaling pathways (Bonavida 2007). However, high energy beta radiation (0.6 MeV) would cause additional damage to tumor cells and the magnitude of damage gets enhanced due to localization of radioisotope very close to cellular targets such as membrane, cytoplasm and nucleus level. It may be pertinent to mention here that during kinetics of internalization,  $^{131}\text{I}$ -rituximab gets almost equally distributed to membrane and cytoplasm at 12 h period of incubation (Fig. 3.4.8a). Even though, beta radiation emitted from  $^{131}\text{I}$ -rituximab has an average range of 2.3 mm, at the time of equal distribution of  $^{131}\text{I}$ -rituximab to membrane and cytoplasm, there will be possibility of maximum damage to cellular targets including nucleus. Hence, one could expect higher tumor cytotoxicity at 12 h or longer periods, which is similar to the observation in cytotoxicity studies using LDH (Fig. 3.4.10) and apoptosis (Fig. 3.4.11) reported in this thesis.

To elucidate the mechanism underlying the cytotoxicity and apoptotic death in Raji cells after  $^{131}\text{I}$ -rituximab treatment, the expression of p53 and cleavage of PARP were studied. The results showed that in  $^{131}\text{I}$ -rituximab treated Raji cells, expression of p53 was maximum at 6 h. However, cleavage of PARP begins at 6 h and was maximum at 24 h (Fig. 3.4.12). The p53 being DNA damage sensor protein is known to be

upregulated at early time and also responsible for induction of apoptotic machinery. It was further interesting to observe that tumor cells treated with  $^{131}\text{I}$ -rituximab showed p53 upregulation and cleavage of PARP compared to the cells treated with  $^{131}\text{I}$ -rituximab (Fig. 3.4.12) suggesting the role of beta radiation from  $^{131}\text{I}$ -rituximab in tumor cell killing. These studies prove the enhanced cytotoxic effect of  $^{131}\text{I}$ -rituximab and the potential role of radioimmunotherapy in treatment of cancer.

## CHAPTER 4

# **Study on Effects of <sup>131</sup>I-rituximab in Combination with Doxorubicin on Raji Cells**

## 4.1 INTRODUCTION

NHL is a group of hematological malignancies of which more than 90 % originates from the B-cells (Freedman et al. 1991). There are various therapeutic modalities available for NHL, which includes chemotherapy, radiation therapy, immunotherapy, radioimmunotherapy etc. However, the combined approach of different modes of therapy, adds on benefit by mitigating the limitations of each therapeutic modalities. It is reported that combining the approach of radioimmunotherapy with chemotherapy has synergistic effect (Jang et al. 2012). The present study combines the approach of chemotherapy (doxorubicin) and radioimmunotherapy ( $^{131}\text{I}$ -rituximab). Raji cells were treated with doxorubicin in combination with  $^{131}\text{I}$ -rituximab and the underlying mechanism of cell toxicity was elucidated.

Doxorubicin is an anthracycline antibiotic and commonly used chemotherapeutic drug for the wide range of cancers, including leukemia and lymphoma (Tan et al. 1967). It induces formation of free radicals and superoxide (Rajagopalan et al. 1988, Schimmel et al. 2004) and also inhibits the enzyme topoisomerase II, thereby stops the process of replication and subsequently the progression of cell cycle (Fornari et al. 1994). There are pharmacological and biological evidence for doxorubicin resistance in human cancer cell lines (Slovak et al. 1988, Salmon et al. 1989, Trock et al. 1997), in patients (Shen et al. 2008, Aas et al. 1996, Smith et al. 2006) and associated side effects of myocardiopathy (Zhang et al. 2012). The drug-resistance and associated side effects, warrants the development of combinatorial approach for cancer therapy.

Rituximab is one of the chimeric monoclonal immunotherapeutic agents against CD20, developed by genetic engineering. It has been approved by FDA in 1997 (Reff et

al 1994, Boye et al. 2003, Lim et al. 2010, Olazoglu et al. 2010). Even though, rituximab is used for treatment of NHL patients, it induces resistance during course of therapy (Smith 2003, Scott et al. 2008). It has been found that only 50 % patients showed clinical response to the rituximab (Bonavida 2007). To overcome the resistance and enhance the therapeutic efficacy in B-cell lymphoma patients, rituximab was administered in combination with chemotherapeutic regimen like CHOP (Mounier et al. 2003, Dillman et al. 2007). Rituximab treatment has also been tried in combination with various chemotherapeutic drugs such as paclitaxel, gemcitabine, cisplatin and vinorelbine and increase in cytotoxicity was observed involving various signalling pathways (Alas et al 2001, Emmanouilides et al. 2002, Alas et al. 2002, Coiffier 2003, Jazirehi et al 2003, Jazirehi et al 2005a & b, Bonavida 2007).

Radioimmunotherapy using  $^{131}\text{I}$ -rituximab for NHL (Rao et al. 2005, Bienert et al. 2005, Kersten 2011), relapsed indolent NHL patients (Leahy et al. 2006, 2011) and in Burkitt lymphoma cell line (Kumar et al. 2013b) are reported in literature. The combined approach of rituximab with low LET radiation (X-rays and  $\gamma$ -rays) triggered apoptosis in NHL cancer cells (Skvortsova et al. 2006) and Burkitt lymphoma cell line (Fengling et al. 2009) showing enhanced cell killing. The mechanism of effect of doxorubicin in combination with  $^{131}\text{I}$ -rituximab has not been reported. Hence, this study has been carried out to explore the underlying mechanism of cell killing and cellular signalling in Raji cells induced by  $^{131}\text{I}$ -rituximab in combination with doxorubicin.

## 4.2 SCOPE AND OBJECTIVES OF THE CHAPTER

It was observed from the studies described in the Chapter 3, that  $^{131}\text{I}$ -rituximab induced higher cell toxicity in Raji cells compared to rituximab (Kumar et al. 2013b). To further

enhance the cellular toxicity, combinatorial approach was used with the well known anti cancer drug, doxorubicin. Efficacy of rituximab in combination with paclitaxel, gemcitabine, cisplatin, vinorelbine, adriamycin and cyclophosphamide are known (Coiffier 2003, Jazirehi et al. 2003 and 2007, Alas et al. 2001 and 2002, Dillman et al. 2007), but the effect and underlying mechanisms of  $^{131}\text{I}$ -rituximab and in combination with doxorubicin is not known. Here, Raji cells were treated with doxorubicin along with  $^{131}\text{I}$ -rituximab and induced cell death was compared with  $^{131}\text{I}$ -rituximab as well as doxorubicin treated controls. Furthermore, the cell toxicity, apoptosis and MAPK signaling pathways were investigated in Raji cells.

## **4.3 MATERIALS AND METHODS**

### **4.3.1 Reagents**

Doxorubicin purchased from Sigma Chemicals Inc. (USA) was dissolved in Dulbecco's phosphate buffer saline (2 mg/mL). Primary antibody of MAPK and phospho-MAPK, and peroxidase labeled secondary antibody were purchased from Cell Signaling Technology, Danvers, MA. All other reagents used were of cell culture grade.

### **4.3.2 Cell culture**

Raji cells obtained from the National Center for Cell Sciences (NCCS), Pune, India, was cultured in RPMI-1640 supplemented with 10 % serum (Invitrogen), and antibiotic/antimycotic solution. All culture was maintained in humidified 5 % CO<sub>2</sub> atmosphere at 37 °C.

### **4.3.3 Determination of effect of doxorubicin on Raji cell line**

Raji cells ( $1 \times 10^6$ /well) were plated in 24 well plates and different concentrations of doxorubicin (0.5-15 µg/mL) were added followed by incubation for 6 h, to find the effect of doxorubicin. Cells were harvested, washed with PBS and further incubated ( $1 \times 10^3$  cells / well) for 12 and 24 h in 96 well plates. MTT assay was carried out according to protocol described by Kumar et al (2013a). Briefly, after completion of incubation, 10 µL of MTT solution (5 mg/mL) was added to each well and incubated for 2 h. Formazan crystal was solubilized by addition of 100 µL of solubilizing buffer (20 % SDS in 50 % DMF). Color was quantified at 570 nm with reference to 630 nm in BioTek Universal Microplate Reader (BioTek U.S., Winooski, VT, USA). Percent cell proliferation/viability was calculated as ratio of OD of treated to control samples,



multiplied by 100.

#### 4.3.4 Treatment of Raji cells with $^{131}\text{I}$ -rituximab and doxorubicin

Raji cells ( $1 \times 10^6$ ) were plated in 24 well plates and treated with doxorubicin (0.5, 1, 2 and 10  $\mu\text{g/mL}$ ) for 4 h followed by 1.85 MBq of  $^{131}\text{I}$ -rituximab for 2 h. Hence, total incubation time for the doxorubicin was 6h. Concentration of 1.85 MBq of  $^{131}\text{I}$ -rituximab was chosen from the studies described in Chapter 3 (Kumar et al. 2013b). The cells were harvested after completion of 6 h, washed thrice with PBS and further incubated for 12 h at 37 °C in an incubator to carry out further experiments.

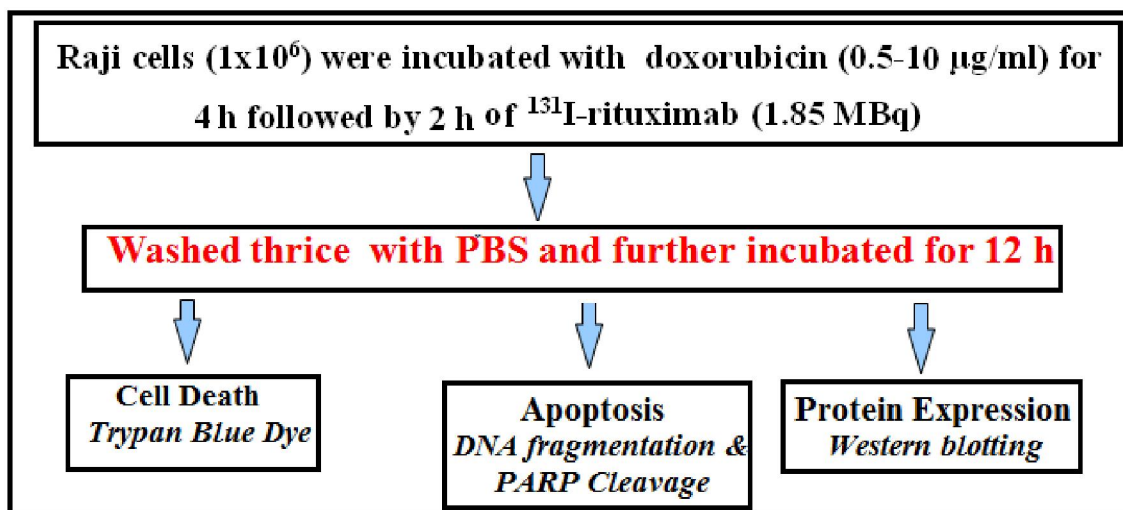


Figure 4.1 Flow chart of experimental plan

#### 4.3.5 Estimation of cell death of Raji cells in combinatorial treatment of doxorubicin and $^{131}\text{I}$ -rituximab by trypan blue dye uptake

Raji cells were treated with doxorubicin (0.5, 1, 2 and 10  $\mu\text{g/mL}$ ), rituximab (5  $\mu\text{g/mL}$ ),  $^{131}\text{I}$ -rituximab (1.85 MBq) alone and in combination with doxorubicin, for desired time periods as mentioned in Section 4.3.4, washed and further incubated for 12 h. Cells were harvested and the magnitude of cell death in control and treated cells was determined by

mixing cells with equal volume of 0.4 % (w/v) trypan blue dye (Kumar et al. 2013a). Living cells exclude while dead cells take up the dye, which was counted using haemocytometer and expressed as percent cell death. Percent cell death was calculated as the ratio of dead to total cells multiplied by 100.

#### **4.3.6 Study of apoptosis by DNA fragmentation study**

Raji cells ( $\sim 1 \times 10^5$ ) were harvested after treatment with doxorubicin and  $^{131}\text{I}$ -rituximab and were lysed in lysis buffer provided with kit. The supernatant was used to determine apoptosis by DNA fragmentation study using ELISA method, according to method described in earlier Section 2.3.6.

#### **4.3.7 Study of apoptosis by estimation of PARP cleavage**

PARP protein is one of the active components of induction of apoptotic cell death. The protein was isolated from doxorubicin and  $^{131}\text{I}$ -rituximab treated Raji cells and estimation of PARP cleavage was carried out according to method described in earlier Section 2.3.7.

#### **4.3.8 Study of expression of protein related to apoptotic cell death**

Raji cells were harvested after desired treatment (refer Section 4.3.4) and lysed in cell lysis buffer and protease inhibitor cocktail (Kumar et al. 2013a). Where ever required protein concentration in samples was estimated by Bio-Rad Protein assay (Bio-Rad). Protein (40  $\mu\text{g}$ ) was loaded on 10 or 15 % SDS PAGE gel and electrophoresis was carried out. Protein was transferred onto nitrocellulose membrane by electroblotting. The membrane was blocked using 5 % non-fat milk protein followed by incubation with primary antibodies for PARP, bclxl, MAPK pathways proteins (p44/42, p38 and their phosphoprotein) and beta-actin (loading control) for 1.5 h. The membrane was washed

with Tris buffer saline with Tween 20 (0.1 %) followed by treatment with secondary antibody for 2 h. The membrane was incubated with ECL (enhanced chemiluminescence) reagents (Cell Signaling Tech.), followed by exposure to Hyper film. Film was processed and developed by Kodak developer and fixer solution. Protein blot densitometry was carried out using UVIbandmap (UVITEC Limited Cambridge, UK).

#### **4.3.9 Statistical analysis**

Unless mentioned, the results are mean  $\pm$  SD of at least three independent experiments, where t-test was used to compare control and irradiated samples. Significance level was determined by considering  $p$  values below 0.05.

## 4.4 RESULTS

### 4.4.1 Effect of doxorubicin on proliferation of Raji cells

To optimize the doxorubicin concentration and post treatment incubation period, MTT assay was carried out for 12 and 24 h after treatment with increasing concentrations of doxorubicin (0.5-15  $\mu\text{g/ml}$ ). Percent cell proliferation was calculated and plotted against the doxorubicin concentration (Fig. 4. 2). A dose dependent decrease in proliferation of Raji cells was observed, which showed saturation at higher concentrations as 8  $\mu\text{g/mL}$  or above. However, there were marginal differences between the percent cell proliferation of Raji cells at 12 and 24 h of post incubation at higher concentration ( $>8 \mu\text{g/mL}$ ) of doxorubicin.

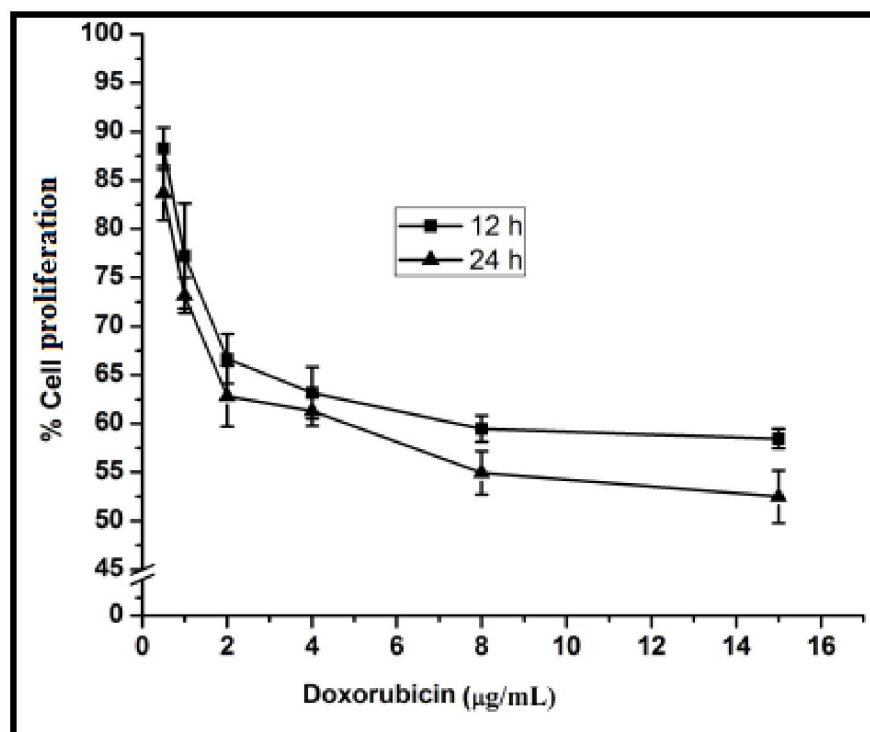


**Figure 4.2** Estimation of percent cell proliferation by MTT assay of Raji cells treated with doxorubicin for 6 h.

#### 4.4.2 Effect of doxorubicin in combination with $^{131}\text{I}$ -rituximab on cell death of Raji cells

In order to investigate efficacy of combinatorial treatment of doxorubicin and  $^{131}\text{I}$ -rituximab, cell death assay was carried out in Raji cells after treatment with 0.5, 1, 2 and 10  $\mu\text{g/mL}$  of doxorubicin concentration in combination of 1.85 MBq of  $^{131}\text{I}$ -rituximab for 12 h (Fig. 4.3). Increased cell death was observed in Raji cells treated with  $^{131}\text{I}$ -rituximab in combination with doxorubicin compared to their respective controls. The magnitude of cell death in case of doxorubicin (2  $\mu\text{g/mL}$ ) in combination with  $^{131}\text{I}$ -rituximab treated Raji cells was ~74 % compared to the doxorubicin (2  $\mu\text{g/mL}$ , ~55 %) and  $^{131}\text{I}$ -rituximab (~22 %) controls (p 0.05).  $^{131}\text{I}$ -rituximab in combination with

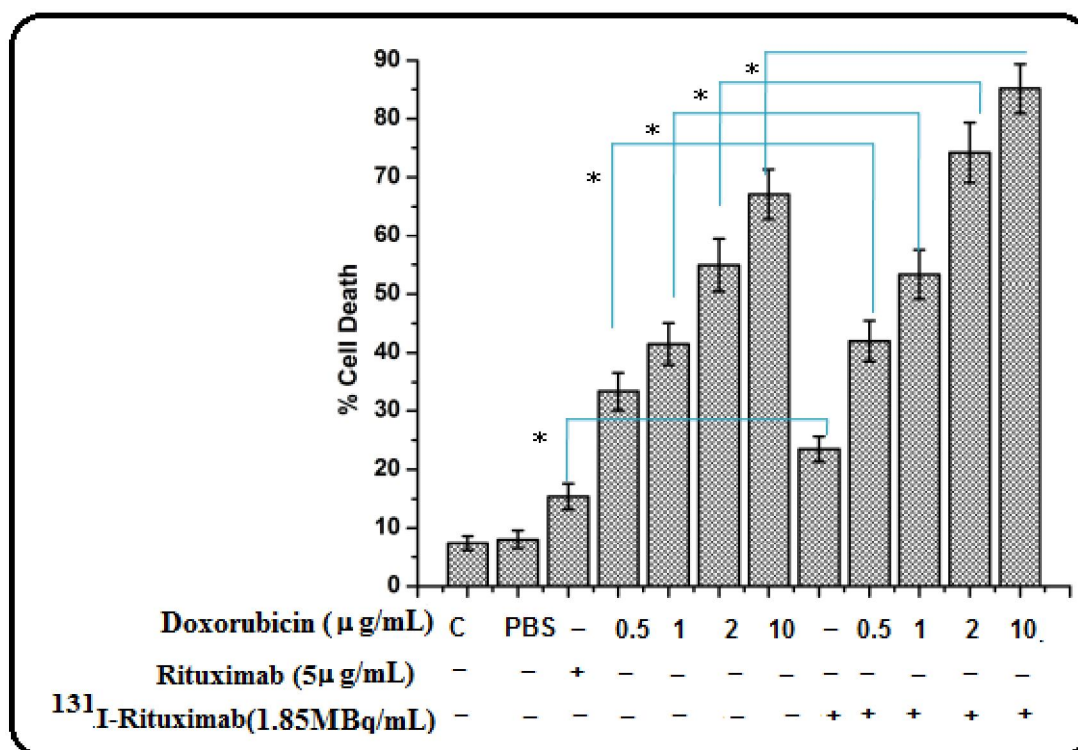


**Figure 4.3** Estimation of cell death in Raji cells treated with doxorubicin in combination with  $^{131}\text{I}$ -rituximab, determined by trypan blue dye. (Where \* p 0.05 and n=3).

10  $\mu\text{g/mL}$  of doxorubicin induced highest amount of cell death, however, a marginal difference was observed in the case of 0.5 and 1  $\mu\text{g/mL}$  of doxorubicin in combinatorial treatment with  $^{131}\text{I}$ -rituximab.

#### 4.4.3 Effect of doxorubicin and $^{131}\text{I}$ -rituximab on induction of apoptotic DNA fragmentation

In order to investigate, the mechanism of cell death in Raji cells, after treatment with doxorubicin in combination of  $^{131}\text{I}$ -rituximab, magnitude of apoptotic DNA fragmentation was estimated by ELISA method. The results showed that there is a significant increase ( $p < 0.05$ ) of EF in the case of combinatorial treatment of doxorubicin (2  $\mu\text{g/mL}$ ) and  $^{131}\text{I}$ -rituximab (EF~9) compared to the corresponding individual controls of doxorubicin (2  $\mu\text{g/mL}$ , EF-4.2) and  $^{131}\text{I}$ -rituximab (EF~2.5) (Fig. 4.4a). However, at higher concentration

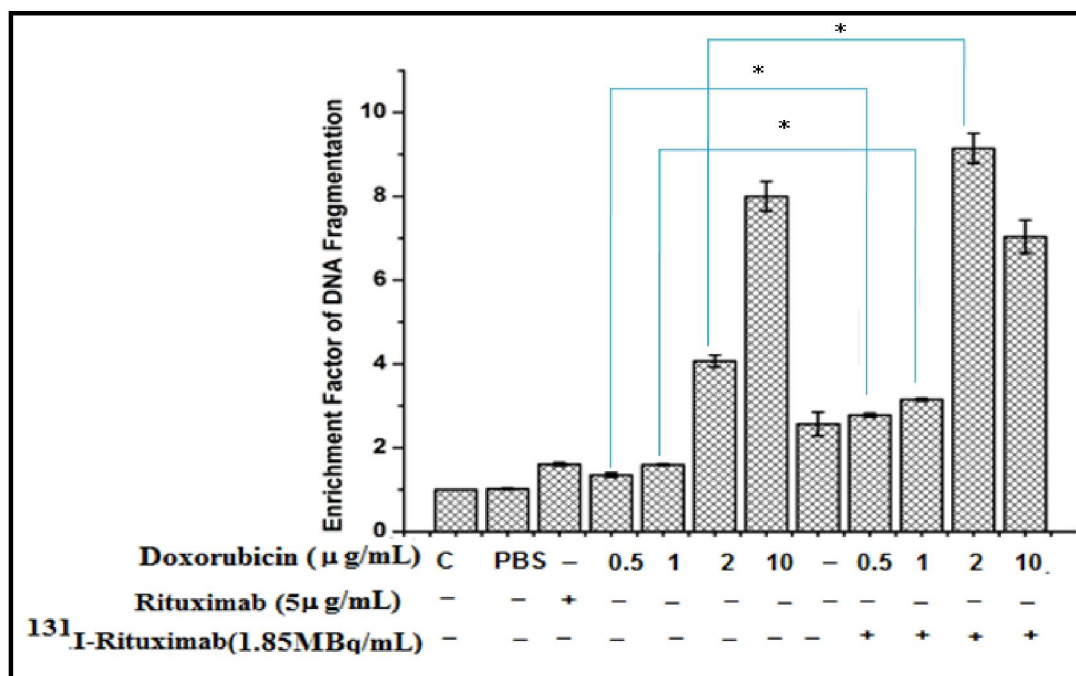


**Figure 4.4a** Estimation of apoptotic DNA fragmentation of Raji cells treated with doxorubicin in combination with  $^{131}\text{I}$ -rituximab. (Where \*  $p < 0.05$  and  $n=3$ ).

of doxorubicin (10  $\mu\text{g/mL}$ ) in combination with  $^{131}\text{I}$ -rituximab showed EF~7 compared to the corresponding doxorubicin (10  $\mu\text{g/mL}$ , EF~8). These results were further expressed in terms of fold change compared to their respective controls in Fig. 4.4b The results suggest prominent combinatorial effect in terms of DNA fragmentation of doxorubicin and  $^{131}\text{I}$ -rituximab at 2  $\mu\text{g/mL}$  than the 0.5, 1 and 10  $\mu\text{g/mL}$  of doxorubicin (Fig. 4.4b) for getting highest apoptotic DNA cleavage.

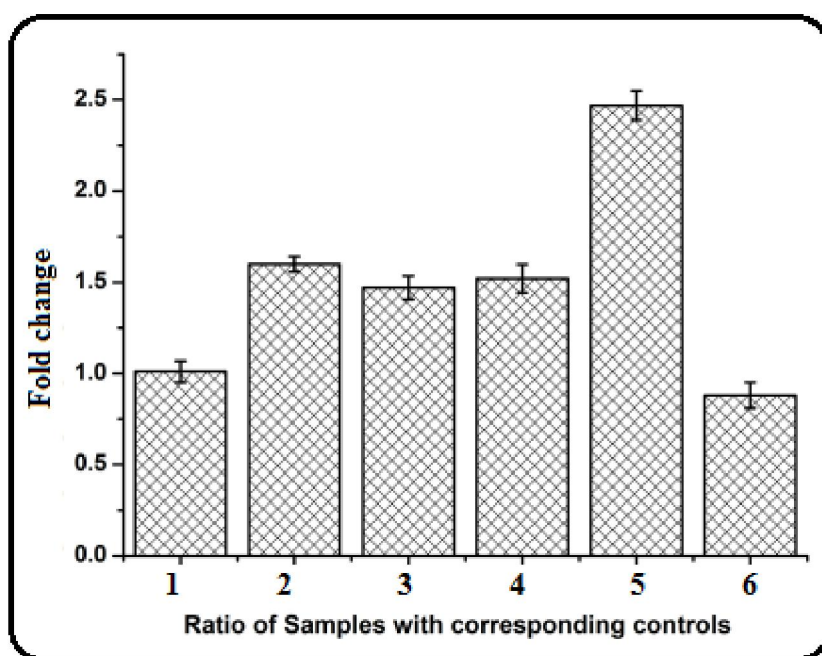


**Figure 4.4b** Fold change in apoptotic DNA fragmentation of Raji cells as a ratio of enrichment factor. (where 1: cells treated in PBS/ control cells, 2: Cells treated with 1.85 MBq of  $^{131}\text{I}$ -rituximab /5  $\mu\text{g}$  of rituximab, 3: Cells treated with 0.5  $\mu\text{g/mL}$  of doxorubicin in combination with 1.85 MBq of  $^{131}\text{I}$ -rituximab /0.5  $\mu\text{g/mL}$  of doxorubicin, 4: Cells treated with 1  $\mu\text{g/mL}$  of doxorubicin in combination with 1.85 MBq of  $^{131}\text{I}$ -rituximab /1  $\mu\text{g/mL}$  of doxorubicin, 5: Cells treated with 2  $\mu\text{g/mL}$  of doxorubicin in combination with 1.85 MBq of  $^{131}\text{I}$ -rituximab / 2  $\mu\text{g/mL}$  of doxorubicin and 6: Cells treated with 10  $\mu\text{g/mL}$  of doxorubicin in combination with 1.85 MBq of  $^{131}\text{I}$ -rituximab / 10  $\mu\text{g/mL}$  of doxorubicin)

#### 4.4.4 Effect of doxorubicin and $^{131}\text{I}$ -rituximab on cleavage of PARP protein

This study was carried out to estimate the cleavage of PARP protein by ELISA method in control and treated Raji cells (Fig. 4.5a). The results showed that there was a significant increase ( $p < 0.05$ ) of PARP cleavage in cells treated with doxorubicin ( $2 \mu\text{g/mL}$ ) in combination with  $^{131}\text{I}$ -rituximab ( $\text{EF} \sim 7.5$ ) compared to their corresponding controls i.e. doxorubicin ( $2 \mu\text{g/mL}$ ,  $\text{EF} \sim 3.45$ ) and  $^{131}\text{I}$ -rituximab ( $\text{EF} \sim 2.75$ ) (Fig. 4.5a). There was also a significant increase ( $p < 0.05$ ) of PARP cleavage in combinatorial treatment of 0.5 and  $1 \mu\text{g/mL}$  of doxorubicin. Further analysis of results in terms of fold change with respect to their controls (Fig. 4.5b), showed highest amount of PARP cleavage at  $2 \mu\text{g/mL}$  of doxorubicin combination with  $^{131}\text{I}$ -rituximab.

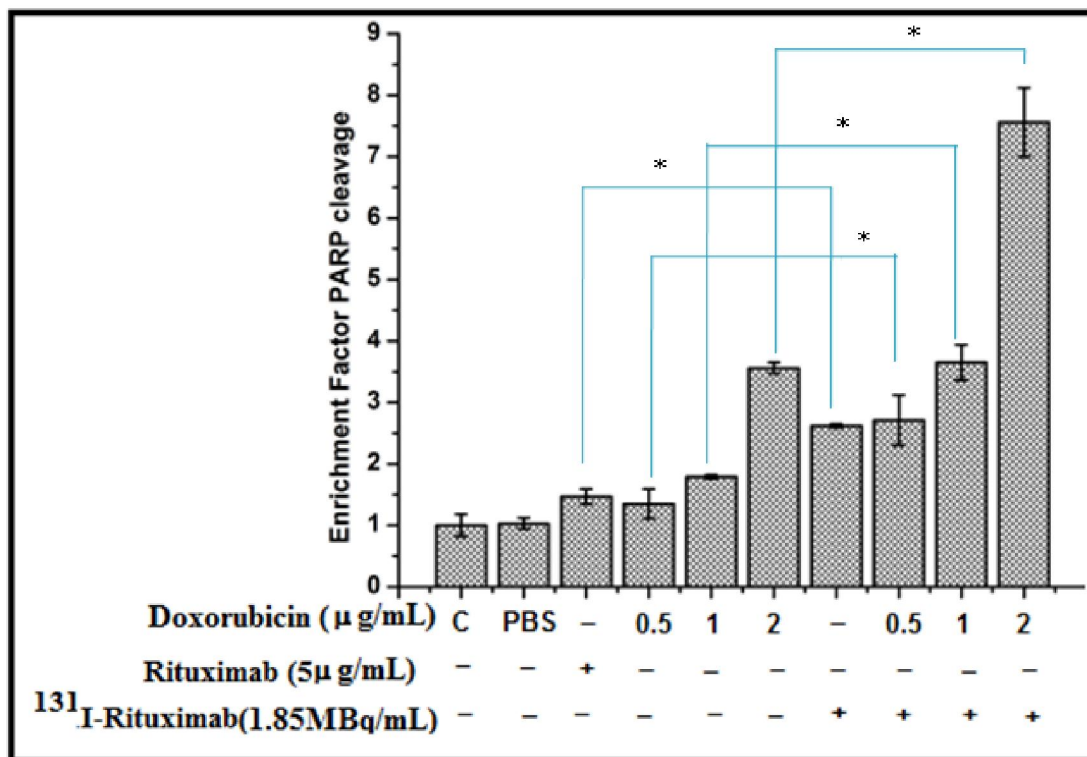


**Figure 4.5a** Estimation of PARP cleavage in Raji cells treated with doxorubicin in combination with  $^{131}\text{I}$ -rituximab. (Where \*  $p < 0.05$  and  $n=3$ ).



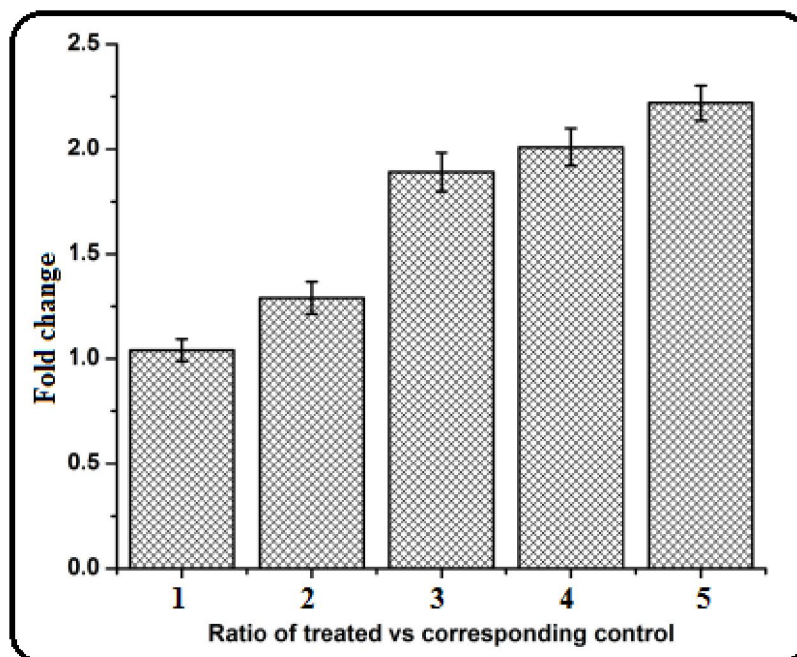


**Figure 4.5b** Fold change in PARP cleavage of Raji cells as a ratio of enrichment factor. (where 1: cells treated in PBS/ control cells, 2: Cells treated with 1.85 MBq of  $^{131}\text{I}$ -rituximab /5  $\mu\text{g}$  of rituximab, 3: Cells treated with 0.5  $\mu\text{g}/\text{mL}$  of doxorubicin in combination with 1.85 MBq of  $^{131}\text{I}$ -rituximab /0.5  $\mu\text{g}/\text{mL}$  of doxorubicin, 4: Cells treated with 1  $\mu\text{g}/\text{mL}$  of doxorubicin in combination with 1.85 MBq of  $^{131}\text{I}$ -rituximab /1  $\mu\text{g}/\text{mL}$  of doxorubicin and 5: Cells treated with 2  $\mu\text{g}/\text{mL}$  of doxorubicin in combination with 1.85 MBq of  $^{131}\text{I}$ -rituximab / 2  $\mu\text{g}/\text{mL}$  of doxorubicin)

#### 4.4.5 Effect of doxorubicin and $^{131}\text{I}$ -rituximab on expressions of proteins involved in apoptosis and MAPK

The previous results from trypan blue, DNA fragmentation and PARP cleavage assays showed efficacy of combinatorial approach of doxorubicin and  $^{131}\text{I}$ -rituximab. Hence, to further illustrate the underlying molecular players and signaling pathways, regulation of bclxl in control and treated cells was studied. Moreover, the PARP cleavage observed by ELISA method was also verified by Western blotting (Fig. 4.6a). The results showed that the expression of anti-apoptotic protein (bclxl) was downregulated and cleaved PARP

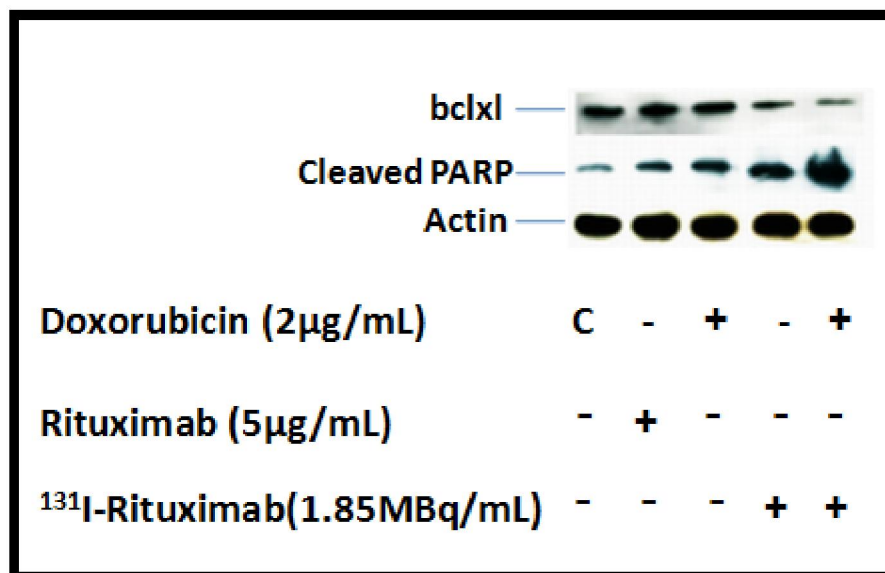


**Figure 4.6a** Expressions of apoptotic proteins in Raji cells treated with doxorubicin in combination with  $^{131}\text{I}$ -rituximab

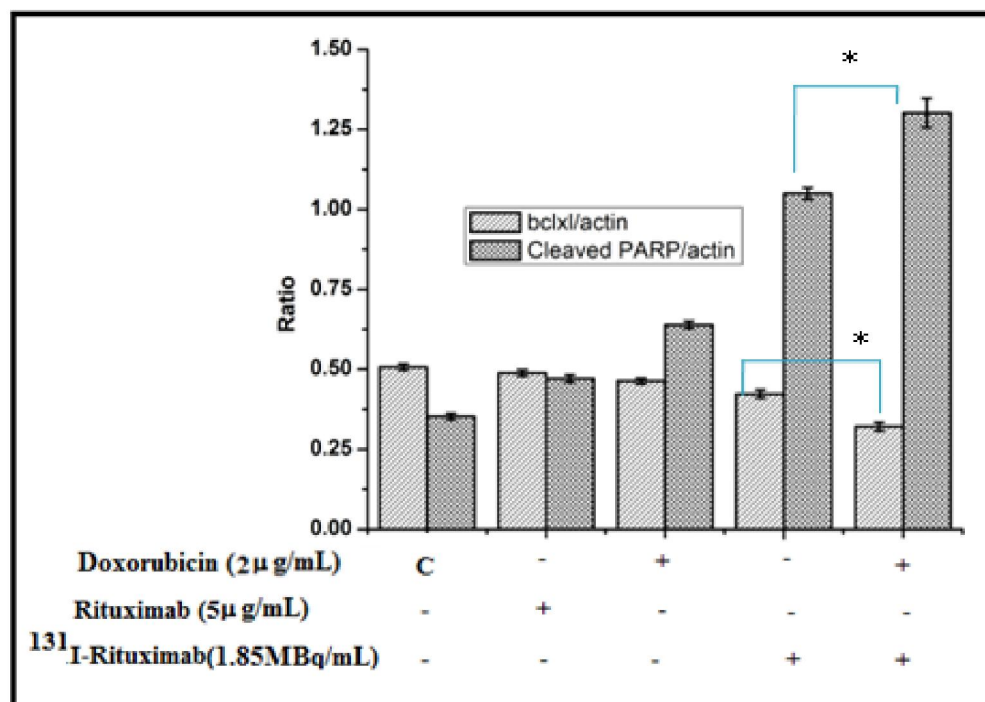


**Figure 4.6b** Ratio of intensity of expression of apoptotic proteins by Western blotting with respect to the beta actin (loading control). (Where \* p < 0.05 and n=3).

was higher in the cells treated with  $^{131}\text{I}$ -rituximab in combination with doxorubicin (2  $\mu\text{g/mL}$ ) compared to the individual controls (Fig. 4.6a). Densitometry of bclxl and cleaved PARP proteins from Western blotting was performed and expressed as a ratio of protein of interest to the corresponding beta actin protein as a loading control (Fig. 4.6b). It was found that maximum downregulation of bclxl and maximum cleavage of PARP protein was observed in the combinatorial treatment compared to the individual controls.

Western blotting was also carried out for MAPK pathway proteins p44/42, p38 and their phosphorylated form in control and treated cells. An increase in expression of p38 proteins was observed in cells treated with  $^{131}\text{I}$ -rituximab in combination with doxorubicin compared to the individual controls, which was not much affected for p44/42 (except marginal decrease in rituximab/ $^{131}\text{I}$ -rituximab controls,  $p < 0.05$ ) (Fig. 4.6c & d). However, strong phosphorylation of p38 was observed in  $^{131}\text{I}$ -rituximab treated cells while phosphorylation of p38 was lower in cells treated with  $^{131}\text{I}$ -rituximab in combination of doxorubicin. However, in the case of phospho p44/42 proteins (Fig. 4.6c & d) phosphorylation was lower in doxorubicin and combinatorial treatment. Densitometry of p38, p44/42, phospho p38 and phospho p44/42 were analyzed and expressed as a ratio of protein of interest to the corresponding beta actin protein as a loading control (Fig. 4.6d). It was found that almost complete downregulation of phospho p44/42 was observed in the combinatorial treatment. Likewise, it was observed that phospho p38 was downregulated in the combinatorial treatment compared to the  $^{131}\text{I}$ -rituximab controls.

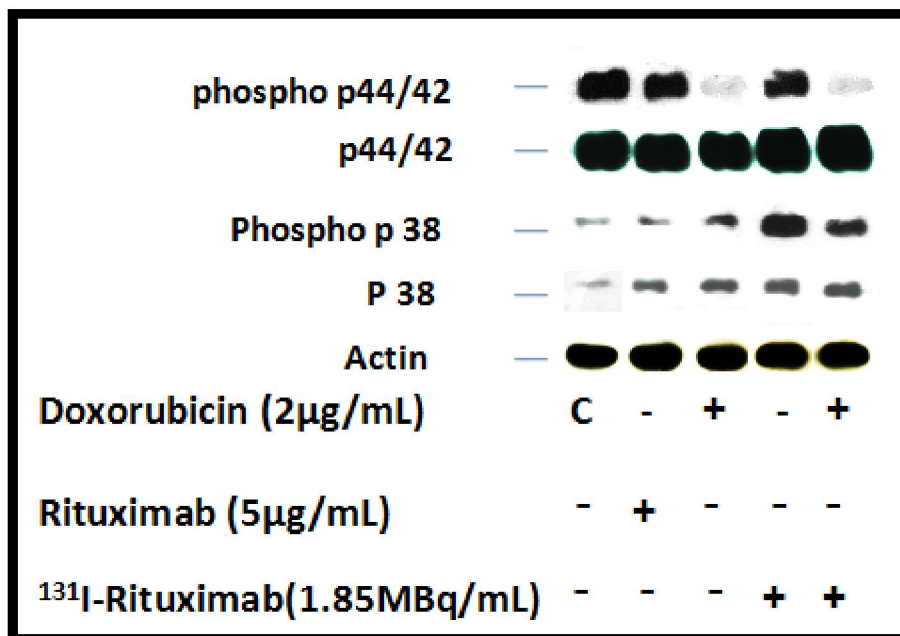


**Figure 4.6c** Expressions of MAPK proteins in Raji cells treated with doxorubicin in combination with <sup>131</sup>I-rituximab

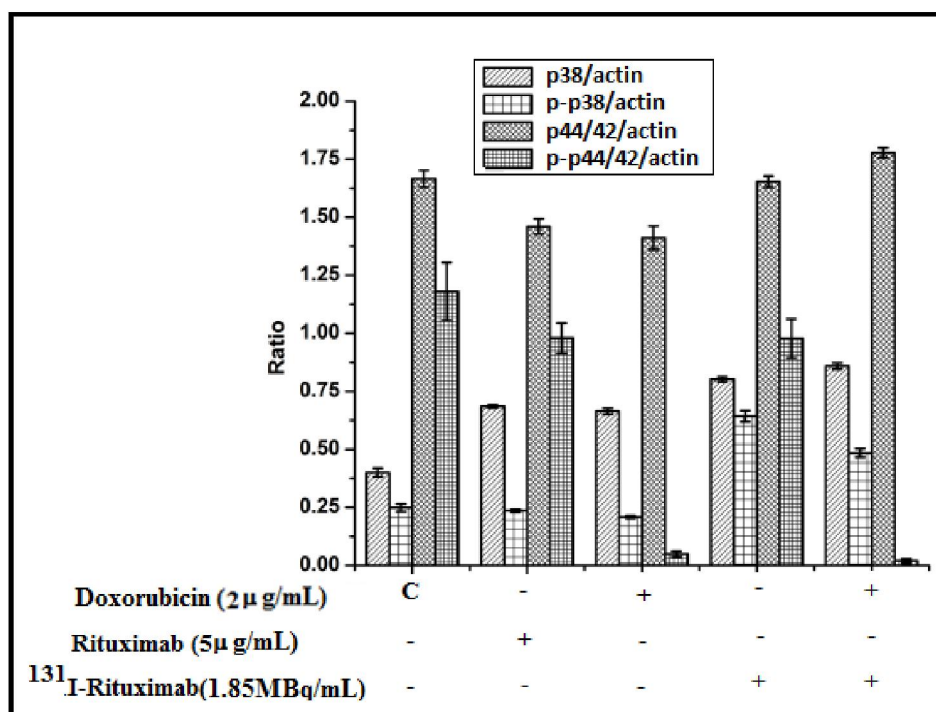


**Figure 4.6d.** Ratio of intensity of expression of MAPK proteins by Western blotting with respect to the beta actin (loading control)

## 4.5 DISCUSSION

The dosage of doxorubicin administered is 60-75 mg/m<sup>2</sup> or 1.2-2.4 mg/kg at every three weeks in cancer chemotherapy. However, these dosages cause toxicity to cardiomyocytes (Zhang et al. 2012) and resistance to therapy (Slovak et al. 1988, Salmon et al. 1989, Trock et al. 1997, Shen et al. 1987, Aas et al. 1996, Smith et al. 2006). To elucidate the mechanism underlying the cytotoxicity in Raji cells after doxorubicin and <sup>131</sup>I-rituximab treatment, we have estimated cell death, apoptosis by DNA fragmentation and PARP cleavage and, regulation of MAPK signaling pathways. Rituximab is known to cause cytotoxicity in tumor cells involving various cellular signaling pathways (Emmanouilides et al. 2002, Jazirehi et al. 2003, Jazirehi et al. 2005a and 2005b, Alas et al. 2001 and 2002 and Chow et al. 2002). Additional killing of lymphoma cells by <sup>131</sup>I-rituximab will be due to associated high energy beta radiation (0.6 MeV of <sup>131</sup>I). The enhanced magnitude of damage is due to localization of radioisotope very close to cellular targets at membrane and cytoplasm level (Kumar et al. 2013b).

The highest magnitude of cell death measured by trypan blue dye was observed after treatment of doxorubicin (10 µg/mL) in combination with <sup>131</sup>I-rituximab, compared to other combinatorial treatments of doxorubicin (0.5, 1 and 2 µg/mL) and <sup>131</sup>I-rituximab. However, the extent of DNA fragmentation was more in case of treatment of doxorubicin (2 µg/mL) in combination with <sup>131</sup>I-rituximab. The DNA fragmentation in the combinatorial treatment of doxorubicin (10 µg/mL) was lower compared to combinatorial treatment of 2 µg/mL. This might be due to combinatorial treatment of doxorubicin at higher concentration result in higher apoptosis and thus number of cell lysis at the advanced stage of cell death. The fragmented DNA from these lysed cells

would be lost in the supernatant while harvesting the cells for DNA fragmentation analysis by ELISA. Similarly, the effects of combinatorial treatments of 0.5 and 1 µg/mL of doxorubicin were lower than that of 2 µg/mL. Thus the western blotting studies were aimed to investigate efficacy of  $^{131}\text{I}$ -rituximab in combination with doxorubicin of 2 µg/mL concentration.

The result of cleaved PARP protein determined by Western blotting was similar to the observation found in the estimation of PARP cleavage by ELISA method for the given concentration of doxorubicin and  $^{131}\text{I}$ -rituximab. This apoptotic cell death is higher in the combinatorial treatment which was validated with the apoptosis results of DNA fragmentation. In Western blotting studies, downregulation of bclxl and the corresponding PARP cleavage confirms the apoptotic cell death (Fig. 4.7), which is in agreement with observation of enhanced cytotoxicity in the NHL B cell line treated with rituximab and drugs (cisplatin, adriamycin, vinblastine, 5-fluorouracil and paclitaxel) (Emmanouilides et al. 2002, Jazirehi et al. 2003, Jazirehi et al. 2005a and 2005b, Alas et al. 2001 and 2002, Chow et al. 2002).

In general, p38 are poorly activated by mitogens but strongly activated by inflammatory cytokines and a wide variety of cellular stress inducers and its activation occurs through phosphorylation. After activation, these cytosolic proteins translocate to the nucleus and activate numerous proteins and/or transcription factors (Wagner et al. 2009, Johnson et al. 2002). So the increase in expression of p38 protein in the combination of 2 µg/mL of doxorubicin with the  $^{131}\text{I}$ -rituximab might be due to the radiation stress. The strong phosphorylation of p38 in  $^{131}\text{I}$ -rituximab treated cells and relatively weak phosphorylation was observed in combinatorial treatments, which

correspond to the maximum apoptotic cell death (Fig. 4.7). Similar results have been observed in the rituximab treated B-cell chronic lymphocytic leukemia cell line where p38 has a role in induction of apoptosis (Mathas et al. 2000, Pedersen et al. 2002).

In contrary to p38, p44/42 (also known as ERK1/2) is the key transducers of proliferation signals and is often activated by mitogens and its activation occurs through phosphorylation of threonine and tyrosine residues (Wagner et al. 2009, Johnson et al. 2002). However, there is no change in p44/42 expression in the case of  $^{131}\text{I}$ -rituximab. The increase in cytotoxicity in case of  $^{131}\text{I}$ -rituximab in combination of doxorubicin may be due to a decrease in phosphorylation of p44/42. On downstream signaling, p44/42 is known to inhibit bclxl (Jazirehi et al. 2003) leading to cell death, which may explain the association of the signaling pathway in enhanced killing of Raji cells treated with  $^{131}\text{I}$ -rituximab in combination with doxorubicin, which ultimately induce apoptotic cell death. However, detailed mechanistic pathways need to be investigated.

There is a report that unlabeled rituximab used in combination with doxorubicin (Chow et al. 2002) enhanced cell death. The author (Kumar et al. 2013b) has reported in Chapter 3 that  $^{131}\text{I}$ -rituximab is more potent in induction of apoptotic cell death than the unlabeled rituximab. In this Chapter, the author has reported that combined treatment of doxorubicin and  $^{131}\text{I}$ -rituximab induced higher cell death than the corresponding controls. Hence, it has concluded that doxorubicin has the potential to sensitize  $^{131}\text{I}$ -rituximab induced cell death in Raji cells involving MAPK signaling pathways.

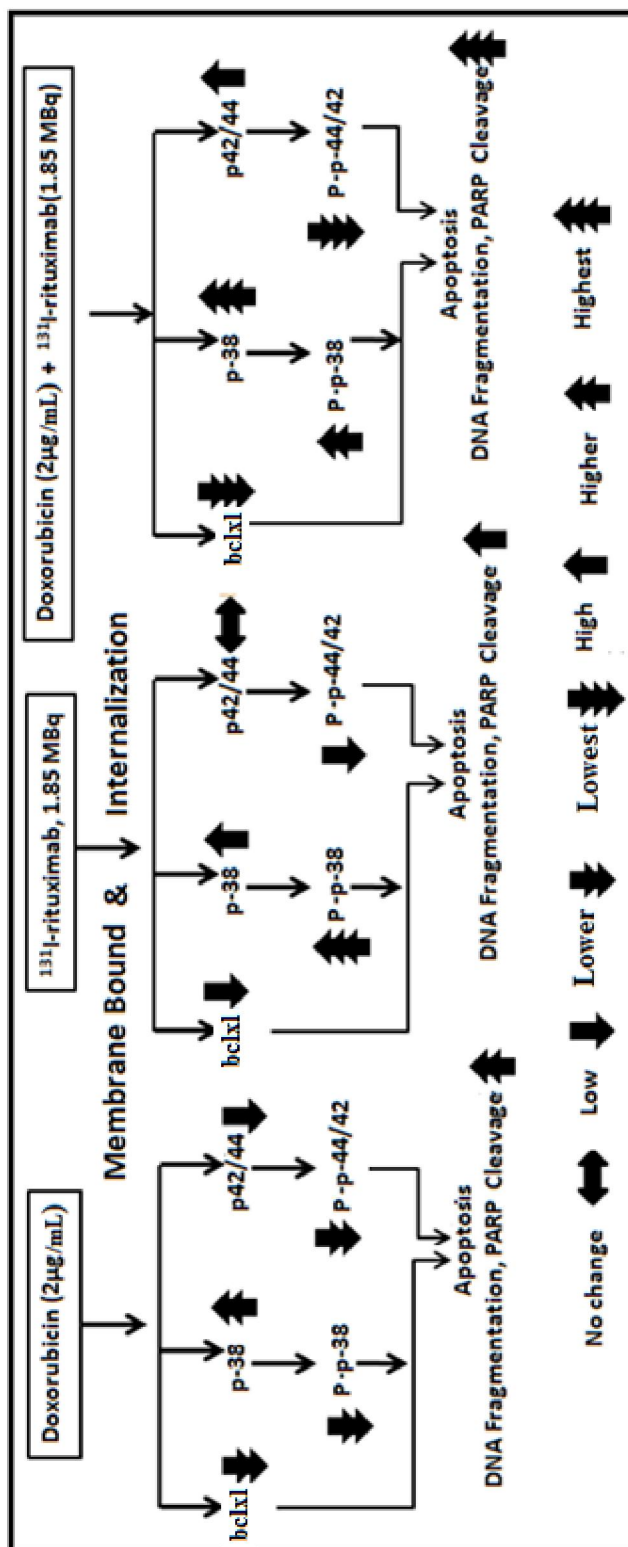


**Figure 4.7** Schematic diagram of signaling associated with <sup>131</sup>I-rituximab, doxorubicin and combinatorial treatment



## CHAPTER 5

# Summary, Conclusions and Future Directions

## 5.1 SUMMARY OF THE THESIS

The use of external beam radiation is one of the therapeutic modalities for the treatment of various types of cancer. However, beta radiation emitted from radiopharmaceuticals is more effective in selected cancers (thyroid cancer, lymphoma etc). The radiation has limitations during cancer therapy because cancer cells have different status of p53, antioxidant, hypoxia etc. The different stages and origins of tumors also play a major role in treatment outcome. Alpha and beta radiation overcome most of the limitations, since their effect is independent of oxygen level. Radioiodine is one of the oldest known radionuclides used in therapy. The beta radiation emitted from radioiodine is used for therapy, while  $\gamma$ -rays are used for diagnosis. The effects of  $\alpha$  and X-rays emitted from  $^{131}\text{I}$  on therapy are insignificant because it mostly escapes and deposit energy other than the target sites. The mechanisms of cell death induced by beta radiation are not well understood. Hence, the author has chosen tumor cells of various tissue origin (Raji, MCF-7, A431 and U937 cells), which were irradiated with beta radiation emitted from  $^{131}\text{I}$  and this effect was compared with an equivalent dose of  $\gamma$  radiation. It was found that the cellular toxicity and apoptosis was higher in the case of beta irradiated tumor cells compared to the cells that received equivalent dose of  $\gamma$  radiation. The differential expressions of RAD51 and P21 genes have a major role in discriminating the effect of beta and gamma radiation in cancer cells.

The scope of targeted delivery of radionuclides for cancer therapy is increasing rapidly due to higher therapeutic gain. Hence, beta emitting radionuclides viz.  $^{131}\text{I}$ ,  $^{177}\text{Lu}$ ,  $^{90}\text{Y}$  etc. were targeted to tumor cell receptors using suitable ligands. The targeted therapy will not only enhance the effect of beta radiation but sometime effect get further

enhanced due to the internalization of the radiolabeled ligands. There are various antibody available in clinics which can be labeled with beta emitting radionuclides and can be used for the treatment of various cancers. Bexxar and Zevalin are commercially available  $^{131}\text{I}$  and  $^{90}\text{Y}$  labeled antibody respectively, being used for the treatment of NHL. Being mouse origin, these antibodies induce HAMA response. So, in this study rituximab, a chimeric antibody was selected for radiolabeling with  $^{131}\text{I}$  and evaluated in CD20 overexpressing cancer cells (Raji). Being chimeric in nature, HAMA response will be minimum for the rituximab. The  $^{131}\text{I}$  is easily available radionuclides amongst others and is the oldest one used in the clinics. Thus, rituximab was labeled with  $^{131}\text{I}$  by Iodogen method and characterized by HPLC. Cell binding and internalization study was carried out in Raji cells. It was observed that cell binding decrease with the increase in time of incubation. Here it was found that cellular internalization increase with the time of incubation, which corresponds to the increase in cell death and apoptosis. The stability of  $^{131}\text{I}$ -rituximab bound with CD20 was analyzed in the cell supernatant media. It was observed that there was a maximum of 10 % deiodination at 24 h time period of incubation. The extent of cell toxicity induced by  $^{131}\text{I}$ -rituximab was compared to unlabeled rituximab and it was concluded from the results that cellular toxicity and apoptosis was more in  $^{131}\text{I}$ -rituximab compared to the rituximab.

Combining different therapeutic modalities impart the decrease of tumor resistance against the cancer therapy, which has corroborated by synergistic or additive effects. Considering the legacy of combining therapeutic approach, studies were carried out to explore the possibility of synergistic effect of combining  $^{131}\text{I}$ -rituximab (radioimmunotherapy) with doxorubicin (chemotherapy). Doxorubicin was chosen,

because it is commonly used for the treatment of a wide range of cancers including leukemia and lymphoma. However, there are evidences for doxorubicin resistance in patients and associated side effects of myocardiopathy. These drug-resistance and associated side effects, warrants the development of combinatorial approach for cancer therapy. To overcome the resistance and enhance the efficacy in Raji cells, doxorubicin was treated in combination with  $^{131}\text{I}$ -rituximab. Higher cell toxicity was observed in the combinatorial treatment compared to the individual controls. It was found that cell death was governed by the MAPK signalling pathways, which is corroborated with inhibition of anti-apoptotic proteins. Downstream of these cellular signalling, the apoptotic DNA fragmentation and cleavage of PARP proteins was observed, which are the hallmark features of apoptosis.

The overall understanding at cellular and molecular level after various treatment conditions is schematically shown in Fig. 5.1.

On the whole, the thesis provides basic understanding at cellular and molecular level, the effect of beta radiation from  $^{131}\text{I}$ , in diffused as well as selective targeting by  $^{131}\text{I}$ -rituximab and/or in combination with doxorubicin, which may be helpful in developing better radio-immunotherapeutic strategies for cancer therapy.

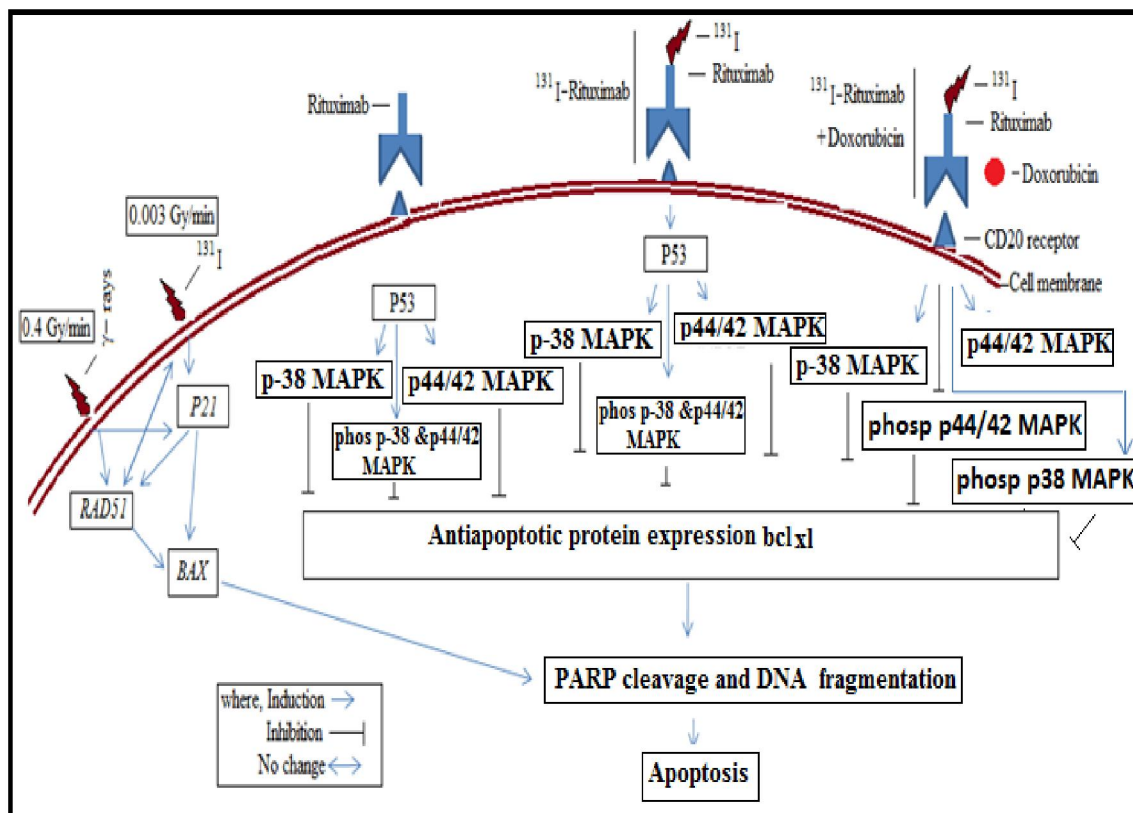


**Figure 5.1** Schematic of cell signaling pathways induced in Raji cells by  $\gamma$ -rays,  $^{131}\text{I}$ , rituximab,  $^{131}\text{I}$ -rituximab and doxorubicin in combination with  $^{131}\text{I}$ -rituximab

## 5.2 MAJOR CONCLUSIONS OF THE THESIS

1. Beta radiation emitted from radionuclides is more potent in induction of cell toxicity in tumor cells compared to the equivalent dose and very high dose rate of  $\gamma$  radiation.
2. *RAD51* and *P21* have major role in discriminating the effect of beta and gamma radiation in tumor cells.
3.  $^{131}\text{I}$ -rituximab enhanced Raji cells toxicity compared to the unlabeled rituximab.
4. Increase in Raji cell death corresponds to the extent of cellular internalization of the  $^{131}\text{I}$ -rituximab.
5. Efficacy of  $^{131}\text{I}$ -rituximab involves apoptotic cell death, where p53 play major role during early incubation periods.
6. Combinatorial approach of doxorubicin and  $^{131}\text{I}$ -rituximab enhanced toxicity in Raji cell line compared to the individual controls, which involve regulation by bclxl and the MAPK signaling pathways.

### 5.3 FUTURE DIRECTIONS

1. There is a need of detailed studies of the mechanism of DNA damage and repair kinetics of beta radiation and the equivalent dose of gamma rays, which may determine the radiosensitivity of various cancer cell lines. The estimation of SSB and DSB of DNA damage by comet assay will give an insight of nature of damage. Moreover, deeper understanding about role of *RAD51* and other DNA damage response genes/proteins (like *KU70/80*) after beta radiation using knockdown/inhibitors approach will further elucidate the underlying molecular mechanism in cellular radiosensitivity.
2. Understand the effect of  $^{131}\text{I}$ -rituximab on cytotoxicity and underlying signaling pathways, there is need to evaluate the efficacy in drug/radiation resistant cell lines.
3. Validate the effect of  $^{131}\text{I}$ -rituximab and its combination with doxorubicin in in-vivo mouse models.

# REFERENCES



- Aas T, Børresen AL, Geisler S, Sorensen BS, Johnsen H, Varhaug JE, Akslen LA, Lønning PE. Specific P53 mutations are associated with de novo resistance to doxorubicin in breast cancer patients. *Nat Med* 1996; 2: 811-814.
- Alas S, Bonavida B. Rituximab in activates STAT3 activity in B-non-Hodgkin's lymphoma through inhibition of the interleukin10 autocrine/paracrine loop and results in down-regulation of Bcl-2 and sensitization to cytotoxic drugs. *Cancer Res* 2001; 61: 5137– 44.
- Alas S, Ng CP, Bonavida B. Rituximab modifies the cisplatin-mitochondrial signalling pathway, resulting in apoptosis in cisplatin-resistant non-Hodgkin's lymphoma. *Clin Cancer Res* 2002; 8: 836-845.
- Anderson KC, Bates MP, Slaughenhaupt BL, Pinkus GS, Schlossman SF, Nadler LM. Expression of human B cell -associated antigens on leukemia and lymphomas: a model of human B cell differentiation. *Blood* 1984; 63:1424-33.
- Antonescu C, Bischof DA, Kosinski M, Monnin P, Schaffland AO, Ketterer N, Grannavel C, Kovacsovics T, Verdun FR, Buchegger F. Repeated injections of <sup>131</sup>I-rituximab show patient-specific stable biodistribution and tissue kinetics. *Eur J Nucl Med Mol Imaging* 2005; 32:943-51.
- Aurlen E, Larsen RH, Kvalheim G, Bruland OS. Dmonstration of highly specific toxicity of the alpha-emitting radioimmunoconjugate <sup>211</sup>At-rituximab against non-Hodgkin's lymphoma cells. *Br J Cancer* 2000;83:1375-9.
- Baechler S, Hobbs RF, Jacene HA, Bochud FO, Wahl RL and Sgouros G. Predicting hematologic toxicity in patients undergoing radioimmunotherapy with <sup>90</sup>Y-

- ibritumomab tiuxetan or  $^{131}\text{I}$ - tositumomab. J Nucl Med 2010; 51(12): 1878-1884
- Balkrishna BY. Trends in the incidence of non-Hodgkin's lymphoma in India. Asian Pacific J Cancer Prev 2008; 9: 433-436.
- Beers SA, Chan CHT, French RR, Cragg MS, Glennie MJ. CD20 as a Target for therapeutic type I and ii monoclonal antibodies Semen Hematol 2010; 47:107-114.
- Bhaktisiddhanta, STGM. Sri Brahma Samhita 1932, pg 58-59. The Bhaktivedanta Book Trust, 1932.
- Bienert M, Reisinger I, Srock S, Humplik BI, Reim C, Kroessin T, Avril N, Pezzutto A, Munz DL. Radioimmunotherapy using  $^{131}\text{I}$ -rituximab in patients with advanced stage B-cell non-Hodgkin's lymphoma: initial experience. Eur J Nucl Med Mol Imaging 2005; 32:1225-33.
- Biersack HJ, Grünwald F, Editors. Thyroid Cancer. 2nd Ed. New York; Springer: 2005.
- Boelaert K, Franklyn JA. Sodium iodide symporter: a novel strategy to target breast, prostate and other cancers Lancet 2003;361:796-797.
- Bonavida B. Rituximab -induced inhibition of antiapoptotic cell survival pathways: implications in chemo/immuno-resistance, rituximab unresponsiveness, prognostic and novel therapeutic interventions. Oncogene 2007; 26:3629-3636.
- Boswell CA, Brechbiel MW. Development of radioimmunotherapeutic and diagnostic antibodies: an inside-out view. Nucl Med Biol 2007; 34:757-778.
- Boye J, Elter T, Engert A. An overview of the current clinical use of the anti CD20

- monoclonal antibody Rituximab. *Ann Oncol* 2003; 14: 520-535.
- Bracey TS, Miller JC, Preece A, Paraskeva C. Gamma-radiation-induced apoptosis in human colorectal adenoma and carcinoma cell lines can occur in the absence of wild type p53. *Oncogene* 1995;15: 2391-2396.
- Calais PJ, Turner JH. Outpatient  $^{131}\text{I}$ -rituximab radioimmunotherapy for non-Hodgkin lymphoma: a study in safety. *Clin Nucl Med* 2012; 37:732-737.
- Carrasquillo JA, Krohn KA, Beaumier P, et al. Diagnosis of and therapy for solid tumors with radiolabeled antibodies and immune fragments. *Cancer Treat Rep* 1984;68:317–328.
- Castillo J, Winer E, Quesenberry P. Newer monoclonal antibodies for haematological malignancies. *Exp Hematol* 2008; 36:755-768.
- Chamrathy MR, Williams SC, Moadel RM. Radioimmunotherapy of non Hodgkin's lymphoma: from the magic bullets to radioactive magic bullets. *Yale J Biol Med* 2011; 84:391-407.
- Chinn PC, Leonard JE, Rosenberg J, Hanna N, Anderson DR. Preclinical evaluation of  $^{90}\text{Y}$ -labeled anti-CD20 monoclonal antibody for treatment of non- Hodgkin's lymphoma. *Int J Oncol* 1999; 15:1017–1025.
- Chow KU, Sommerlad WD, Boehrer S, Schneider B, Seipelt G, Rummel MJ, Hoelzer D, Mitrou PS, Weidmann E. Anti-CD20 antibody (IDEC-C2B8,rituximab) enhances efficacy of cytotoxic drugs on neoplastic lymphocytes in vitro: role of cytokines, complement, and caspases. *Haematologica* 2002; 87:33-43.

- Coiffier B. Monoclonal antibodies combined to chemotherapy for the treatment of patients with lymphoma. *Blood Reviews* 2003; 17: 25-31.
- Corinna AM, Palanca W, and Press OW. Improving the efficacy of radioimmunotherapy for non-Hodgkin's lymphomas. *Cancer* 2010; 116(4 Suppl): 1126-1133.
- Cory S, Huang DCS, Adams JM. The Bcl-2 family: role in cell survival and oncogenesis. *Oncogene* 2003; 22:8590-607.
- Cragg MS, Walshe CA, Ivanov AO, Glennie MJ. The biology of CD20 and its potential as a target for mAb therapy. *Curr Dir Autoimmun* 2005; 8: 140–74.
- Dall'Acqua WF, Damschroder MM, Zhang J, Woods RM, Widjaja L, Yu J, Wu H. Antibody humanization by framework shuffling. *Methods* 2005; 36: 43-60.
- Daniel PT, Sturm I, Ritschel S, Friedrich K, Droken B, Bendzko P, Hillebrand T. Detection of genomic DNA fragmentation during apoptosis (DNA ladder) and the simultaneous isolation of RNA from low cell numbers. *Anal Biochem* 1999; 266:110-115.
- Darzynkiewicz Z, Juan G, Li X, Gorczyca W, Murakami T, & Traganos F. Cytometry in cell necrobiology: analysis of apoptosis and accidental cell death (Necrosis). *Cytometry* 1997; 27:1-20.
- Deans J, Li H, Polyak MJ. CD20-mediated apoptosis: signalling through lipid rafts. *Immunology* 2002; 107: 176–182.
- Degterev A, Boyce M, Yuan JA. Decade of caspases. *Oncogene* 2003; 22:8543-67.
- DeNardo SJ, Erickson KL, Benjamini E. Use of I-131 antibodies for radiation therapy.

- Clin Nucl Med 1980; 5:S4-S5.
- DeNardo SJ, Erickson KL, Benjamini E, et al. Radioimmunotherapy for melanoma. Clin Cancer Res 1981;29:434A.
- Di Marco A, Gaetani M, Scarpinato B. Adriamycin (NSC-123,127): a new antibiotic with antitumor activity. Cancer Chemother Rep 1969; 53: 33–7.
- Dillman RO, Schreeder MT, Hon JK, Connelly EF, Priest CD, Cutter K. Community-based phase II trial of pentostatin, cyclophosphamide, and rituximab (PCR) biochemotherapy in chronic lymphocytic leukaemia and small lymphocytic lymphoma. Cancer Biother Radiopharm 2007; 22:185-193.
- Dolmans DE, Fukumura D, Jain RK. Photodynamic therapy for cancer. Nat Rev Cancer 2003; 3:380–387.
- Ehrlich P. The collected papers of Paul Ehrlich, vol 3. London: Pergamon; 1960.
- Ekins RP, Slater JD. A method for the simultaneous estimation of total exchangeable sodium and potassium in man. Phys Med Biol 1960; 4:264-70.
- El-Deiry WS, Tokino T, Velculescu VE, Levy DB, Parsons R, Trent JM, Lin D, Mercer E, Kinzler KW and Vogelstein B. BAX, a potential mediator of p53 tumor suppression. Cell 1993; 75:817-825.
- Elgazzar AH, Elsaid M. Biological effects of ionizing radiation. In: Elgazzar AH, editor. The pathophysiologic basis of nuclear medicine. Berlin: Springer-Verlag; 2001 pp369–70.
- Elmore S. Apoptosis: A review of programmed cell death. Toxic Pathol 2007; 35:495-516.

- Emmanouilides C, Jazirehi AR, Bonavida B. Rituximab-mediated sensitization of B-non-Hodgkin's lymphoma (NHL) to cytotoxicity induced by paclitaxel, gemcitabine, and vinorelbine. *Cancer Biother Radiopharm* 2002; 17:621-30.
- Eriksson D, Blomberg J, Lindgren T, Löfroth PO, Johansson L, Riklund K, Stigbrand T. Iodine -131 induces mitotic catastrophes and activates apoptotic pathways in HeLa Hep2 cells. *Cancer Biother Radiopharm* 2008; 23: 541-549.
- Erwig LP, Henson PM. Clearance of apoptotic cells by phagocytes. *Cell Death Differ* 2008; 15:243-250.
- Fani M, Maecke HR. Radiopharmaceutical development of radiolabeled peptides. *Eur J Nucl Med Mol Imaging* 2012; 39: S11–S30.
- Fengling M, Liu F, Wen W, Zhai L, Tong J, Wang Z, Yuan X, Gao Q. Rituximab sensitizes a Burkitt lymphoma cell line to cell killing by X-irradiation. *Radiat Environ Biophys* 2009; 48: 371-378.
- Finlay IG, Mason MD, Shelley M. Radioisotopes for the palliation of metastatic bone cancer: a systematic review. *Lancet Oncol* 2005; 6: 392-400.
- Fornari FA, Randolph JK, Yalowich JC, Ritke MK, Gewirtz DA. Interference by doxorubicin with DNA unwinding in MCF-7 breast tumor cells. *Mol Pharmacol* 1994; 45: 649–56.
- Forrer F, Oechsli-Oberholzer C, Campana B, Herrmann R, Maecke HR, Mueller-Brand J, Lohri A. Radioimmunotherapy with <sup>177</sup>Lu-DOTA-rituximab: final results of a phase I/II Study in 31 patients with relapsing follicular, mantle cell, and other indolent B-cell lymphomas. *J Nucl Med* 2013; 54:1045-52.

- Fournier C, Taucher-Scholz G. Radiation induced cell cycle arrest: an overview of specific effects following high-LET exposure. *Radiother Oncol* 2004;73:S119-S22.
- Fraker P, Speck J. Protein and cell membrane iodinations with a sparingly soluble chloroamide, 1, 3, 4, 6-tetrachloro-3a, 6a-diphenylglycoluril. *Biochem Biophys Res Commun* 1978; 80:849-857.
- Frederick CA, Williams LD, Ughetto G, van der Marel GA, van Boom JH, Rich A, Wang AH. Structural comparison of anticancer drug-DNA complexes: adriamycin and daunomycin. *Biochemistry* 1990; 29: 2538–49.
- Freedman A, Nadler L. Immunologic markers in non -Hodgkin's lymphoma. *Hematol Oncol Clinics North Am* 1991; 5: 871-889.
- Friedman AH. Radiation induced signal transduction and stress response. *Radiat Res* 1998; 150: S102-S108.
- Friesen C, Lubatschowski A, Kotzerke J, Buchmann I, Reske SN, Debatin KM. Beta-irradiation used for systemic radioimmunotherapy induces apoptosis and activates apoptosis pathways in leukaemia cells. *Eur J Nucl Med Mol Imaging* 2003; 30:1251-61.
- Gerbaulet A, Pötter R, Mazeron J, Limbergen EV. The GEC ESTRO handbook of brachytherapy. Belgium: ACCO. 2005.
- Gholipour N, Jalilian AR, Khalaj A, Johari-Daha F, Yavari K, Sabzevari O, Khanchi AR, Akhl. Preparation and radiolabeling of a lyophilized (kit) formulation of DOTA-rituximab with Y and <sup>111</sup>In for domestic radioimmunotherapy and

- radioscintigraphy of non-Hodgkin's lymphoma. Daru 2014 ;29:22:58.
- Goddu SM, Rao DV, Howell RW. Multicellular dosimetry for micrometastases: dependence of self-dose versus cross-dose to cell nuclei on type and energy of radiation and subcellular distribution of radionuclides. J Nucl Med 1994; 35:521-530.
- Goldenberg DM. Advancing role of radiolabeled antibodies in the therapy of cancer. Cancer Immunol Immunother 2003; 52:281-296.
- Govindan SV, Griffiths GL, Hansen HJ, Horak ID, Goldenberg DM. Cancer therapy with radiolabeled and drug/toxin-conjugated antibodies. Tech Cancer Res Treat 2005; 4:375-91.
- Harms-Ringdahl M, Nicotera P, Radford IR. Radiation induced apoptosis. Mut Res 1996; 366:171-9.
- Harun-Or-Rashid M, Asai M, Sun XY, Hayashi Y, Sakamoto J, Murata Y. Effect of thyroid statuses on sodium/iodide symporter (NIS) gene expression in the extrathyroidal tissues in mice. Thyroid Res 2010; 3: 3.
- Hertz S, Roberts A. Radioactive iodine as an indicator in thyroid physiology. The Am J of Physiology 1940; 128: 565-576.
- Hu Y, Hellweg CE, Baumstark-Khan C, Reitz G, Lau P. Cell cycle delay in murine pre-osteoblasts is more pronounced after exposure to high-LET compared to low-LET radiation. Radiat Environ Biophys 2014; 53:73-81.
- Jamous M and Mier UHW. Synthesis of peptide radiopharmaceuticals for the therapy and



- diagnosis of tumor diseases. *Molecules* 2013; 18: 3379-3409.
- Jang BS, Lee SM, Kim HS, Shin IS, Razjouyan F, Yao SWZ, Pastan I , Dreher MR, Paik CH. Combined-modality radioimmunotherapy: synergistic effect of paclitaxel and additive effect of bevacizumab. *Nucl Med Biol* 2012; 39: 472-483.
- Jayakumar S, Bhilwade HN, Pandey BN, Sandur SK, Chaubey RC. The potential value of the neutral comet assay and the expression of genes associated with DNA damage in assessing the radiosensitivity of tumor cells. *Mutat Res* 2012; 748: 52-59.
- Jazirehi AR, Gan XH, Vos SD, Emmanouilides C and Bonavida B. Rituximab (anti-CD20) selectively modifies Bcl-xL and apoptosis protease activating factor-1 (Apaf-1) expression and sensitizes human non-Hodgkin's lymphoma B cell lines to paclitaxel-induced apoptosis. *Mol Cancer Ther* 2003; 2:1183-1193.
- Jazirehi AR. Yepez SH, Cheng G, Bonavida B (a). Rituximab (Chimeric Anti-CD20 monoclonal antibody) inhibits the constitutive nuclear factor- IKB signalling pathway in non-Hodgkin's lymphoma B-cell lines: role in sensitization to chemotherapeutic drug-induced apoptosis. *Cancer Res* 2005; 65:264-276.
- Jazirehi, AR., Bonavida B (b). Cellular and molecular signal transduction pathways modulated by rituximab (rituxan antiCD20 mAb) in non-Hodgkin's lymphoma implications in chemo-sensitization and therapeutic intervention. *Oncogene* 2005; 24:2121–2143.
- Johnson GL, Lapadat R. Mitogen-activated protein kinase pathways mediated by ERK, JNK, and p38 Protein Kinases. *Science* 2002; 298: 1911-1912.

- Jones PT, Dear PH, Foote J, Neuberger MS, and Winter G. Replacing the complementarity-determining regions in a human antibody with those from a mouse. *Nature* 1996; 321: 522-525.
- Kang GW, Kang HJ, Shin DY, Gu HR, Choi HS, Lim SM. Radioimmunotherapy with  $^{131}\text{I}$ -rituximab in a patient with diffuse large B-cell lymphoma relapsed after treatment with  $^{90}\text{Y}$ -ibritumomab tiuxetan. *Nucl Med Mol Imaging* 2013; 47:281-4.
- Kankaanranta L, Seppälä T, Koivunoro H, Saarilahti K, Atula T, Collan J, Salli E, Kortensniemi M, Uusi-Simola J, Välimäki P, Mäkitie A, Seppänen M, Minn H, Revitzer H, Kouri M, Kotiluoto P, Seren T, Auterinen I, Savolainen S, Joensuu H. Boron neutron capture therapy in the treatment of locally recurred head-and-neck cancer: final analysis of a phase i/ii trial. *Int J Radiat Oncol Biol Phys* 2012; 82: e67–75.
- Kaplan, I. *Nuclear Physics*, New York: Addison-Wesley, 1964.
- Karran P. DNA double strand break repair in mammalian cells. *Curr Opin Genet Dev* 2000; 10:144–150.
- Kawabata S, Miyatake S, Kuroiwa T, Yokoyama K, Doi A, Iida K, Miyata S, Nonoguchi N, Michiue H, Takahashi M, Inomata T, Imahori Y, Kirihata M, Sakurai Y, Maruhashi A, Kumada H, Ono K. Boron neutron capture therapy for newly diagnosed glioblastoma. *J Radiat Res* 2009; 50: 51–60.
- Kersten MJ. Radioimmunotherapy in follicular lymphoma: Some like it hot.. *Transfus Apher Sci* 2011; 44:173-178.
- Khanna KK and Jackson SP. DNA double strand breaks: signaling, repair and the cancer

- connection. Nat Genet 2001; 27: 247-254.
- Kim SJ, Park Y, Hong HJ. Antibody engineering for the development of therapeutic antibodies. Mol Cells 2005; 20:17-29.
- Kocher DC. Radioactive decay data tables, springfield: national technical information service, 1981 DOE/TIC-11026.
- Köhler G, Milstein C. Continuous cultures of fused cells secreting antibody of predefined specificity. Nature 1975; 256:495–49.
- Kramer GH, Hauck BM, Chamberlain MC. Biological half life of iodine in normal and athyroidic persons. Radiat Prot Dosimetry 2002;102:129–135.
- Kuijpers TW, Bende RJ, Baars PA, Grummels A, Derks IA, Dolman KM, Beaumont T, Tedder TF, van Noesel CJ, Eldering E, van Lier RA. CD20 deficiency in humans results in impaired T cell-independent antibody responses. J Clin Invest 2010; 120: 214–22.
- Kumar C, Korde A, Kusum K, Das T and Samuel G (a). Cellular toxicity and apoptosis studies in osteocarcinoma cells, a comparison of <sup>177</sup>Lu-EDTMP and Lu-EDTMP. Curr Radiopharm 2013; 6: 146-151.
- Kumar C, Pandey BN, Samuel G, Venkatesh M (b) Cellular internalization and mechanism of cytotoxicity of 131I-rituximab in Raji cells J Environ Pathol Toxicol Oncol 2013; 32:91-99.
- Kunala S, Macklis RM. Ionizing radiation induces CD20 expression on human B cells. Int J Cancer 2001; 96:178-181.

- Leahy MF, Seymour JF, Hicks RJ, Turner JH. Multicenter phase II clinical study of iodine-131-rituximab radioimmunotherapy in relapsed or refractory indolent non-Hodgkin's lymphoma. *J Clin Oncol* 2006; 24:4418-25.
- Leahy MF, Turner JH. Radioimmunotherapy of relapsed indolent non-Hodgkin lymphoma with  $^{131}\text{I}$ -rituximab in routine clinical practice: 10-year single-institution experience of 142 consecutive patients. *Blood* 2011; 117:45-52.
- Lei L, Story M and Legerski RJ. Cellular responses to ionizing radiation damage. *Int J Radiat Oncol Biol Phys* 2001; 49:1157-1162.
- Lewington VJ, Bone seeking radionuclides for therapy. *J Nucl Med* 2005; 46:38S-47S.
- Lim SH, Beers SA, French RR, Johnson PM, Glennie MJ, Cragg MS Anti-CD20 monoclonal antibodies: historical and future perspectives. *Haematologica* 2010; 95:135-143.
- Lim SJ, Kim EH, Woo KS, Chung WS, Choi CW, Lim SM. Induction of G2 arrest and apoptosis of Raji cells by continuous low dose beta irradiation with  $^{188}\text{Re}$ -perrhenate. *Cancer Biother Radiopharma* 2006; 21:314-320.
- Liu S. Radiolabeled cyclic RGD peptides as integrin  $\alpha_v\beta_3$ -targeted radiotracers: maximizing binding affinity via bivalency. *Bioconjug Chem* 2009; 20 :2199-213.
- Mathas S, Rickers A, Bommert K, Dörken B, Mapara MY. Anti-CD20 and B-cell receptor-mediated apoptosis: evidence for shared intracellular signaling pathways. *Cancer Res* 2000; 60:7170-7176.
- McQuillan AD, Macdonald WB, Turner JH. Phase II study of first-line  $^{131}\text{I}$ -rituximab

- radioimmunotherapy in follicular non-Hodgkin lymphoma and prognostic  $^{18}\text{F}$ -fluorodeoxyglucose positron emission tomography. *Leuk Lymphoma* 2014;19:1-7.
- Meerten TV, Rozemarijn SR, Samantha H, Anton H and Saskia BE. Complement-induced cell death by rituximab depends on cd20 expression level and acts complementary to antibody-dependent cellular cytotoxicity. *Clin Cancer Res* 2006; 12:4027-4035.
- Meijer AE, Ekedahl J, Joseph B, Castro J, Harms-Ringdahl M, Zhivotovsky B, Lewensohn R. High-LET radiation induces apoptosis in lymphoblastoid cell lines derived from atazia-telangiectasia patients. *Int J Radiat Biol* 2001; 77(3): 309-17.
- Meng Z, Lou S, Tan K, Xu J, Jia Q, Zheng W. Nuclear factor-kappa B inhibition can enhance apoptosis of differentiated thyroid cancer cells induced by  $^{131}\text{I}$ . *PloS One* 2012; 7: (3) e33597.
- Milenic DE, Brady ED, Brechbiel MW. Antibody-targeted radiation cancer therapy. *Nat Rev Drug Disc* 2004; 3:488-96.
- Mirzayans R, Andrais B, Scott A, Murray D. New insights into p53 signaling and cancer cell response to DNA damage: implications for cancer therapy. *J Biomed Biotechnol* 2012; 2012: 170325.
- Momparler RL, Karon M, Siegel SE, Avila F. Effect of adriamycin on DNA, RNA, and protein synthesis in cell-free systems and intact cells. *Cancer Res* 1976; 36: 2891-2895.
- Morgenroth A, Dinger C, Zlatopolskiy BD, Al-Momani E, Glatting G, Mottaghy FM, Reske SN. Auger electron emitter against multiple myeloma targeted endo-radio-

- therapy with  $^{125}\text{I}$ -labeled thymidine analogue 5-iodo-4'-thio-2'-deoxyuridine. Nucl Med Biol 2011;38: 1067-77.
- Morrison SL, Johnson MJ, Herzenberg LA, and Oi VT. Chimeric human antibody molecules; mouse antigen-binding domains with human constant region domains. Proc Natl Acad Sci USA 1984; 21: 6851-6855.
- Mounier N, Briere J, Gisselbrecht C, Emile JF, Lederlin P, Sebban C, Berger F, Bosly A, Morel P, Tilly H, Bouabdallah R, Reyes F, Gaulard P, Coiffier B. Rituximab plus CHOP (R-CHOP) overcomes bcl-2--associated resistance to chemotherapy in elderly patients with diffuse large B-cell lymphoma (DLBCL). Blood 2003; 101:4279-84.
- Multani PS, Grossbard ML. Monoclonal antibody-based therapies for hematologic malignancies. J Clin Oncol 1998; 16:3691-3710.
- Nadler LM, Ritz J, Hardy R, Pesando JM, Schlossman SF, Stashenko P. A unique cell surface antigen identifying lymphoid malignancies of B cell origin. J Clin Invest 1981; 67:134-40.
- Neshasteh-Riz A, Mairs RJ, Angerson WJ, Stanton PD, Reeves JR, Rampling R, Owens J, Wheldon TE. Differential cytotoxicity of  $^{123}\text{IUdR}$ ,  $^{125}\text{IUdR}$  and  $^{131}\text{IUdR}$  to human glioma cells in monolayer or spheroid culture: effect of proliferative heterogeneity and radiation cross-fire. Br J Cancer 1998; 77:385-90.
- Ng DCE. Radioimmunotherapy: a brief overview. Biomed Imaging Interv J 2006; 2:e23.
- O'Connor PM, Jackman J, Jondle D, Bhatia K, Magrath I, Kohn KW. Role of the p53 tumor suppressor gene in cell cycle arrest and radiosensitivity of Burkitt's

- lymphoma cell lines. *Cancer Res* 1993; 53: 4776-80.
- Okarvi SM. Peptide-based radiopharmaceuticals and cytotoxic conjugates: potential tools against cancer. *Cancer Treat Rev* 2008; 34:13-26.
- Olazoglu E, Audoly LP. Evolution of anti-CD20 monoclonal antibody therapeutics in oncology. *MAbs* 2010; 2:14-19.
- Pandey BN, Mishra KP. In vitro studies on radiation induced membrane oxidative damage in apoptotic death of mouse thymocytes. *Int J Low Radiat* 2003;1:113-119.
- Pedersen IM, Buhl AM, Klausen P, Geisler CH, Jurlander J. The chimeric anti-CD20 antibody rituximab induces apoptosis in B-cell chronic-kinase-lymphocytic leukaemia cells through a p38 mitogen activated protein dependent mechanism. *Blood* 2002; 99: 1314-1319.
- Peter BP, West SC. Role of the human RAD51 protein in homologous recombination and double stranded break repair. *Trends Biochem Sci* 1998; 23: 247-251.
- Pfaffl MW, Horgan GW, Dempfle L. Relative expression software tool (REST) for group-wise comparison and statistical analysis of relative expression results in real-time PCR, *Nucleic Acids Res* 2002; 30: e36.
- Pigram WJ, Fuller W, Hamilton LD. Stereochemistry of intercalation: interaction of daunomycin with DNA. *Nat New Biol* 1972; 235: 17-9.
- Plosker GL, Fliggitt DP. Rituximab: a review of its use in non-Hodgkin's lymphoma and chronic lymphocytic leukaemia. *Drugs* 2003; 63:803-843.

- Pohlman B, Sweetenham J, Macklis RM. Review of clinical radioimmunotherapy. *Expert Rev Anticancer Ther* 2006; 6: 445–61.
- Presta L. Antibody engineering for therapeutics. *Curr Opin Struct Biol* 2003; 13:519-525.
- Rajagopalan S, Politi PM, Sinha BK, Myers CE. Adriamycin- induced free radical formation in the perfused rat heart:implication for cardiotoxicity. *Cancer Res.* 1988; 48:4766-4769.
- Rao AV, Akabani G, Rizzieri DA. Radioimmunotherapy for non-Hodgkin's lymphoma. *Clin Med Res* 2005; 3:157-165.
- Reff ME, Carner K, Chambers KS, Chinn PC, Leonard JE, Rabb R, Newman RA, Hanna N, Anderson DR. Depletion of B cells in vivo by a chimeric mouse human monoclonal antibody to CD20. *Blood* 1994; 83:435-445.
- Salmon SE, Grogan TM, Miller T, Scheper R, William S, Dalton WS. Prediction of doxorubicin resistance in vitro in myeloma, lymphoma, and breast cancer by P-glycoprotein staining. *J Natl Cancer Inst* 1989; 81: 696-701.
- Scheidhauer K, Wolf I, Baumgartl HJ, Schilling CV, Schmidt B, Reidel G, Peschel C, Schwaiger M. Biodistribution and kinetics of <sup>131</sup>I-labelled anti-CD20 MAB IDEC-C2B8 (rituximab) in relapsed non-Hodgkin's lymphoma. *Eur J Nucl Med* 2002; 29:1276-1282.
- Schimmel K, Richel D, Brink RVD, Guchelaar HJ. Cardiotoxicity of cytotoxic drugs. *Cancer Treat Rev* 2004; 30:181-191.
- Schipler A, Iliakis. DNA double-strand-break complexity levels and their possible



- contributions to the probability for error-prone processing and repair pathway choice. *Nucleic Acids Res* 2013; 41:7589-605.
- Scott HO, Francisco JH, James LC, Myron SC. Acquired resistance to rituximab is associated with chemotherapy resistance resulting from decreased bax and bak expression. *Clin Cancer Res* 2008; 14:1550-1560.
- Sharkey RM, Burton J, Goldenberg DM. Radioimmunotherapy of non-Hodgkin's lymphoma: a critical appraisal. *Expert Rev Clin Immunol* 2005; 1:47-52.
- Shen F, Chu S, Bence AK, Bailey B, Xue X, Erickson PA, Montrose MH , Beck WT, Erickson LC. Quantitation of doxorubicin uptake, efflux, and modulation of multidrug resistance (MDR) in mdr human cancer cells. *J Pharmacol Exp Ther* 2008; 324:95–102.
- Shen J, Hughes C, Chao C, Cai J, Bartels C, Gessner T, Subjeck J. Coinduction of doxorubicin glucose-regulated proteins in resistance Chinese hamster cells (stress proteins/anoxia/calcium ionophores). *Proc Natl Acad Sci USA* 1987; 84:3278-3282.
- Shih LB, Thorpe SR, Griffiths GL, Diril H, Ong GL, Hansen HJ, Goldenberg DM, Mattes MJ. The processing and fate of antibodies and their radiolabels bound to the surface of tumor cells in vitro: a comparison of nine radiolabels. *J Nucl Med* 1994; 35:899-908.
- Skoog ML, Ollinger K, Skogh M. Microfluorometry using fluorescein diacetate reflects the integrity of the plasma membrane in UVA-irradiated cultured skin fibroblasts *Photodermatol Photoimmunol Photomed* 1997; 13:37-42.

- Skvortsova I, Skvortsova S, Popper BA, Haidenberger A, Saurer M, Gunkel AR, Zwierzina H, Lukas PJ. Rituximab enhances radiation-triggered apoptosis in Non-Hodgkin's lymphoma cells via caspase dependent and independent mechanisms. *Radiat Res* 2006; 47:183-196.
- Slovak ML, Hoeltge GA, Dalton WS, Trent JM. Pharmacological and biological evidence for differing mechanisms of doxorubicin resistance in two human tumor cell lines. *Cancer Res* 1988; 48:2793-2797.
- Smith L, Watson MB, O'Kane SL, Drew PJ, Lind MJ, Cawkwell L. The analysis of doxorubicin resistance in human breast cancer cells using antibody microarrays. *Mol Cancer Ther* 2006; 5: 2115-20.
- Smith MR. Rituximab (monoclonal anti CD20 antibody): mechanisms of action and resistance. *Oncogene* 2003; 22:7359–7368.
- Sood DD, Ready AVR, Ramamoorthy N. *Fundamental of Radiochemistry*. India: IANCAS; 2000.
- Spitzweg C, Joba W, Eisenmenger W, Heufelder AE. Analysis of human sodium iodide symporter gene expression in extrathyroidal tissues and cloning of its complementary deoxyribonucleic acids from salivary gland, mammary gland, and gastric mucosa. *J Clin Endocrinol Metab* 1998; 83: 1746-51.
- Steel GG, Deacon JM, Duchesne GM, Horwich A, Kelland LR, Peacock JH. The dose-rate effect in human tumor cells. *Radiother Oncol* 1987; 9: 299-310.
- Stel AJ, Cate BT, Jacobs S, Kok JW, Spierings DCJ, Dondorff M, Helfrich W, Kluin-Nelemans HC, de Leij LFMH, Withoff S, Kroesen BJ. Fas receptor clustering and

- involvement of the death receptor pathway in rituximab-mediated apoptosis with concomitant sensitization of lymphoma b cells to fas-induced apoptosis. J Immunol 2007; 178:2287-2295.
- Stewart AJ et al. Radiobiological concepts for brachytherapy. In Devlin P. Brachytherapy. Applications and Techniques. Philadelphia: LWW. 2007.
- Szumiel I. Ionizing radiation induced cell death. Int J Radiat Biol 1994; 66:329-341.
- Tan C, Tasaka H, Yu KP, Murphy ML, Karnofsky DA. Daunomycin, an antitumor antibiotic, in the treatment of neoplastic disease. Clinical evaluation with special reference to childhood leukemia. Cancer 1967; 20: 333–53.
- Thakral P, Singla S, Yadav MP, Vasisht A, Sharma A, Gupta SK, Bal CS; Snehlata, Malhotra A. An approach for conjugation of (177) Lu- DOTA-SCN- Rituximab (BioSim) & its evaluation for radioimmunotherapy of relapsed & refractory B-cell non Hodgkins lymphoma patients. Indian J Med Res 2014;139:544-54.
- Tran L, Baars JW, de Boer JP, Hoefnagel CA, Beijnen JH, Huitema AD. The pharmacokinetics of <sup>131</sup>I-rituximab in a patient with CD20 positive non-Hodgkin Lymphoma: evaluation of the effect of radioiodination on the biological properties of rituximab. Hum Antibodies 2011; 20:37-40.
- Trock BJ, Leonessa F, Clarke R. Multidrug Resistance in Breast Cancer: a Meta-analysis of MDR1/gp170 Expression and Its Possible Functional Significance. J Natl Cancer Inst 1997; 89: 917-93.
- Tsurushita N, Hinton PR, Kumar S. Design of humanized antibodies: from anti-Tac to Zenapax. Methods 2005; 36: 69-83.

- Urashima T, Nagasawa H, Wang K, Adelstein KJ, Little OB, Kassis AI. Induction of apoptosis in human tumor cells after exposure to Auger electrons: comparison with  $\gamma$ -ray exposure. Nucl Med Biol 2006; 33: 1055 -106.
- Vandenbulcke K, De Vos F, Offner F, Philippé J, Apostolidis C, Molinet R, Nikula TK, Bacher K, de Gelder V, Vral A, Lahorte C, Thierens H, Dierckx RA, Slegers G. In vitro evaluation of  $^{213}\text{Bi}$ -rituximab versus external gamma irradiation for the treatment of B-CLL patients: relative biological efficacy with respect to apoptosis induction and chromosomal damage. Eur J Nucl Med Mol Imaging 2003; 30:1357-64.
- Wagner EF, Nebreda ÁR. Signal integration by JNK and p38 MAPK pathways in cancer development. Nature Reviews Cancer 2009; 9: 537-549.
- Ward JF. DNA damage produced by ionizing radiation in mammalian cells: identities, mechanisms of formation and reparability. Prog Nucleic Acid Res Mol Biol 1998; 35:95–125.
- Wei L, Luo RC, Zhang JY, Yan X, Lü CW. In vitro cytotoxicity of  $^{131}\text{I}$ -Rituximab against B-cell lymphoma cells. Nan Fang Yi Ke Da Xue Xue Bao 2009; 29: 40-3.
- Wei L., Luo RC, Zhang JY, Yan X, Fang YX, Fei LH. Biological response of B-cell lymphoma cells in vitro to  $^{131}\text{I}$ -rituximab. Nan Fang Yi Ke Da Xue Xue Bao 2006; 26:211-213.
- Weiner GJ. Rituximab: mechanism of action. Semin Hematol 2010; 47: 115–123.
- Weiss RB. The anthracyclines: will we ever find a better doxorubicin? Semin Oncol 1992; 19: 670–86.

- Wheat JM, Currie GM, Davidson R, Kiat, H. Radionuclide therapy. The Radiographer 2011; 58: 53-59.
- Wilkins DK, Mayer A. Development of antibodies for cancer therapy. Expert Opin Biol Ther 2006; 6:787-96.
- Willhauck MJ, Sharif-Samani B, Senekowitsch-Schmidtke R, Wunderlich N, Göke B, Morris JC, Spitzweg C. Functional sodium iodide symporter expression in breast cancer xenografts in vivo after systemic treatment with retinoic acid and dexamethasone. Breast Cancer Res Treat 2008; 109: 263-272.
- Yalow RS, Berson SA. Immunoassay of endogenous plasma insulin in man. J Clin Invest 1960; 39: 1157–75.
- Yasui LS, Andorf C, Schneider L, Kroc T, Lennox A, Saroja KR. Gadolinium neutron capture in glioblastoma multiforme cells. Int J Radiat Biol 2008; 84: 1130–9.
- Zhang S, Liu X, Bawa-Khalfe T, Lu LS, Lyu YL, Liu LF, Yeh ET. Identification of the molecular basis of doxorubicin-induced cardiotoxicity. Nat Med 2012; 18:1639-42.
- Zhou X, Hu W, Qin X. The role of complement in the mechanism of action of rituximab for b-cell lymphoma: implications for therapy. Oncologist 2008; 13: 954–966.

# **PUBLICATIONS**

## Journal Publications

- [1.] **Kumar C**, Pandey BN, Samuel G, Venkatesh M. Cellular internalization and mechanism of cytotoxicity of  $^{131}\text{I}$ -rituximab in Raji cells. *J Environ Pathol Toxicol Oncol* 2013; 32(2): 91-99.
- [2.] **Kumar C**, Jayakumar S, Pandey BN, Samuel G, Venkatesh M. Cellular and Molecular Effects of Beta Radiation from I-131 on Human Tumor Cells a Comparison with Gamma Radiation. *Current Radiopharmaceuticals*. Jul 16. 2014, [Epub ahead of print].
- [3.] **Kumar C**, Pandey BN, Samuel G, Venkatesh M. Doxorubicin enhances  $^{131}\text{I}$ -rituximab induced cell death in Raji cells. *Journal of Cancer Research & Therapeutics*. 2014, [Journal ahead of print].

## Conference Publications

- [1.] **Kumar C**, Pandey BN, Korde A, Samuel G. Radioiodinated rituximab induced p21 dependent cell death in Raji cell. *SNMICON 2012*, Bhubaneswar, 29<sup>th</sup> Nov-2<sup>nd</sup> Dec 2012.
- [2.] **Kumar C**, Pandey BN, Samuel G, Venkatesh M. Doxorubicin enhances  $^{131}\text{I}$ -rituximab induced apoptotic cell death in Raji cells. *Indian j Nucl Med* 2013; 28:S34. SNMICON 2013, Mumbai.
- [3.] **Kumar C**, Jayakumar S, Pandey BN, Shinde, SN, Korde A, Samuel G, Dash A. Differential role of RAD51 in repair of DNA damage induced by  $\beta$ -rays of I-131 in Raji cells: a comparison with the  $\gamma$ -rays. *ICRB 2014*, 11-13<sup>th</sup> Nov 2014, New Delhi.

# Cellular Internalization and Mechanism of Cytotoxicity of $^{131}\text{I}$ -Rituximab in Raji Cells

Chandan Kumar,<sup>1</sup> B.N. Pandey,<sup>2</sup> Grace Samuel,<sup>1,\*</sup> & Meera Venkatesh<sup>1</sup>

<sup>1</sup>Radiopharmaceuticals Division, Bhabha Atomic Research Centre, Mumbai, India; <sup>2</sup>Radiation Biology and Health Sciences Division, Bhabha Atomic Research Centre, Mumbai, India

\*Address all correspondence to: Grace Samuel, Radiopharmaceuticals Division, Bhabha Atomic Research Centre, Mumbai 400 085, India; grace@barc.gov.in

**ABSTRACT:** Rituximab labeled with radioiodine ( $^{131}\text{I}$ -rituximab) has a large potential to be employed for targeted therapy of non-Hodgkin's lymphoma. Studies of parameters such as cellular internalization, stability of  $^{131}\text{I}$ -rituximab bound to CD20 receptor of tumor cells, and the mechanism underlying cytotoxicity induced by  $^{131}\text{I}$ -rituximab will be useful for better clinical application. In this article we describe the efficacy of  $^{131}\text{I}$ -rituximab in CD20-expressing Raji cells. Rituximab labeled with  $^{131}\text{I}$  was purified on a PD-10 column and characterized using high-performance liquid chromatography and paper electrophoresis. Raji cells treated with  $^{131}\text{I}$ -rituximab (1.85 MBq for 2 hours) were washed then incubated. The culture medium collected from treated cells showed increased radioactivity over a longer period (>6 hours), probably due to the deiodination/degradation of  $^{131}\text{I}$ -rituximab. The tumor cells treated with  $^{131}\text{I}$ -rituximab showed time-dependent internalization of radioactivity, and at 12 hours the radioactivity was almost equally distributed in the membrane and cytoplasm. At 24 hours ~70% of the radioactivity was internalized. Cellular toxicity after  $^{131}\text{I}$ -rituximab treatment showed a time-dependent increase in toxicity as estimated by lactate dehydrogenase. Tumor cells treated with  $^{131}\text{I}$ -rituximab showed significantly higher toxicity and apoptosis compared with the those treated with the same concentration of unlabeled rituximab. The increased apoptotic death in cells treated with  $^{131}\text{I}$ -rituximab was associated with cleavage of poly ADP ribose polymerase and upregulation of p53 protein. This study provides a deeper understanding about the cellular internalization/stability of  $^{131}\text{I}$ -rituximab bound to the CD20 receptor and its efficacy in killing Raji cells.

**KEY WORDS:**  $^{131}\text{I}$ -rituximab, rituximab, lymphoma, toxicity, apoptosis, cellular internalization

## I. INTRODUCTION

Rituximab is a genetically engineered chimeric monoclonal antibody against the CD20 receptor<sup>1</sup> that was approved by the U.S. Food and Drug Administration in 1997 for the treatment of non-Hodgkin's lymphoma (NHL). CD20 is a 33- to 37-kDa extracellular surface protein expressed during early B-cell development.<sup>2</sup> Most human B-cell-lineage malignancies express a large amount of the CD20 receptor protein.<sup>3</sup> Hence, CD20 is considered an attractive and possible target for the treatment of NHL.<sup>4,5</sup> Most of the commercially successful monoclonal antibodies on the market or in the final stage of development are unlabeled. The concept of "magic bullets," coined by Ehrlich,<sup>6</sup> became a reality with the use of specific antibodies conjugated to radionuclides<sup>7</sup> as targeting molecules. There are several

radionuclides coupled to antibodies,<sup>8-10</sup> peptides,<sup>11</sup> or other molecules<sup>12-14</sup> that are widely used in the therapy of various diseases, particularly cancer.

Radioiodine ( $^{131}\text{I}$ ) has been largely used for targeted therapy of thyroid disorders because of the uptake of  $^{131}\text{I}$  by the differentiated thyroid tissues.<sup>15</sup> It has the advantage of having both  $\beta^-$  as well as  $\gamma$  radiation and hence can be used for both imaging and therapy. The average range (2.3 mm) of the electrons emitted by  $^{131}\text{I}$  can lead to irradiation of many neighboring tumor cells, and this cross fire may exclude the necessity of a radiopharmaceutical being present within each cell of the targeted tumor. The advantages of  $^{131}\text{I}$ -based radiopharmaceuticals are many and include (1) easy availability at a reasonable cost, (2) convenient half-life of ~8 days for therapy, and, most important, (3) being amenable to labeling with a variety of biomolecules because of



simple chemical reactions that do not alter their bioreactivity. There are currently two radiolabeled anti-CD20 monoclonal antibodies approved for therapy by the US Food and Drug Administration. Zevalin, a  $^{90}\text{Y}$ -labeled ibritumomab tiuxetan, was approved in 2002 and  $^{131}\text{I}$ -labeled Bexxar was approved in 2003—both for the treatment of NHL.<sup>16</sup> These antibodies are of mouse origin and may trigger the human antimouse antibody response, thus posing limitations to their efficacy. Hence, a chimeric monoclonal antibody such as rituximab has been chosen for our study because it may exhibit better therapeutic efficacy. The cell killing ability of rituximab could be enhanced further with the incorporation of therapeutic radionuclides such as  $^{131}\text{I}$  targeted to highly radiosensitive lymphoma cells.  $^{131}\text{I}$ -rituximab has been shown to be effective in lymphoma patients<sup>17</sup>; however, its characterization and evaluation of cytotoxicity<sup>18,19</sup> in cancer cells are limited in the literature. Hence, this study aimed to study the cellular localization/stability of  $^{131}\text{I}$ -rituximab bound with a CD20 receptor and the molecular mechanism underlying the cytotoxicity in Raji cells, a B-cell lymphoma cell line.

## II. MATERIALS AND METHODS

### A. Materials

Chemicals and kits for assays were purchased from Sigma Chemical Inc. (St. Louis, MO) unless otherwise stated. Rituximab and the In Situ Cell Death Detection Kit were purchased from Roche Diagnostics GmbH (Indianapolis, IN).  $^{131}\text{I}$  was obtained from the Radiochemicals Section of the Bhabha Atomic Research Centre, Mumbai, India.

### B. Cell Culture

Raji (CD20 wild type, Burkitt lymphoma cell line) and U937 (p53-ve human histiocytic lymphoma cell line, CD20-ve) cell lines obtained from the National Center for Cell Sciences (Pune, India) were routinely cultured in Roswell Park Memorial Institute 1640 medium supplemented with 10% serum (Invitrogen, Carlsbad, CA), 2 mM L-glutamine, and antibiotic solution. All routine culture was performed in a humidified 5% carbon dioxide atmosphere at 37°C, and cells were passaged every alternate day.

### C. Radiolabeling of Rituximab With $^{131}\text{I}$

Radiolabeling of rituximab was carried out using the Iodogen method.<sup>20</sup> Rituximab (100  $\mu\text{g}$ ),  $\text{Na}^{131}\text{I}$  (~1 mCi), and 100  $\mu\text{L}$  of 0.5 M phosphate buffer (pH, 7.5) were combined in a tube coated with Iodogen (1  $\mu\text{g}$ ) and mixed for 10 minutes. The reaction mixture was purified on a PD-10 column (GE Healthcare, Amersham, UK) using phosphate buffer (0.05 M, pH 7.6) as the eluant. The labeling yield and radiochemical purity were analyzed by high performance liquid chromatography (HPLC, JASCO, Japan) and with radiation detector (Raytest, Germany) using a TSKgel column (Tosoh Bioscience, King of Prussia, PA) and paper electrophoresis. For HPLC, 0.05 M phosphate buffer (pH, 6.8) was used as the mobile phase.

### D. Analysis of CD20 Expression by Flow Cytometry

Raji and U937 cells were taken from the confluent culture, fixed in 2% formaldehyde, and stain with 5- $\mu\text{L}$  fluorescein isothiocyanate-labeled mouse monoclonal antibody to the human CD20 antigen (procured from Invitrogen) in 100  $\mu\text{L}$  staining buffer (2% serum in phosphate-buffered saline [PBS]) for an hour. Cells were washed twice with staining buffer and analyzed in a Partec flow cytometry system (Partec GmbH, Münster, Germany) using Flowjo software (Tree Star, Inc., Ashland, OR).

### E. Cell Binding and Inhibition

Inhibition studies were carried out in Raji cells ( $1 \times 10^6$ ) to demonstrate the specificity of the antibody. Raji cells were incubated with 0.037 MBq of  $^{131}\text{I}$ -rituximab along with different amounts (0.1–100  $\mu\text{g}$ ) of rituximab for 2 hours at 37°C. To estimate the extent of nonspecific binding,  $1 \times 10^6$  U937 cells (a CD20-ve cell line) also were incubated with  $^{131}\text{I}$ -rituximab for 2 hours at 37°C. In the case of Raji cells, cell binding studies were performed with varying amounts of  $^{131}\text{I}$ -rituximab (0.037, 0.37, 1.85, and 3.7 MBq, equivalent to 1, 10, 50, and 100  $\mu\text{Ci}$ , respectively) and treated for 30 minutes, 2 hours, and 6 hours at 37°C. A range of radioactivity was chosen to optimize the suitable concentration of  $^{131}\text{I}$ -rituximab. The cells were washed thrice with cold PBS and radioactiv-

ity was measured with sodium iodide doped with thallium (NaI(Tl)), a gamma counter. Cell binding was calculated and expressed as the percentage of cell binding ([radioactivity count in 30 seconds associated with cell/total tracer radioactivity count in 30 seconds]  $\times$  100). The percentage of cell binding inhibition was calculated as:

$$(100 \times [1 - \{\text{percentage of cell binding in the presence of rituximab} / \text{percentage of cell binding in the absence of rituximab}\}]).$$

#### F. Treatment of Tumor Cells With $^{131}\text{I}$ -Rituximab

Raji cells ( $1 \times 10^6$ ) added to 1.85 MBq of  $^{131}\text{I}$ -rituximab were incubated for 2 hours. Cells were harvested and washed thrice with PBS and further incubated for 2, 6, 12, and 24 hours at  $37^\circ\text{C}$  in culture conditions. The dose delivered was calculated by assuming that the energy deposited in the cells by the beta particles was 100%, whereas it was negligible for the gamma rays. The doses delivered to the tumor cells by 1.85 MBq of  $^{131}\text{I}$ -rituximab were calculated based on the S value,<sup>21</sup> which was found to be 0.38 Gy for a 2-hour incubation period. The cumulative dose received by cells during incubation periods of 2, 6, 12, and 24 hours were 0.39, 0.40, 0.42, and 0.46 Gy, respectively.

#### G. Cellular Internalization of $^{131}\text{I}$ -Rituximab

The cells were initially incubated with 1.85 MBq of  $^{131}\text{I}$ -rituximab for 2 hours at  $37^\circ\text{C}$ , washed thrice, and then further incubated in culture media for 2, 6, 12, and 24 hours. After incubation and washing, the cell membrane was stripped with an acidic buffer (200 mM sodium acetate in 500 mM sodium chloride; pH, 2.5), incubated for 5 minutes at  $4^\circ\text{C}$ , and centrifuged ( $1400 \times g$  for 5 minutes). Cell pellets were resuspended and washed twice with the acidic buffer, and the supernatants were pooled. Cell pellets were lysed in 1 N sodium hydroxide, and the radioactivity associated was measured in an NaI(Tl) gamma counter. The percentage distribution of  $^{131}\text{I}$ -rituximab on the membrane (supernatant fraction) and cytoplasm (cell pellet fraction) was calculated as follows:

$$(\text{Radioactivity in either supernatant or cell pellets} / [\text{total radioactivity} \{\text{supernatant} + \text{cell pellets}\}]) \times 100).$$

#### H. Radioiodine Rituximab Degradation/Deiodination

The Raji cells were initially incubated with  $^{131}\text{I}$ -rituximab for 2 hours at  $37^\circ\text{C}$  followed by washing and further incubation in culture conditions. The supernatant culture media were collected at different time periods to determine deiodination or degradation. For this, 500  $\mu\text{L}$  of media was mixed with 2 mg of immunoglobulin (as a carrier) in ice-cold 10% trichloroacetic acid (TCA). The mixture was vortexed and centrifuged at  $10,000 \times g$  for 10 minutes. The supernatant was carefully transferred and pellets were dissolved in 1 mL of 2 N sodium hydroxide. The radioactivity in both fractions was measured in an NaI(Tl) gamma counter and calculated as follows:

$$(\text{Radioactivity in either supernatant or protein pellets} / [\text{total radioactivity} \{\text{supernatant} + \text{protein pellets}\}]) \times 100.$$

For paper chromatography, a Whatman paper strip was soaked in 0.025 M phosphate buffer (pH, 7.6) and allowed to partially dry in air. Cell supernatant (20  $\mu\text{L}$ ) from each time point was spotted onto a paper strip and underwent electrophoresis at 245 V for an hour. The paper strip was dried and cut into 1-cm pieces, and the radioactivity of each piece was counted in an NaI(Tl) gamma counter. To find the position of migration on the paper strip,  $^{131}\text{I}$ -rituximab and  $^{131}\text{I}$  were used as controls. The percentage of radioactivity at different spots was calculated as follows:

$$(\text{Radioactivity in either point of spotting [intact or high molecular weight } ^{131}\text{I}\text{-rituximab] or point of radioiodide [deiodinated]} / [\text{total radioactivity} \{\text{intact} + \text{deiodinated} + \text{degraded}\}]) \times 100.$$

#### I. Estimation of Cell Toxicity

##### 1. Lactate Dehydrogenase Assay in Cell Supernatant

The tumor cells were treated with  $^{131}\text{I}$ -rituximab (1.85 MBq) or an equivalent amount of rituximab (control) in complete medium in culture conditions followed by washing of cells (as mentioned earlier). After completion of different periods of incubation, cells were centrifuged and the supernatant culture medium was collected to estimate

the release of lactate dehydrogenase (LDH). The LDH assay was carried out according to the protocol described in the kit. In brief, the LDH assay mixture was prepared by mixing equal volumes of LDH assay substrate, cofactor, and dye just before use. The reaction mixture was added to culture media (2:1, v/v) and placed in 96-well plates. They were mixed well, covered with aluminum foil to protect the mixture from light, and incubated for 25 minutes at room temperature. The reaction was terminated by adding one-tenth of the volume of 1 N hydrogen chloride, and the absorbance was measured at 490 nm. The percentage of release of LDH was calculated as  $[\text{optical density (OD) of treated sample} / \text{OD of control sample}] \times 100$ .

## 2. Apoptotic DNA Fragmentation

To determine the magnitude of apoptosis, a DNA fragmentation study was carried out according to protocol described in In Situ Cell Death Detection Kit. This method is based on the fact that during apoptosis the fragmented nuclear DNA and histone exudes to cytoplasm, which can be detected by enzyme-linked immunosorbent assay (ELISA) and expressed as an enrichment factor. Raji cells ( $\sim 1 \times 10^5$ ) harvested after treatment were lysed for 30 minutes using a lysis buffer and centrifuged to  $20,000 \times g$  for 10 minutes. The supernatant was carefully transferred to new tubes and stored at  $-40^\circ\text{C}$  until analysis. The ELISA plate was coated overnight with antihistone antibody at  $4^\circ\text{C}$  followed by incubation of 100  $\mu\text{L}$  of cell lysates for 90 minutes. Thereafter, the wells were washed thrice and incubated with anti-DNA horseradish peroxidase for 90 minutes. The wells again were washed thrice, and substrate solution was added and incubated for 20 minutes. The color developed was quantified at 405 nm. DNA fragmentation was expressed as an enrichment factor, which is the ratio of the OD of the treated and control samples.

## J. Western Blotting

Raji cells were harvested after the desired treatment and lysed in cellLytic MT reagent, and protein was estimated using the Bio-Rad Protein Assay (Bio-Rad lab Inc. Hercules CA). Protein (50  $\mu\text{g}$ ) was loaded on 10% sodium dodecyl sulfate polyacrylamide gel electrophoresis gel and transferred

onto a nitrocellulose membrane by electroblotting. The membrane was processed for blocking using 5% nonfat milk protein (Cell Signaling Technology, Danvers, MA) followed by incubation with primary antibodies (poly ADP ribose polymerase [PARP], p53, and  $\beta$ -actin) for 1.5 hours. The membrane was washed with Tris buffer saline with tween 20 followed by treatment with a secondary antibody. The membrane was developed using a BM chemiluminescence kit (Roche Diagnostics) using ECL hyperfilm (GE Healthcare).

## K. Statistical Analysis

Unless mentioned, results are mean  $\pm$  standard deviation of at least 3 independent experiments.  $P \leq 0.05$  was considered statistically significant.

## III. RESULTS

### A. Flow Cytometric Analysis of Cells

Flow cytometric data (Fig. 1a) shows 3.5% and 69.4% fluorescein isothiocyanate-positive cells in U937 and Raji cell lines, respectively.

### B. Specificity of $^{131}\text{I}$ -Rituximab With CD20-Positive Tumor Cells

Rituximab was labeled with  $^{131}\text{I}$  using the Iodogen method. The radioiodination yield was  $\sim 95\%$  and the radiochemical purity of  $^{131}\text{I}$ -rituximab was  $>99\%$  after purification in a PD-10 column, as determined by HPLC and paper electrophoresis. The specific radioactivity of  $^{131}\text{I}$ -rituximab was 0.37 MBq/ $\mu\text{g}$ . To demonstrate the unaltered specificity of the antibody (rituximab) after labeling with  $^{131}\text{I}$ , a competitive binding inhibition study was performed in the presence of rituximab. Raji cells were treated with  $^{131}\text{I}$ -rituximab (0.037 MBq) for 2 hours along with increasing concentrations (0.1–100  $\mu\text{g}$ ) of rituximab (Fig. 1b). Our results showed that with an increase in the concentration of rituximab, the percentage of inhibition was increased, which reached a saturation ( $\sim 90\%$  inhibition) at concentrations of  $\geq 50 \mu\text{g}$  rituximab. These results suggest that the immunoreactivity of rituximab was retained after labeling with  $^{131}\text{I}$ .

To further confirm the specificity of  $^{131}\text{I}$ -rituximab to Raji cells with a CD20 receptor, the percentage of cell binding of  $^{131}\text{I}$ -rituximab (0.037

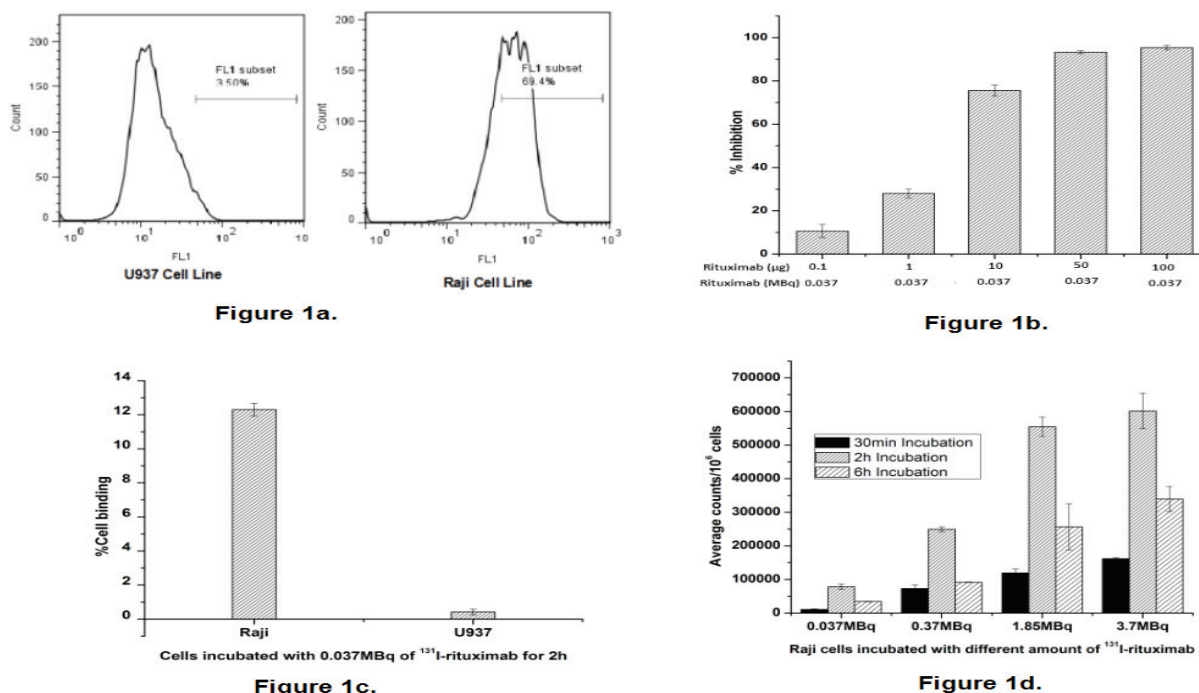


**FIG. 1:** **a:** CD20 expression analysis by flow cytometry in U937 (left) and Raji (right) cell lines. **b:** Percentage of cell binding inhibition in a Raji cell line incubated with  $^{131}\text{I}$ -rituximab. **c:** Percentage of cell binding in Raji and U937 cell lines incubated with  $^{131}\text{I}$ -rituximab. **d:** Average counts per  $10^6$  cells of Raji incubated with  $^{131}\text{I}$ -rituximab.

MBq; 2-hour incubation) was compared with that in U937 (CD20-negative) tumor cells. Our results showed that the U937 cells showed very low binding (<0.5%) compared with Raji cells (~12% binding) (Fig. 1c), further suggesting the specificity of  $^{131}\text{I}$ -rituximab to tumor cells with CD20 receptors.

To optimize the time and concentration of  $^{131}\text{I}$ -rituximab required for optimal tumor cell binding, Raji cells were treated with varying amounts of  $^{131}\text{I}$ -rituximab (0.037–3.7 MBq), and cells were harvested after different periods of incubation (0.5–6 hours) (Fig. 1d). The maximum radioactivity per million cells was observed for 2-hour incubation irrespective of the amount of  $^{131}\text{I}$ -rituximab used. However, we observed saturation of cell bound radioactivity at 1.85 and 3.7 MBq of  $^{131}\text{I}$ -rituximab, incubated for 2-hour, with one million cells. Hence, 1.85-MBq radioactivity and a 2-hour period of incubation were used for further experiments.

### C. Cellular Internalization of $^{131}\text{I}$ -Rituximab

To study whether the  $^{131}\text{I}$ -rituximab associated with tumor cells was internalized (cytoplasmic) or bound to the membrane, the membrane was

stripped at different time periods of  $^{131}\text{I}$ -rituximab treatment. It was observed that a major fraction (~70% of total radioactivity associated with cells) was membrane bound up to 6 hours (Fig. 2a), whereas at 24 hours the membrane-bound radioactivity decreased to ~30%. Furthermore, to investigate the stability of  $^{131}\text{I}$ -rituximab bound with CD20 receptors in Raji cells during the incubation period (2–24 hours), radioactivity was determined in culture medium (supernatant) and cell pellets (Fig. 2b). Our results suggest that radioactivity in the supernatant was increased from  $59.85 \pm 1.55\%$  at 2 hours to  $83.82 \pm 1.51\%$  at 24 hours of incubation, whereas the radioactivity associated with cells decreased from  $40.15 \pm 0.369\%$  at 2 hours to  $16.17 \pm 0.12\%$  at 24 hours of incubation.

### D. Determination of Deiodination and Degradation of Rituximab in Raji Cells Labeled With $^{131}\text{I}$ -Rituximab

From the observations described above, it is an obvious speculation that the change in radioactivity in the cell-bound fraction during the course of incubation may be due to 3 reasons, either independent



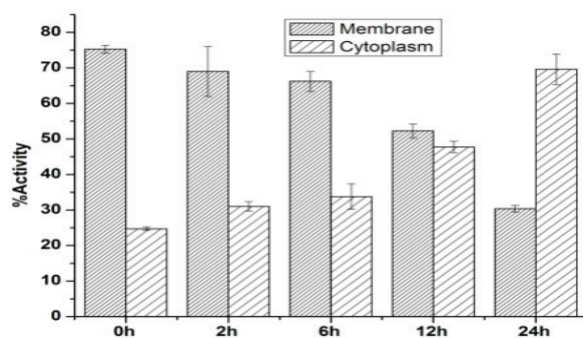


Figure 2a.

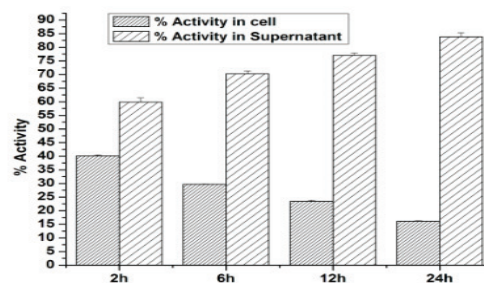


Figure 2b.

**FIG. 2:** a: Distribution of radioactivity in cell cytoplasm and on cell membrane in Raji cells after incubation with  $^{131}\text{I}$ -rituximab b: Percentage of radioactivity associated with Raji cells and its supernatant media after incubation with  $^{131}\text{I}$ -rituximab.

or in combination: (1) detachment of  $^{131}\text{I}$ -rituximab from the cell receptor; (2) degradation of  $^{131}\text{I}$ -rituximab, and (3) deiodination of  $^{131}\text{I}$ -rituximab. Hence, to prove the mechanism of changes in radioactivity in the cell-bound fraction during incubation, the following experiments were performed. The supernatant culture media of Raji cells was obtained after different time periods of  $^{131}\text{I}$ -rituximab incubation. The magnitude of degradation/deiodination of  $^{131}\text{I}$ -rituximab was estimated in these culture media by TCA precipitation (Fig. 3a). It was found that the radioactivity associated with TCA precipitate was almost constant (90–95%) up to 12 hours of incubation, which decreased to ~75% at 24 hours. The observation from TCA precipitation was analyzed further by paper electrophoresis (Fig. 3b). It was found that the radioactivity associated with the point of spotting remains high (~90–95%) for up to 6 hours, which subsequently decreased to 75–80% at longer periods of incubation (12 and 24 hours). However, the radioactivity in the iodide zone, which represents free iodide, showed only ~10%, even at the 24-hour time point.

#### E. Effect of $^{131}\text{I}$ -Rituximab on Toxicity of Raji Cells

LDH, a marker of cell toxicity, is released from the cells when the cell membrane is damaged and permeable. Cell toxicity of Raji cells treated with 1.85 MBq of  $^{131}\text{I}$ -rituximab after different incubation periods (2, 6, 12, and 24 hours) was studied using LDH assay (Fig. 4a). An equivalent concentration

(5  $\mu\text{g}$ ) of rituximab was used as vehicle control. It was observed that cells treated with rituximab followed by incubation showed an increase in LDH release (1.5- to 3-fold), depending on the increase in the length of the incubation period. However, when the cells were treated with  $^{131}\text{I}$ -rituximab, 3- to 7.5-fold increase in the release of LDH was observed, which was significantly higher than vehicle control (rituximab). These results suggest the efficacy of  $^{131}\text{I}$ -rituximab in Raji cells.

#### F. Effect of $^{131}\text{I}$ -Rituximab on the Induction of Apoptotic Death in Raji Cells

To elucidate the underlying mechanism and mode of cell death in Raji cells after  $^{131}\text{I}$ -rituximab treatment, the magnitude of apoptosis was determined by in situ cell death detection ELISA (Fig. 4b). Our results showed that the enrichment factor of Raji cells treated with rituximab increased from ~2.5-fold at 2 hours to ~4-fold at 24 hours, whereas in Raji cells treated with  $^{131}\text{I}$ -rituximab it increased from ~2.5-fold at 2 hours to ~25-fold at 24 hours.

#### G. Effect of $^{131}\text{I}$ -Rituximab on the Expression of DNA Damage and Apoptotic Proteins in Raji Cells

The role of DNA damage and apoptotic proteins in the mechanism underlying in induction of apoptotic death was studied in Raji cells after  $^{131}\text{I}$ -rituximab treatment (Fig. 5). In Raji cells treated with  $^{131}\text{I}$ -rituximab, p53, a marker of DNA damage, was

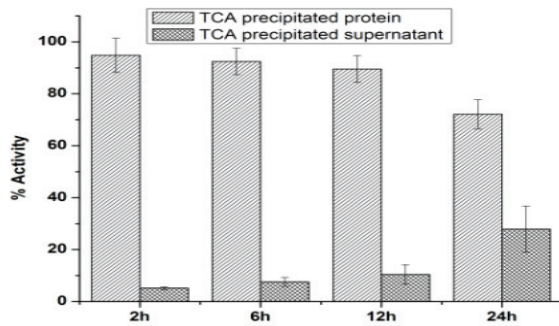


Figure 3a.

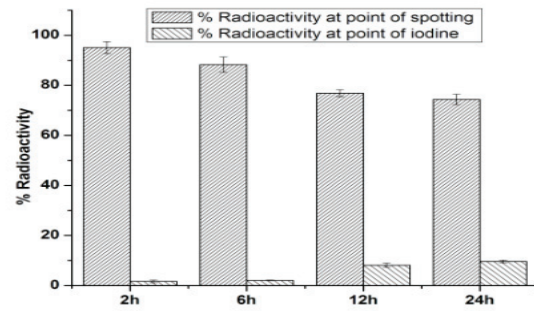


Figure 3b.

**FIG. 3: a:** Estimated  $^{131}\text{I}$ -rituximab degradation and deiodination in supernatant media of Raji cells by trichloroacetic acid precipitation. **b:** Estimated extent of  $^{131}\text{I}$ -rituximab degradation and deiodination in supernatant media of Raji cells by paper electrophoresis.

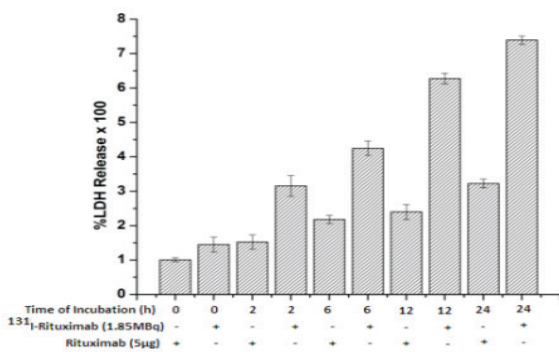


Figure 4a.

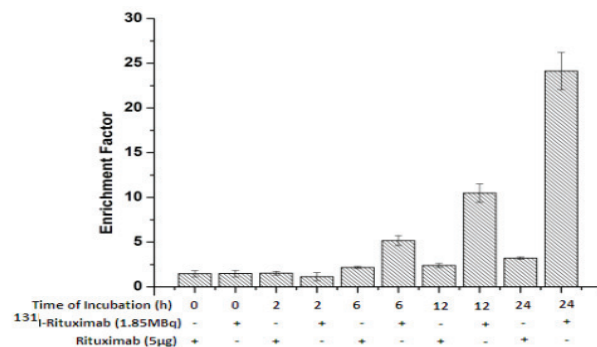


Figure 4b.

**FIG. 4: a:** Percentage of lactate dehydrogenase (LDH) released in Raji cells after incubation with  $^{131}\text{I}$ -rituximab. **b:** Apoptosis in Raji cells after incubation with  $^{131}\text{I}$ -rituximab.

upregulated after 6 hours, which showed down-regulation at 12- and 24-hour time points. PARP which gets cleaved during apoptosis, showed a cleaved fraction at 6 hours and a maximum cleavage at 24 hours of  $^{131}\text{I}$ -rituximab treatment. Compared with cells treated with  $^{131}\text{I}$ -rituximab, cells treated with rituximab showed lower expression of p53 and cleavage of PARP at different time points.

#### IV. DISCUSSION

The objective of this work was to study the internalization and understand the fate of  $^{131}\text{I}$ -rituximab and the mechanism of cytotoxicity in Raji cells treated with  $^{131}\text{I}$ -rituximab. We followed the Iodogen method for radiolabeling  $^{131}\text{I}$  with rituximab. In our study, radiolabeling yield was ~95%, which

is similar to previous reports.<sup>18,19</sup> Moreover, we have shown binding of  $^{131}\text{I}$ -rituximab specific to a CD20-positive tumor cell line, which is in agreement with previous studies.<sup>18,19</sup> The low binding of  $^{131}\text{I}$ -rituximab to CD20-negative U937 cells (<0.5%) is because of nonspecific binding of  $^{131}\text{I}$ -rituximab. The significantly higher binding of  $^{131}\text{I}$ -rituximab to CD20-positive cells indicates its positive aspect as a potential radiopharmaceutical. In one previous study, the stability of antibodies labeled with radioisotopes ( $^{125}\text{I}$ ,  $^{188}\text{Re}$ ,  $^{111}\text{In}$ ) was studied up to 7 days in renal carcinoma and ovarian cancer cells.<sup>22</sup> Our results are in agreement with this study, suggesting instability of  $^{131}\text{I}$ -rituximab bound with Raji cells with respect to incubation time, which was explained based on the deiodination and degradation of radiopharmaceuticals.

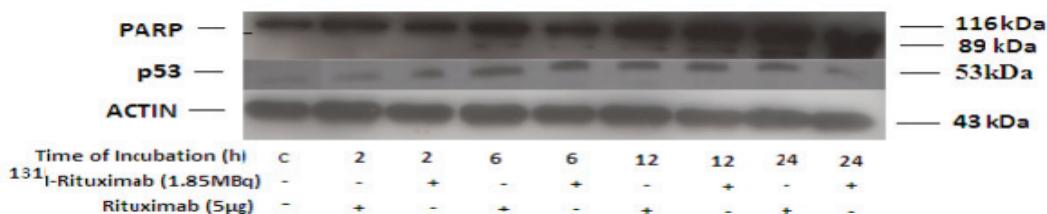


**FIG: 5:** Expression of p53 and poly ADP ribose polymerase (PARP) proteins in Raji cells after incubation with  $^{131}\text{I}$ -rituximab.  $\beta$ -Actin was used as the loading control.

However, deiodination and degradation in a previous study<sup>22</sup> occurred during longer periods of time than those in our study, which showed deiodination and degradation of  $^{131}\text{I}$ -rituximab bound to Raji cells at 24 hours, which may be due to the higher energy of  $^{131}\text{I}$ . Study of cellular internalization showed that radioactivity retained in tumor cells decreased with the time of incubation; its degraded/deiodinated products in supernatant concomitantly increased with incubation time, as estimated by TCA precipitation and paper electrophoresis. The difference (15%) in the degraded  $^{131}\text{I}$ -rituximab radioactivity observed at 24 hours between TCA precipitation and paper chromatography could be due to low molecular weight fragmented  $^{131}\text{I}$ -rituximab, which is not precipitated by the TCA and remains in the TCA supernatant.

Cellular toxicity by  $^{131}\text{I}$ -rituximab was higher compared with rituximab. Rituximab is known to cause cytotoxicity in tumor cells involving cellular signaling pathways.<sup>23</sup> However, additional damage to tumor cells resulted because of high-energy beta radiation (0.6 MeV), and the magnitude of damage is enhanced further because of the localization of radioisotopes close to cellular targets at the membrane and cytoplasm (nucleus). It may be pertinent to mention here that during kinetics of internalization,  $^{131}\text{I}$ -rituximab is almost equally distributed to the membrane and cytoplasm at 12 hours of incubation (Fig. 2a). Even though beta radiation emitted from  $^{131}\text{I}$ -rituximab has an average range of 2.3 mm, at the time of equal distribution of  $^{131}\text{I}$ -rituximab to the membrane and cytoplasm, there will be the possibility of maximum damage to cellular targets, including the nucleus. Hence, we may expect higher tumor cytotoxicity at incubation periods of 12 hours or longer, which is similar to our observation in cytotoxicity studies using LDH and apoptosis.

To elucidate the mechanism underlying the cytotoxicity of and apoptotic death in Raji cells after  $^{131}\text{I}$ -rituximab treatment, we have studied expression of p53 and cleavage of PARP. Our results showed that in Raji cells treated with  $^{131}\text{I}$ -rituximab, maximum expression of p53 was seen at 6 hours; however, cleavage of PARP begins at 6 hours and was maximal at 24 hours (Fig. 5). The DNA damage sensor protein p53 is known to be upregulated early and is responsible for the induction of apoptotic machinery. Furthermore, it was interesting to observe that tumor cells treated with only rituximab showed a lower level of p53 upregulation and cleavage of PARP than cells treated with  $^{131}\text{I}$ -rituximab (Fig. 5), suggesting a greater role of beta radiation from  $^{131}\text{I}$ -rituximab in tumor cell killing.

## V. CONCLUSION

Our results showed that  $^{131}\text{I}$ -rituximab has a synergistic benefit in terms of killing Raji cells when compared with unlabeled rituximab, and the efficacy of  $^{131}\text{I}$ -rituximab involves apoptotic death associated with regulation of p53 and PARP.

## ACKNOWLEDGMENTS

The authors are grateful to Dr. Mahesh Subramanian, Bio-organic Division, Bhabha Atomic Research Centre, India, for flow cytometry analysis of cells and are deeply grateful to Dr M. R. A. Pillai, Head, Radiopharmaceuticals Division, Bhabha Atomic Research Centre, India, for his suggestions and direction for the work. The authors thank Shri P. V. Joshi and his colleagues of the Radiochemical Section, Radiopharmaceuticals Division, Bhabha Atomic Research Centre, India, for providing in-house  $\text{Na}^{131}\text{I}$  to carry out the radiolabeling studies.

## REFERENCES

- Boye J, Elter T, Engert A. An overview of the current clinical use of the anti CD20 monoclonal antibody rituximab. *Ann Oncol*. 2003;14:520–35.
- Reff ME, Carner K, Chambers KS, Chinn PC, Leonard JE, Rabb R, Newman RA, Hanna N, Anderson DR. Depletion of B cells *in vivo* by a chimeric mouse human monoclonal antibody to CD20. *Blood*. 1994;83:435–45.
- Anderson KC, Bates MP, Slaughenhaupt BL, Pinkus GS, Schlossman SF, Nadler LM. Expression of human B cell-associated antigens on leukemias and lymphomas: a model of human B cell differentiation. *Blood*. 1984;63:1424–33.
- Multani PS, Grossbard ML. Monoclonal antibody-based therapies for hematologic malignancies. *J Clin Oncol*. 1998;16:3691–710.
- Kunala S, Macklis RM. Ionizing radiation induces CD20 expression on human B cells. *Int J Cancer*. 2001;96:178–81.
- Ehrlich P. The collected papers of Paul Ehrlich. Vol. 3. London: Pergamon; 1960.
- Pohlman B, Sweetenham J, Macklis RM. Review of clinical radioimmunotherapy. *Expert Rev Anticancer Ther*. 2006;6:445–61.
- Mach JP, Carrel S, Merenda C, Sordat B, Cerottini JC. *In vivo* localisation of radiolabelled antibodies to carcinoembryonic antigen in human colon carcinoma grafted into nude mice. *Nature*. 1974;248:704–6.
- Milenic DE, Brady ED, Brechbiel MW. Antibody-targeted radiation cancer therapy. *Nat Rev Drug Discov*. 2004;3:488–99.
- Govindan SV, Griffiths GL, Hansen HJ, Horak ID, Goldenberg DM. Cancer therapy with radiolabeled and drug/toxin-conjugated antibodies. *Technol Cancer Res Treat*. 2005;4:375–91.
- Britz-Cunningham SH, Adelstein SJ. Molecular targeting with radionuclides: state of science. *J Nucl Med*. 2003;44:1945–61.
- Chinol M, Vallabhajosula S, Goldsmith SJ, Klein MJ, Deutsch KF, Chinen LK, Brodack JW, Deutsch EA, Watson BA, Tofe AJ. Chemistry and biological behavior of samarium-153 and rhenium-186-labeled hydroxyapatite particles: potential radiopharmaceuticals for radiation synovectomy. *J Nucl Med*. 1993;34:1536–42.
- Finlay IG, Mason MD, Shelley M. Radioisotopes for the palliation of metastatic bone cancer: a systematic review. *Lancet Oncol*. 2005;6:392–400.
- Otte A, Mueller-Brand J, Dellas S, Nitzsche EU, Herrmann R, Maecke HR. Yttrium-90-labelled somatostatin-analogue for cancer treatment. *Lancet*. 1998;351:417–8.
- Boelaert K, Franklyn JA. Sodium iodide symporter: a novel strategy to target breast, prostate and other cancers? *Lancet*. 2003;361:796–7.
- Sharkey RM, Burton J, Goldenberg DM. Radioimmunotherapy of non-Hodgkin's lymphoma: a critical appraisal. *Expert Rev Clin Immunol*. 2005;1:47–62.
- Tran L, Baars JW, de Boer JP, Hoefnagel CA, Beijnen JH, Huitema AD. The pharmacokinetics of <sup>131</sup>I-rituximab in a patient with CD20 positive non-Hodgkin lymphoma: evaluation of the effect of radioiodination on the biological properties of rituximab. *Hum Antibodies*. 2011;20:37–40.
- Wei L, Luo RC, Zhang JY, Yan X, Lü CW. *In vitro* cytotoxicity of <sup>131</sup>I-Rituximab against B-cell lymphoma cells. *Nan Fang Yi Ke Da Xue Xue Bao*. 2009;29:40–3.
- Wei L, Luo RC, Zhang JY, Yan X, Fang YX, Fei LH. Biological response of B-cell lymphoma cells *in vitro* to <sup>131</sup>I-rituximab. *Nan Fang Yi Ke Da Xue Xue Bao*. 2006;26:211–3.
- Fraker P, Speck J. Protein and cell membrane iodinations with a sparingly soluble chloroamide, 1,3,4,6-tetrachloro-3a,6a-diphrenylglycoluril. *Biochem Biophys Res Commun*. 1978;80:849–57.
- Goddu SM, Rao DV, Howell RW. Multicellular dosimetry for micrometastases: dependence of self-dose versus cross-dose to cell nuclei on type and energy of radiation and subcellular distribution of radionuclides. *J Nucl Med*. 1994;35:521–30.
- Shih LB, Thorpe SR, Griffiths GL, Diril H, Ong GL, Hansen HJ, Goldenberg DM, Mattes MJ. The processing and fate of antibodies and their radio-labels bound to the surface of tumor cells *in vitro*: a comparison of nine radiolabels. *J Nucl Med*. 1994;35:899–908.
- Bonavida B. Rituximab-induced inhibition of antiapoptotic cell survival pathways: implications in chemo/immuno-resistance, rituximab unresponsiveness, prognostic and novel therapeutic interventions. *Oncogene*. 2007;26:3629–36.



